Novel methods of chemical speciation of Pt(IV/II) complexes in acid halide-rich solutions by ion-pair RP-HPLC coupled to ICP-OES/MS in conjunction with ^{195}Pt NMR

by
Pieter-Hugo van Wyk

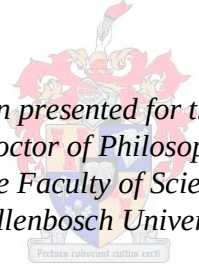

Dissertation presented for the degree of
Doctor of Philosophy
in the Faculty of Science at
Stellenbosch University

Supervisor: Prof. Klaus R. Koch
Co-Supervisor: Dr. Wilhelmus J. Gerber

March 2013

Declaration

By submitting this thesis/dissertation electronically, I declare that the entirety of the work contained therein is my own, original work, that I am the sole author thereof (save to the extent explicitly otherwise stated), that reproduction and publication thereof by Stellenbosch University will not infringe any third party rights and that I have not previously in its entirety or in part submitted it for obtaining any qualification.

Date: March 2013

"I listen to the wind

To the wind of my soul

Where I'll end up well I think,

Only God really knows"

Cat Stevens, 1971

Opgedra aan Ma en Pa (1956-2009)

Dankie vir so baie

Acknowledgements

So many people have contributed in one way or another to the work compiled in this thesis, it truly is the sum of many parts. I would like to express my gratitude to the following:

My supervisor, Professor Klaus Koch, to whom I am indebted for welcoming me into his research group, that shift has had so many positive repercussions in my life, both academically and personally. His guidance in my research, belief in my abilities and inspirational enthusiasm with which he takes on challenges. His knowledge of chemistry and science in general, not to mention the worldly wisdom he added to so many topical discussions. The opportunities I have been given to travel locally and abroad are also greatly appreciated.

My co-supervisor, Doctor Wilhelmus Gerber, for the everyday thoughtful discussions, the challenges he put before me and constantly pushing me to improve myself, I would not be where I am without it. His patient editing of those first written attempts and the lessons I have learnt towards becoming a better scientific writer over the years. Last but not least, his willingness to always support his losing Bulls team when it comes to putting a wager on the game.

The PGM research group, for creating an enjoyable working environment, for all the discussions; scientific, philosophical and those totally arbitrary, it has been a pleasure.

Doctor André de Villiers, an endless source of chromatography knowledge and experience, his advice and helpful discussions are greatly appreciated. As well as the occasional loan of spare HPLC parts.

Doctor Marietjie Stander, her invaluable contribution to the mass spectrometry experiments and her willingness to put her high resolution instrument at the mercy of ion-pairing reagents.

Doctor Jaco Brand and Elsa Malherbe at the NMR lab for their advice and assistance.

The technical staff at the Analytical Chemistry Department, Shafiek Mohammed, Deidre Davids and Roger Lawrence.

The University of Stellenbosch, Anglo Platinum and the Harry Crossley Foundation for financial support.

My mother and my late father, for creating a safe, motivating and inspiring environment to grow up in, for always believing in me, your love and support have been the key ingredients.

Conference Proceedings

Aspects of this work have been presented at the following conferences:

Conference Poster Presentations

1. P-H van Wyk, W. J. Gerber, K. R. K Koch. Speciation and characterization of the $[PtCl_{6-n}Br_n]^{2-}$ (n = 0 - 6) complex anions using RP-IP-HPLC. *RSC SACI Inorg*, University of Free State, Bloemfontein, South Africa, September 2009.
2. P-H van Wyk, W. J. Gerber, K. R. K Koch. Reversed phase HPLC ion-pairing separation and quantification of $[PtCl_{4-n}Br_n]^{2-}$ (n = 0 - 4) and $[PtCl_{6-n}Br_n]^{2-}$ (n = 0 - 6) anions with UV-VIS and ICP-OES/MS detection. *Analitika*, Stellenbosch University, South Africa, December 2010.
3. P-H van Wyk, W. J. Gerber, K. R. K Koch. Reversed phase HPLC ion-pairing separation and quantification of $[PtCl_{4-n}Br_n]^{2-}$ (n = 0 - 4) and $[PtCl_{6-n}Br_n]^{2-}$ (n = 0 - 6) anions with UV-VIS and ICP-OES/MS detection. *RSC SACI*, Wits University, Johannesburg, South Africa, January 2011.

Conference Poster Prizes

1. Best poster prize, *RSC SACI Inorg*, 2009, University of Free State, Bloemfontein, South Africa.
2. Best poster prize, *RSC SACI*, 2011, Wits University, Johannesburg, South Africa.

Conference Oral Presentations

4. P-H van Wyk, W. J. Gerber, K. R. K Koch. Reversed phase HPLC ion-pairing separation and quantification of $[PtCl_{4-n}Br_n]^{2-}$ (n = 0 - 4) and $[PtCl_{6-n}Br_n]^{2-}$ (n = 0 - 6) anions with UV-VIS and ICP-OES/MS detection. *Analitika*, Stellenbosch University, South Africa, December 2010.
5. P-H van Wyk, W. J. Gerber, K. R. K Koch. Chemical speciation of mixed halide Platinum(II/IV) complex anions by ion-pairing RP-HPLC coupled to ICP-MS/OES: Toward Determination of metal to halide ratios. *Twelth Symposium on Hyphenated Techniques in Chromatography and Hyphenated Chromatographic Analyzers*, Bruges, Belgium, February 2012.

Abbreviations

CZE	Capillary Zone Electrophoresis
ESI-MS	Electrospray Ionization- Mass Spectrometry
HPLC	High Performance Liquid Chromatography
ICP-MS	Inductively coupled plasma-Mass Spectrometry
ICP-OES	Inductively coupled plasma-Optical Emission Spectroscopy
IP	Ion-pairing
LOD	Limit of detection
LOQ	Limit of quantification
NMR	Nuclear Magnetic Resonance
PDA	Photodiode Array
PGMs	Platinum Group Metals
ppm	parts per million
RP	Reversed Phase
TBA^+Cl^-	Tetrabutylammonium Chloride
$TBA^+NO_3^-$	Tetrabutylammonium Nitrate
TriBA	Tributylamine
UHPLC	Ultra High Performance Liquid Chromatography
UV-Vis	Ultra Violet-Visible
Q	Quadrupole
TOF	Time-of-flight

Abstract

In this work a robust reversed phase ion-pairing high performance liquid chromatographic (RP-HPLC) method has been developed for the separation, characterization and quantification of all possible $[PtCl_{6-n}Br_n]^{2-}$ (n = 0 – 6) and $[PtCl_{4-n}Br_n]^{2-}$ (n = 0 – 4) complex anions using UV-Vis detection. High resolution ^{195}Pt NMR of more concentrated $Pt^{II/IV}$ solutions served to validate the relevant species assignments, particularly those of the stereoisomer species, *cis*- and *trans*-$[PtCl_4Br_2]^{2-}$, $[PtCl_2Br_4]^{2-}$ and *mer*- and *fac*-$[PtCl_3Br_3]^{2-}$. Quantification of the $Pt^{II/IV}$ species was achieved by means of IP-RP-HPLC coupled to either ICP-MS or ICP-OES, and together with the UV-Vis absorption spectra obtained by photodiode array (PDA) recording of all eluted species, allowed for the determination of the photometric characteristics (λ_{max} and ε) of all the $Pt^{II/IV}$ species. This data enables practical speciation studies of such $Pt^{II/IV}$ complex anions using standard analytical equipment.

The hyphenation of ion-pairing RP-HPLC to ICP-OES allows for the successful determination of the Pt to halide mole ratios of individually separated species in order to characterize these species in a novel manner. The Pt to chloride and/or Pt to bromide mole ratio of the $[PtCl_4]^{2-}$ and the series of $[PtCl_{6-n}Br_n]^{2-}$ (n = 0 – 6) complexes were determined using HPLC-ICP-OES based on the 177.708 nm Pt, 134.724 nm Cl and 148.845 nm Br emission lines and served as a technique for the unambiguous chemical speciation of such complexes.

An increase in sensitivity of the developed method was achieved by the use of an ion-pairing reversed phase ultra high performance liquid chromatography electrospray ionization quadrupole time-of-flight mass spectrometry (UHPLC-ESI-Q-TOF-MS) method. This method proved capable of separating and characterizing the homoleptic and heteroleptic $[Pt^{IV}Cl_{6-n}Br_n]^{2-}$ (n = 0 – 6) and mono-aquated $[Pt^{IV}Cl_{5-n}Br_n(H_2O)]^{-}$ (n = 0 – 5) complex anions in well defined acidic aqueous solutions. Ion-pairing ultra high performance liquid chromatography separation

based on the volatile ion-pairing reagent, tributylamine, provided adequate chromatographic resolution as well as sufficiently low background noise for high resolution ESI-Q-TOF-MS detection. The wealth of structural information contained in the mass spectra obtained for each Pt^{IV} species simplified the identification of individual species. Moreover, the general fragmentation trends encompassing a constant incremental change of 44 Da ($^{79/81}Br$ - $^{35/37}Cl$) resulting from the successive substitution of Cl^- by Br^-, in combination with the observed elution order, facilitated the relevant species assignments. The developed method enabled the relative rapid (<13 min) characterization of all 22 $[PtCl_{6-n}Br_n]^{2-}$ (n = 0 – 6) and mono-aquated $[PtCl_{5-n}Br_n(H_2O)]^-$ (n = 0 – 5) species.

Quantification of each individual $[PtCl_{6-n}Br_n]^{2-}$ (n = 0 – 6) species by means of ion-paring HPLC-UV-Vis allowed for the determination of all 17 stability constants for the Pt^{IV} chlorido-bromido halide exchange reaction network. Determination of the associated Gibbs free energies for each ligand exchange reaction step, $\Delta G^{o}_{rxnK_n}$ (n = 1 - 17), together with energy conservation relationships, served to validate the accuracy of the experimentally calculated stability constants. The experimentally determined overall formation constant, or ΔG^{o}_{rxn}, and those calculated using the standard reaction half cell reduction potentials of $[PtCl_6]^{2-}$ and $[PtBr_6]^{2-}$ were in good agreement, further confirming the experimentally obtained thermodynamic parameters. The thermodynamic driving force for the Pt^{IV} chloride-bromido exchange reactions is attributed to the hydration of the halide ligands, which drives the reaction towards the bromido Pt^{IV} species in aqueous solutions, even though the chlorido Pt^{IV} complexes are energetically favoured in this reaction network. Evaluation of other metal cation halido exchange reactions shows that all metal halido complexes exhibit the $F^- >> Cl^- > Br^- > I^-$ order of thermodynamic stability and is only inverted due to the solvation of the relevant halide ligands. Furthermore, density functional theory (DFT) was used to predict the thermodynamic stabilities with respect to the isodesmic reactions involving chlorido-bromido Pt^{IV} stereoisomer pairs and chlorido-bromido Pt^{IV} ligand exchange reactions of the $[PtCl_{6-n}Br_n]^{2-}$ (n = 0 – 6) species and confirm the $F^- >> Cl^- > Br^- > I^-$ order of thermodynamic stability as well as determining the $\Delta\Delta G^{o}_{rxn}$ within the range of 8 - 20 $kJ.mol^{-1}$ to the experimentally determined $\Delta\Delta G^{o}_{rxn}$.

Opsomming

Tydens hierdie studie is ‘n robuuste “reverse-phase” ioonparing hoë-verrigting vloeistof chromatografie, RP-IP-HPLC, metode ontwikkel vir die skeiding, karakterisering en kwantifisering van alle moontlike $[PtCl_{6-n}Br_n]^{2-}$ (n = 0 – 6) en $[PtCl_{4-n}Br_n]^{2-}$ (n = 0 – 4) kompleks anione waar UV-Vis as detektor gebruik word. Die relavante spesies toedelings wat gemaak is, veral ten opsigte van die *cis*- en *trans*-$[PtCl_4Br_2]^{2-}$, $[PtCl_2Br_4]^{2-}$ en *mer*- en *fac*-$[PtCl_3Br_3]^{2-}$ stereo-isomeerpare, is deur middel van hoë-resolusie ^{195}Pt KMR van meer gekonsentreerde $Pt^{II/IV}$ oplossings bevestig. Die $Pt^{II/IV}$ spesies was gekwantifiseer deur die IP-RP-HPLC aan of ‘n ICP-MS of ‘n ICP-OES te koppel. Daarenbowe was dit moontlik om die fotometriese eienskappe (λ_{max} en ε) van elke individuele $Pt^{II/IV}$ komplex anion te bepaal deur die UV-Vis absorpsie spektrum van elke elueerende spesies met PDA op te neem. Die nuwe metode wat tydens hierdie studie ontwikkel is het dit dus moontlik gemaak om sulke $Pt^{II/IV}$ komplek sanione met standaard analitiese toerusting prakties te skei.

Verder is gevind dat deur IP-RP-HPLC aan ICP-OES te koppel dit moontlik is om die Pt tot halied mol verhoudings van elke individueel geskeide spesies te bepaal en dus hierdie spesies op ‘n oorspronklike, nuwe manier te karakteriseer. Die Pt tot chloried en/of Pt tot bromied mol verhoudings van die $[PtCl_4]^{2-}$ en die reeks van $[PtCl_{6-n}Br_n]^{2-}$ (n = 0 – 6) kompleks anione, soos bepaal deur gebruik te maak van HPLC-ICP-OES, is gebasseer op die 177.708 nm Pt, 134.724 nm Cl en 148.845 nm Br emissie lyne. Hierdie metode kan gebruik word vir die eenduidige chemiese skeiding van hierdie komplekse.

Die sensitiwiteit van hierdie metode was egter verder verbeter deur gebruik te maak van ioonparing “reverse-phase” ultra hoë-verrigting vloeistof chromatografie gekoppel met elektrosprei ionisasie quadropool “time-of-flight” massa spektrometrie (UHPLC-ESI-Q-TOF-MS). Deur dit te doen is dit nou selfs moontlik om die homoleptiese en heteroleptiese

$[Pt^{IV}Cl_{6-n}Br_n]^{2-}$ (n = 0 – 6) spesies, asook die "mono-aqauted" $[Pt^{IV}Cl_{5-n}Br_nH_2O]^-$ (n = 0 – 5) spesies in 'n goed gedefinieërde aangesuurde waterige oplossings te skei en te karakteriseer. Die vlugtige ioon-paringsreagent, tributielamien, is vir die skeidingsproses op die IP-UHPLC gebruik om te verseker dat voldoende chromatografiese resolusie, so wel as lae genoeg agtergrondgeraas, verkry word vir hoë-resolusie ESI-Q-TOF-MS deteksie. Die rykdom informasie vervat in die massaspektrum van elke Pt^{IV} spesies het die indentifikasie van elke spesies vergemaklik. Daarenbowe het die fragmentasie tendens, aanduidend van 'n konstante inkrementele verandering van 44 amu (71/81Br – 35/37Cl) weens die opeenvolgende substitusie van Cl^- met Br^-, tesame met die elusie volgorde, die spesies-toedelings gefasiliteer. Met hierdie nuut ontwikkelde metode is dit nou moontlik om al 22 $[PtCl_{6-n}Br_n]^{2-}$ (n = 0 – 6) en "mono-aquated" $[PtCl_{5-n}Br_nH_2O]^-$ (n = 0 – 5) spesies in 'n relatiewe kort tydperk (< 13 min) te karakteriseer.

Deurdat elke $[PtCl_{6-n}Br_n]^{2-}$ (n = 0 – 6) spesies nou individueel met IP-HPLC-UV-Vis gekwantifiseer kan word, is dit moontlik om al 17 stabiliteitskonstantes vir die Pt^{IV} chlorido-bromido halied uitruilingsreaksienetwerk te bepaal. Die geassosieerde Gibbs vrye energie, $\Delta G°_{rxnKn}$ (n = 0 – 17), wat vir elke stap in die uitruilingsreaksienetwerk bepaal is, tesame met die energiebewaring verhoudings, was gebruik om die akkuraatheid van die eksperimenteel bepaalde stabiliteitskonstantes te bekragtig. Verdermeer was die waarde van die algehele formasie konstante wat eksperimenteel bepaal is, $\Delta G°_{rxn}$, in goeie ooreenstemming met dit wat bereken is deur die standaard reaksie halfsel reduksie potensiale van $[PtCl_6]^{2-}$ en $[PtBr_6]^{2-}$. Dus is die eksperimenteel verkrygde termodinamiese parameters bevestig. Die termodinamiese dryfkrag vir die Pt^{IV} chloried-bromied uitruilingsreaksies is toegereken aan die hidrasie van die halied ligande, wat in waterige oplossings die reaksie na die bromied Pt^{IV} spesies dryf, al is die chloried Pt^{IV} spesies energeties bevoordeel in hierdie reaksienetwerk. Evaluering van ander metaal-katioon-halied-uitruilreaksies wys dat alle metaal-halied komplekse die $F^- >> Cl^- > Br^- > I^-$ orde van termodinamiese stabiliteit volg en dat hierdie volgorde slegs omgekeer sal word weens solvasie van hierdie halied ligande. Darenbowe digtheids funksionele teorie (DFT) gebruik om die termodinamiese stabiliteit met betrekking tot isodesmiese reaksies wat chloried-bromied Pt^{IV} stereoisomeer pare behels te voorspel, sowel as van chloried-bromied Pt^{IV} liganduitruilingsreaksies van die $[PtCl_{6-n}Br_n]^{2-}$ (n = 0 – 6) spesies, en bevestig die $F^- >> Cl^- > Br^- > I^-$ volgorde van termodinamiese stabiliteit. Verder was dit ook moontlik om met DFT die $\Delta\Delta G°_{rxn}$ tot so naby as 8 – 20 $kJ.mol^{-1}$ te bereken.

Contents

1 Introduction

1.1 General introduction

A recent compilation of the Earth's platinum group metals (PGMs) resources has singled out the Bushveld complex, Figure 1.1, as host to the vast majority of technologically attainable PGMs known to exist.[1] This uniquely disproportionate accumulation of PGMs (Pt, Pd, Rh, Ru, Ir and Os) is unrivalled in size and by all forecasts will remain such as the unearthing of an equal (350 km x 400 km) or greater ore body is highly improbable.[1]

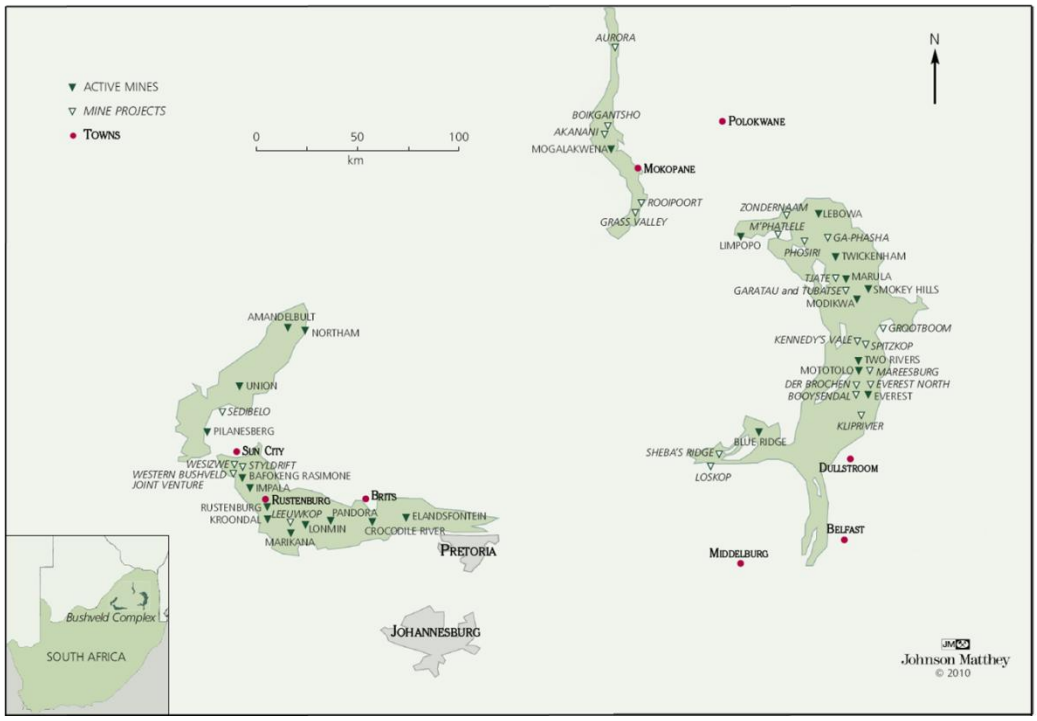

Figure 1.1 Map of the Bushveld complex (eastern, western and northern limbs) situated in the North West province of South Africa.[2] This area is host to 75, 82 and 52 % of the world's resources of Pt, Rh and Pd, respectively.[1]

The significance gained by PGMs in recent decades above the traditional decorative industries, is a result of the rapid advances made in technology incorporating these metals.[3] The ability of PGMs to facilitate both oxidation and reduction reactions[4] and proven high catalytic activity of these metals involving a wide range of substrates, have increased the use of PGMs in a host of important industrial synthetic processes. These include organic oxidation reactions such as the Wacker process,[5] inorganic oxidation reactions such the Ostwald and Brauer[6] process, hydrogenation and dehydrogenation reactions[7, 8, 9] in the pharmaceutical industry and reforming reactions in the petroleum refining industry.[10]

Recognition of mankind's ever-growing negative impact on the environment has made the development of 'clean' technology a priority, an effort which is highlighted by the application of PGMs in automotive emission control catalysts (so-called catalytic converters). CO, various nitrogen oxides and smaller hydrocarbons present in vehicle exhaust emissions are catalytically converted to CO_2, H_2O and N_2, thus reducing pollutants.[11] The assessment that 60 % of the annual world production of Pt, Pd and Rh was used in automotive exhaust catalysts in the year 2000 is testament to its success.[12] Given that approximately 10 g of PGMs are used in each catalytic converter, and that minimal amounts of PGMs are lost to the environment during the lifetime of an automotive emission control catalyst,[13] the recycling of these converters has become increasingly important and accounts for 20% of the world's demand in 2009.[14] Furthermore, PGM catalysts are also used for the development of zero-emission vehicles powered by hydrogen fuel cells in which platinum composite electrodes find application.[15]

PGMs are also used in the high temperature industries wherein the excellent mechanical and oxidation-resistant properties that these metals and their alloys exhibit at high temperatures are utilized. These include coatings for turbine blades used in jet engines, nozzles for spinning textiles and materials for processing highly corrosive molten glass.[12, 15]

The scarcity of commercially viable ore deposits (0.005 ppm Pt in the Earth's crust),[16] increase in mining costs (energy and labour related) and struggling world economy have placed the PGMs industry under immense pressure in recent times.[17] In addition, the production of a single ounce of Pt (28.25 g) entails that roughly 10 tons of ore must be processed via a 5 month extraction and refinement procedure.[16] The development of highly efficient extraction and refinement procedures are thus of the utmost importance.

1.2 PGMs refining methodology

The extraction and refinement of PGMs are mostly dependent on the differences in their chlorido and/or bromido anionic complexes. Until the early 1970's refining of PGMs was achieved using a series of chemical and selective precipitation reactions, in the mid 1970's several solvent extraction methods using anion exchangers such as tributylphosphate were introduced, many of which are still in use today. More recently solid-phase extraction methods were incorporated making use of a high level of molecular recognition.[10] Each of the above-mentioned methods are highly dependent on the relevant chemical species in solution. The International Union for Pure and Applied Chemistry (IUPAC) defines speciation as follows:[18]

"*speciation analysis is the analytical activity of identifying and/or measuring the quantities of one or more individual chemical species in a sample; the chemical species are specific forms of an element defined as to isotopic composition, electronic or oxidation state, and/or complex or molecular structure; the speciation of an element is the distribution of an element amongst defined chemical species in a system.*"

In chloride and bromide rich matrices, Pt^{IV} for instance will undergo several ligand exchange reactions, furnishing in principle the mixed chlorido-bromido Pt^{IV} species shown in Diagram 1.1.

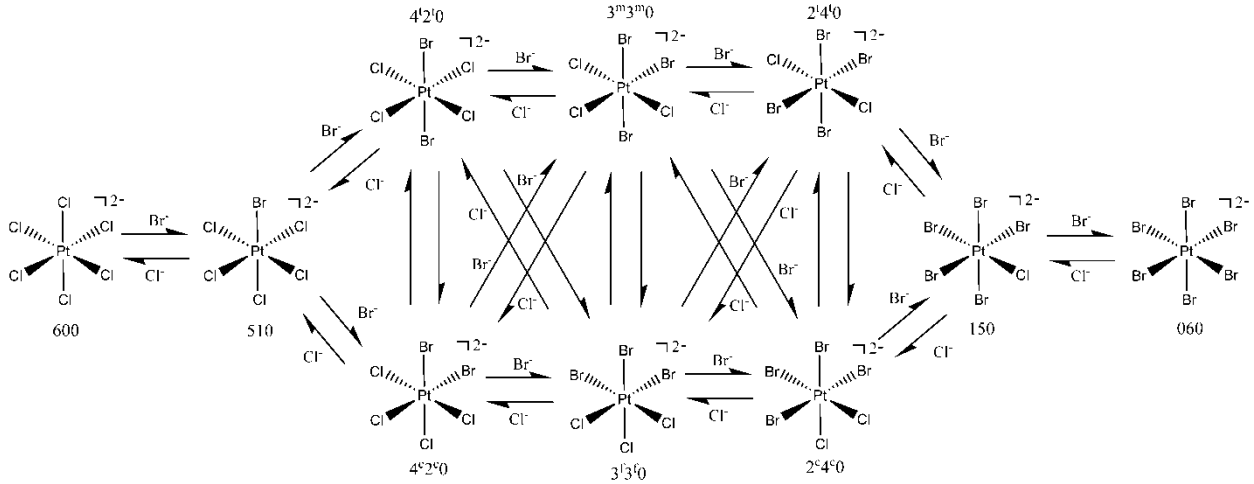

Diagram 1.1 The reaction network formed by the $[PtCl_{6-n}Br_n]^{2-}$ (n = 0 – 6) anionic complexes. The nomenclature used for species assignment states that the first numeral represents the number of chloride ions and the second numeral the number of bromide ions coordinated to the Pt^{IV} ion, respectively. The superscripts c, t, m and f denote the stereoisomer species; *cis*, *trans*, *mer* and *fac*, respectively.

1.3 Analytical methods for the determination and speciation of PGMs in aqueous solutions

The detection and speciation of PGMs in aqueous halide-rich solutions has been an on-going challenge to the analyst. Considerations of the detection power, reliability, precision, selectivity and cost have to be taken into account when evaluating a particular analytical method. A brief overview of analytical methods applied to the determination and speciation in aqueous solutions of Pt species in particular is presented below. Certain methods such as UV-Vis spectrophotometry and ^{195}Pt nuclear magnetic resonance (^{195}Pt NMR) are discussed in terms of direct analysis, whereas others such as inductively coupled plasma-mass spectrometry or-optical emission spectroscopy (ICP-MS/OES) and electrospray ionization-mass spectrometry (ESI-MS) are discussed in terms of direct analysis and as detectors in hyphenated techniques. This section concludes with a review of separation and chromatographic methods pertaining to PGMs analysis.

1.3.1 UV-Vis spectroscopy

In the 1960 to 1970's, several kinetic and equilibrium investigations with respect to aquation, annation and halide exchange of PGM complexes were undertaken using UV-Vis spectroscopy.[19,20] From these studies the reaction mechanisms involved in annation reactions of a variety of Pt^{IV} complexes, including the bromido and chlorido annation reactions of Pt^{IV} aqua complexes and the catalytic effect Pt^{II} has on these reactions could be deduced.[21, 22] Furthermore, Elding *et al* evaluated the equilibrium constants for the reactions of various Pt^{II} complexes with halides and thiocyanate in aqueous solution.[20,24] Robb and Harris investigated the aquation of the $[RhCl_6]^{3-}$ complex, observing that exchange of a chloride *trans* to another chloride is preferred.[25] Analyses such as these necessitate the 'clever' use of isosbestic points,[τ] the investigation of stereochemical specific reaction routes and the availability of heteroleptic PGM complexes as starting reagents.[ζ] However, UV-Vis spectroscopy is a low resolution technique due to the broad bands, and considerable overlap of absorption spectra that occur for these PGM complexes in solution.[26] For example, when 5 or more species of related Pt^{IV} complexes are simultaneously present, speciation and quantification using UV-Vis spectroscopy will not be possible.

[τ] The wavelength at which the total absorbance of a sample does not change during a chemical reaction or a physical change of the sample.
[ζ] Synthesis of pure heteroleptic species is challenging and inevitably involves the formation of mixtures.

1.3.2 ^{195}Pt NMR spectroscopy in Pt speciation

Multinuclear NMR spectroscopy is an ideal high resolution tool to study mixed ligand complexes containing NMR active nuclei due to its response to the magnetic properties of nuclei with $I = 1/2$ in the local environment of the nucleus. Given that the separation and subsequent detection of mixed ligand Pt complexes is tedious, NMR spectroscopy has become an attractive element-specific detection method for the direct speciation of Pt complexes in solution.[27]

NMR spectroscopy has successfully been employed in the speciation of numerous mixed ligand PGM complexes. Of particular interest are the mixed ligand complexes arising from Pt. The natural abundance of the NMR-active ^{195}Pt isotope (33.7%), together with a receptivity of 19.1 relative to ^{13}C implies that ^{195}Pt NMR spectra are relatively easily obtainable.[26] ^{195}Pt shieldings are especially sensitive to oxidation state, the nature of the directly bound ligands and the molecular structure of the complex in solution. ^{195}Pt NMR is thus ideally suited to probe the chemical environment of individual Pt complexes in solution. Utilizing this powerful tool, Koch *et al* investigated the solvation/hydration shells of $[PtCl_6]^{2-}$ and $[PtCl_4]^{2-}$ as well as demonstrating ion-pairing between Na^+ and $[PtCl_6]^{2-}$ in methanol solutions by using a combination of ^{195}Pt NMR and advanced density functional theory and molecular dynamics calculations.[28] The sensitivity of ^{195}Pt NMR to the detailed structure of the Pt complex together with the extremely large ^{195}Pt chemical shift range (^{195}Pt > 13000 ppm) makes ^{195}Pt NMR spectroscopy an ideal method for speciation studies.[26]

Earlier investigations utilized ^{195}Pt NMR spectroscopy for the analysis of water exchange in the *trans*-$[PtCl_2(H_2O)_2]$ species as well as the oxidative addition of Cl_2 to the $[Pt(H_2O)_4]$ species.[29] Sadler *et al* used ^{195}Pt NMR spectroscopy to investigate the species resulting from Pt^{IV} nitrito-chlorido-bromido series.[30] More recently, Koch *et al* successfully assigned δ (^{195}Pt) belonging to the Pt^{IV} hydroxo-halide series of chloride and bromide utilizing ^{195}Pt chemical shift trend analysis.[31] The chemical shifts of complexes arising from the $[PtCl_{6-n}(OH)_n]^{2-}$ (n = 0 – 5) series displays a monotonic downfield ^{195}Pt shift as Cl^- ions are replaced by OH^- ions, resulting in a distinct second-order correlation between the ^{195}Pt chemical shift and n.[31] Similar correlations of δ (^{195}Pt) as function of n were obtained for the $[PtBr_{6-n}(OH)_n]^{2-}$ (n = 0 – 5) series of complex anions. In an analogous manner Kramer *et al* characterized 56 possible mixed halide hydroxido Pt^{IV} complexes in the $[PtCl_{6-m-n}Br_m(OH)_n]^{2-}$ (m, n = 0 – 6) series, Figure 1.2.[31]

More recently Koch *et al* utilized the characteristic isotopologues and isotopomers[ψ] formed by resolved $^{35}Cl/^{37}Cl$ isotopic shifts in the ^{195}Pt resonances as a fingerprint for the unambiguous identification and assignment of aquated Pt^{IV}-chlorido complexes.[32] While ^{195}Pt NMR has been a very powerful tool for the speciation of such complexes in aqueous solutions, the relatively low receptivity of ^{195}Pt limits such studies to relatively concentrated solutions (> 50 mM Pt).

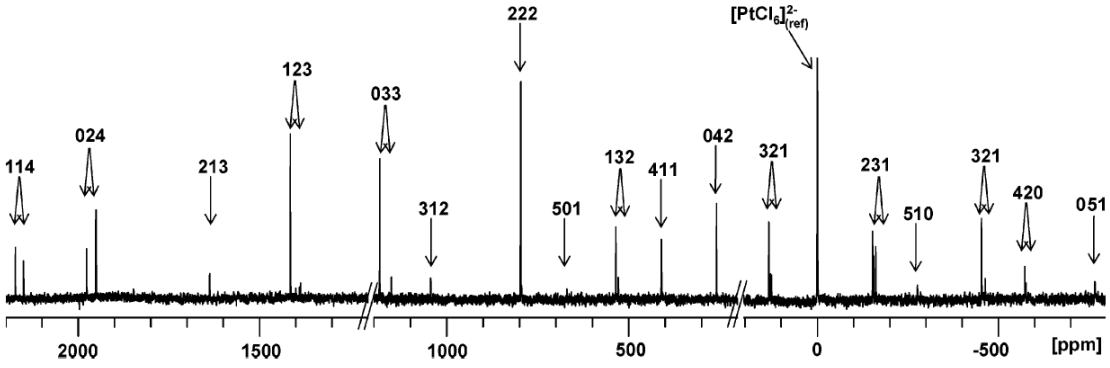

Figure 1.2 ^{195}Pt NMR spectrum of the $[PtCl_{6-m-n}Br_m(OH)_n]^{2-}$ (m, n = 0 – 6) species obtained by Kramer *et al*.[31] The nomenclature used for species assignment states that the first numeral represents the number of chloride ions, the second numeral the number of bromide ions and the third the number of hydroxide ions coordinated to the Pt^{IV} ion respectively.

[ψ] Isotopologue refers to chemical species that differ only in isotopic composition of their molecules or ions. Isotopomers are isomers with the same amount of each isotopic atom, differing in their position in the molecule or ion.[32]

1.3.3 PGMs determination by atomic spectroscopy

1.3.3.1 Inductively coupled plasma-MS/OES

The analysis of PGMs by means of inductively coupled plasma with mass spectrometry or optical emission spectroscopy (ICP-MS/OES) can be divided into two broad areas of application; (i) direct determination of the total elemental concentration of a particular metal (Pt, Pd, Rh, Ru, Ir and Os) in a variety of different matrices ranging from aqueous slurries[33] to complex environmental samples,[34] and (ii) element-specific detection and quantification of several PGM containing species, usually preceded by an appropriate separation technique such as high performance liquid chromatography (HPLC) or capillary electrophoresis (CE). Numerous accounts of direct determination are available in the literature, however, the use of this method in this thesis was limited to well-defined synthetic matrices, and will thus not be discussed further.

ICP-MS/OES as method for on-line detection of species separated by HPLC or CE has emerged as an effective technique, utilizing such capabilities as multi-elemental and multi-isotopic detection.[35] Studies of PGMs using these methods include the analysis of anti-tumor platinum compounds such as cisplatin, carboplatin and oxaliplatin in synthetic samples using both HPLC-ICP-MS[36] and HPLC-ICP-AES,[37] as well as the highly sensitive speciation and trace analysis of such compounds in urine and wastewaters originating from hospitals.[38] Furthermore, the analysis of Pt in environmental samples also utilizes the detection power of HPLC-MS; these include the speciation of Pt metabolites in plants,[39] Pt^{IV} and Pt^{II} chlorido complexes in spiked road dust samples[40] and Pt treated soil.[41] Other uses for this method include the identification and characterization of Rh-containing catalyst reaction intermediates,[42] as well as the high-throughput screening of PGMs in pharmaceutical samples.[43] More recently, Gerber *et al* used this method for the separation and quantification of the $[RhCl_n(H_2O)_{6-n}]^{3-n}$ ($n = 0 – 6$) complexes.[44]

1.3.3.2 Chlorine and bromine determination by means of ICP-OES

In section 1.2 the importance of speciation pertaining to the PGMs refining industry was discussed. Given that PGM chlorido and/or bromido complexes are of considerable importance in this field, thorough analysis of these halides, coordinated and uncoordinated (‘free’), is essential.

The use of ICP-OES to determine chlorine and bromine is limited due to the relatively low emissive sensitivity of these halide atoms in the ultraviolet or visible wavelength range. The most intense spectral lines for these non-metal elements, however, are in the vacuum ultraviolet spectral range, 125-180 nm,[45] wavelengths which are also absorbed by oxygen or water vapour in the air.[45] For example, the 134.724 and 154.065 spectral lines are the most intense for chlorine and bromine, respectively. In order to overcome this problem, earlier spectrometers were purged with an inert gas or the optical system was evacuated.[46-48] There were, however, disadvantages to these approaches: (i) purged systems have high operating costs, (ii) vacuum optical systems often do not reach sufficiently high vacuum, and (iii) deposition of particles on the optical surfaces can occur due to back-streaming of vapours from the oil-filled vacuum pumps.[49] Modern ICP-OES instruments are manufactured with argon-filled spectrometers and can operate in the vacuum ultraviolet spectral range.[49] In order to view the full spectral range, however, the choice of detector is important. With the Spectro ARCOS ICP-OES, detection is achieved through 32 linear CCD detector arrays mounted on the Rowland Circle of the Pachen-Runge double grating spectrometer, allowing access even to the very low UV region (≥130 nm).[50] This is in contrast to other ICP-OES instruments that have an echelle based detection system and are typically limited to a minimum of ~170 nm.[50] The use of the 134.724 and 154.065 spectral lines has enabled the satisfactory determination of chlorine and bromine in a variety of challenging matrices, for example in waste oils[51] as well as in milk samples.[52]

1.3.3.3 Electrospray ionization mass spectrometry

Mass spectrometry techniques have become powerful tools for studying inorganic systems.[53] Most notable is the ESI (Electrospray Ionisation) ionisation technique; a method which is still relatively new for the characterization of inorganic complexes. This ‘soft’ ionisation method generates mass spectral data relating to the composition of the original sample in an accurate and intuitive manner.[53-56] The rapid growth in the use of ESI-MS is testament to the ability of this technique to solve complex analytical problems in organometallic and coordination chemistry, exemplified by several recent studies using ESI-MS to elucidate the structure and mechanism of a range of Pd, Ru and Rh catalysed reactions.[57-60] Moreover, the interaction of Pt^{II} with proteins

and oligonucleotides as well as the speciation of several Pt anti-tumor complexes with such molecules have been studied by ESI-MS.[61-63]

However, the study of PGMs as anionic halide complexes by ESI-MS has been limited to date. One such study by Henderson *et al* investigated the direct infusion of the $[PtCl_6]^{2-}$ species as a function of cone voltage.[53] It was noted that even at a low cone voltage (20 V) the $[PtCl_6]^{2-}$ species exhibited a high degree of fragmentation, yielding besides the molecular ion, $[PtCl_6]^{2-}$, and a potassium adduct, $[KPtCl_6]^-$, and ions such as $[PtCl_5]^-$, $[PtCl_4]^-$ and $[PtCl_3]^-$. These platinum complexes are formed in the gas phase and range from the unusual Pt^{III} and Pt^{I} oxidation states present in the form of $[Pt^{III}Cl_4]^-$ and $[Pt^{I}Cl_2]^-$, respectively, to the well-known 'stable' Pt^{II} oxidation state in the form of a $[Pt^{II}Cl_3]^-$ species. By raising the cone voltage, the molecular ion and $[M+K]^-$ adduct were no longer observed and the lower oxidation state (III, II and I) Pt species abundance increased in a 'stepwise' manner.[53]

The successful analysis of transition metal complexes by direct infusion ESI-MS thus shows much promise, although the complexity and 'interferences' associated with more complicated multi-component samples necessitates the separation of target species prior to ESI-MS analysis. Liquid phase chromatographic separations are especially suited to this task due to the wide range of analyte polarities and molecular mass range covered with for example normal- and reversed phase HPLC.[64] As with many Pt-related studies in the literature, the use of LC-ESI-MS has predominantly focused on the analysis of Pt^{II} based anti-tumor complexes.[65-67]

1.3.4 Separation and chromatographic methods for the speciation of PGMs

In highly acidic chloride-rich solutions the PGMs will exist as relatively kinetically inert anionic $[MCl_x]^{n-x}$ complexes as well as aquated, $[MCl_x(H_2O)_{6-x}]^{n-x}$, and oxo species, $[M_2OCl_x(H_2O)_{10-x}]^{n-x-2}$, where M is the metal, *n* is the oxidation state of the metal, and *x* varies between 4 and 10, Table 1.1.[10,68,69]

Table 1.1 PGM species found in aqueous chloride media[10]

Ruthenium		Rhodium		Palladium	
Ru^{III}	$[RuCl_6]^{3-}$ $[RuCl_5(H_2O)]^{2-}$ $[RuCl_4(H_2O)_2]^{-}$ $[RuCl_3(H_2O)_3]$	Rh^{III}	$[RhCl_6]^{3-}$ $[RhCl_5(H_2O)]^{2-}$ $[RhCl_4(H_2O)_2]^{-}$	Pd^{II}	$[PdCl_4]^{2-}$
Ru^{IV}	$[RuCl_6]^{2-}$ $[Ru_2OCl_{10}]^{4-}$ $[Ru_2OCl_8(H_2O)_2]^{2-}$	Rh^{IV}	$[RhCl_6]^{2-}$	Pd^{IV}	$[PdCl_6]^{2-}$
Osmium		**Iridium**		**Platinum**	
Os^{IV}	$[OsCl_6]^{2-}$	Ir^{III}	$[IrCl_6]^{3-}$ $[IrCl_5(H_2O)]^{2-}$ $[IrCl_4(H_2O)_2]^{-}$	Pt^{II}	$[PtCl_4]^{2-}$
		Ir^{IV}	$[IrCl_6]^{2-}$	Pt^{IV}	$[PtCl_6]^{2-}$

The chromatographic separation of the PGMs has therefore largely focused on the separation of these anionic metal-chlorido complexes from each other.[10] Such separations were achieved in 1989 using gel permeation chromatographic media such as Sephadex® and Biogel® using 1 M hydrochloric acid as eluant.[10] This chromatographic method succeeded in separating the divalent chlorido complexes of Ru^{IV}, Rh^{IV}, Pd^{II}, Pt^{IV}, Ir^{IV} and Os^{IV}.[10] However, uncertainties in the species assignment as well as attempts to use such separations on a large scale brought about the introduction of the Toyopearl® chromatographic media, which focused on the separation of a reduced PGMs feed to avoid uncertainties in the assignment of the observed peaks.[10] High efficiency separations using materials designed for gel permeation chromatography is, however, not possible.

The separation of species resulting from an individual PGM has seldom been reported in the literature. Depending on the acidity, temperature, halide and PGM concentration, and the "age" of the solutions, several $[MCl_n(H_2O)_{6-n}]^{4-n}$ ($n = 4 – 6$) and $[MCl_{6-n}(OH)_n]^{2-}$ ($n = 0 – 6$) species can occur in solution.[70] Additionally, in the presence of two different halides, X and Y, mixed halide complexes of the general form $[MX_{6-n}Y_n]^{2-}$ ($n = 0 – 6$) are formed, which can undergo further aquation and hydrolysis reactions, resulting in a multitude of possible complex species.[28]

Capillary zone electrophoresis (CZE) is increasingly being used in PGMs speciation studies owing to the favourable speed of analysis and high resolution separation capacity.[71] Recently Sastre *et al* succeeded in separating $[PtCl_6]^{2-}$ and $[PdCl_4]^{2-}$ in a 0.01 M HCl matrix, as well as a third peak, which they ascribed to be the mono-aquated $[PtCl_5(H_2O)]^-$ species.[72] CZE studies of Rh^{III} in various acidic halide-rich solutions have shown the existence of several species present in solution during aquation processes.[73-75] Among these studies, Timerbaev *et al* proposed the characterization of the $[RhCl_2(H_2O)_4]^+$, $[RhCl_3(H_2O)_3]$, $[RhCl_4(H_2O)_2]^-$ and $[RhCl_3(OH)(H_2O)_2]^-$ species, resulting from the aquation of $RhCl_3{\cdot}3H_2O$ in a 0.1 M HCl matrix. In a similar study undertaken by Salvadó *et al* it is proposed that at least five Rh species are formed during aquation, including several chlorido- or oxygen-bridged oligomers of Rh^{III}, [76] whereas at equilibrium either $[RhCl_3(H_2O)_3]$ or $[RhCl_2(H_2O)_4]^+$ were found to be the predominant species present in addition to $[RhCl_4(H_2O)_2]^-$. CE has also been utilized by the same research group for the speciation of Ir^{IV} complexes formed during the aquation and hydrolysis of $[IrCl_6]^{2-}$.[77] With this method, the formation of at least seven species were observed, including several Ir^{III} species. The authors allude to the presence of dimers, attributing additional 'unknown' peaks to aquated species bonded by hydroxo bridges.[77] Detection of species prevalent during reactions such as aquation or hydrolysis would normally be impossible using conventional methods (UV-VIS spectroscopy), but with prior separation by means of CZE, the study of such species is made possible. However, the tedious processes involved in obtaining optimal separation conditions in CZE, the difficulty of finding the best peak shapes for quantification of species and unambiguous characterization of peaks, imply that much development in this area is still necessary.[71]

The use of ion-exchange chromatography was proposed by Preetz *et al*,[27] in which [(diethylamino)-ethyl] cellulose (DEAE cellulose) was used as stationary phase. Mobile phases typically consisted of 2 M acids or salt solutions to suppress hydrolysis of mixed ligand PGM complex anions. The chromatographic separation, largely dependent on the effective charge and size of the species, made it possible to separate even some stereoisomers, for example the *cis*- and *trans*-$[OsI_4Cl_2]^{2-}$, $[OsI_2Cl_4]^{2-}$ and *mer*- and *fac*-$[OsI_3Cl_3]^{2-}$ species present in the $[OsI_{6-n}Cl_n]^{2-}$ (n = 0 – 6) series. After successful separation of a mixture, the cellulose was removed from the column, whereupon the zones containing each individual species could be cut out and gathered by displacement elution. In this manner, Preetz succeeded in separating a variety of

hexahalogeno metalates, including the $[OsI_{6-n}Cl_n]^{2-}$ and $[PtCl_{6-n}F_n]^{2-}$ (n = 0 – 6) series.[27] This method is however tedious and involves excessively long analysis times.

Studies by Lederer *et al* using adsorption and anion exchange thin layer chromatography as well as thin layer electrophoresis have led to the successful separation of the series of anionic complexes formed when $[PtCl_6]^{2-}$ is reacted with SCN^-, $[PtCl_{6-n}SCN_n]^{2-}$ (n = 0 – 6).[78] The three sets of stereoisomers prevalent in this series could however only be separated as 3 bands without distinct separation between the individual stereoisomer species.[78] Work done by the same authors on the aquation of Pt^{II} displayed the formation of three distinct peaks ascribed to the $[PtCl_2(H_2O)_2]$, $[PtCl_3(H_2O)]^-$ and $[PtCl_4]^{2-}$ species,[79] and when a solution of $[PtCl_4]^{2-}$ was treated with varying concentrations of KBr solution (0.05 – 0.5 M), 5 peaks were observed assigned to the $[PtCl_{4-n}Br_n]^{2-}$ (n = 0 - 4) species.[79] Separation of the stereoisomer species, *cis*-and *trans*-$[PtCl_2Br_2]^{2-}$, could not be achieved, these species eluted as a single peak.[79] Thin layer chromatography is useful in separating several Pt species, however, the inability to resolve stereoisomer species and to quantify individual Pt anionic complexes limits this method to purely qualitative analyses.

High performance liquid chromatography (HPLC) was considered to be a practical alternative to overcome the inadequate separation efficiencies and quantification difficulties experienced by other methods. Nachtigall *et al* showed that the separation of $[PtCl_6]^{2-}$ and $[PtCl_4]^{2-}$ was possible by means of ion chromatography and also successfully separated the hydrolysis products arising from both these Pt oxidation states, $[PtCl_5(H_2O)]^-$ and $[PtCl_3(H_2O)]^-$.[81] In 1983 Müller *et al* attempted the separation of the mixed bromido-chlorido osmates^{IV}, using a 25 cm column packed with DEAE silica gel (i. d = 4.6 mm, particle size 0.005 mm). Detection in this HPLC separation was performed by means of UV-VIS spectroscopy.[82] This method was successful in separating the $[OsCl_{6-n}Br_n]^{2-}$ (n = 0 – 6) complex anions, however, each stereoisomer pair eluted as a single peak. Later in 1987 Müller, together with Obergfell, developed a HPLC method in which a 25 cm Nucleosil 10 Anion column was used to study the separation of the mixed chlorido-fluorido-osmates^{IV}. This resulted in separation of all the species, including those associated with the stereoisomers.[83] Characterization and detection of the separated species in this study was done by considering the UV-Vis spectra of each individual species obtained by photodiode array (PDA) detection and comparing them to spectra obtained by Preetz in previous studies.[83] In this manner, it was established that the *cis* and *fac* stereoisomers of the $[OsCl_{6-n}F_n]^{2-}$ (n = 0 – 6) series elute

faster than their corresponding *trans* and *mer* congeners.[83] Nevertheless, assignment of stereoisomers in a $[MX_{6-n}Y_n]^{2-}$ (n = 0 – 6) series should be treated with care, as this requires a truly unambiguous method of characterization. This can be illustrated when considering the elution order reported by Preetz for the $[OsI_{6-n}Cl_n]^{2-}$ (n = 0 – 6) series, in which it was found that the *trans* and *mer* stereoisomers elute faster than their corresponding *cis* and *fac* congeners, an elution order which is contrary to that reported for the $[OsF_{6-n}Cl_n]^{2-}$ (n = 0 – 6) series.[83] In 1998 Müller successfully separated the mixed fluorido-chlorido- and fluorido-bromido-rhenates^{IV} including their possible stereoisomers. The assignment of these stereoisomers was not confirmed, but rather inferred to be consistent with similar mixed halide series studied previously.[84] The assignment of stereoisomers must thus remain tentative and should be confirmed experimentally for each individual series in the event that this needed.

Ion-pairing reversed phase HPLC (IP-RP-HPLC) studies have thus far focused on the separation of PGMs, coordinated to a variety of ligands, from each other. Sommer *et al* succeeded in separating Rh^{III}, Ir^{III}, Ru^{III}, Pd^{II}, P^{II}, Os^{IV}, Pt^{IV} and Au^{III} as their bromide complexes using hexadecyltrimethylammonium bromide, CTMA, (0.002 M) as ion pairing reagent on a C18 stationary phase using either methanol or acetonitrile as organic modifiers.[85] The anionic PGM-chelates of the chelones; imino-diacetic (IDA), nitrotriacetic (NTA), ethylendiamine tetraacetic (EDTA) and cyclohexanediamine tetraacetic (CDTA) acids were separated using tetrabutylammonium (TBA) or CTMA bromides as ion pairing reagents,[86-88] but results were not entirely satisfactory. Nonetheless, the Pd^{II} CDTA chelates were successfully separated from the other PGMs and transition metals present in a synthetic solution.[87] A number of N-thiazolylazo dyes were used for the separation of PGMs using RP-HPLC on C18 or C8 silica in the presence of ion pairing reagents such as CTMA and TBA bromide. These include 4-(2-Thiazolylazo) resorcinol[89,90] and 2-(2-Thiazolylazo)-5-diethyl-aminophenol,[91] which were used to separate Rh^{III}, Ru^{IV}, Os^{IV} and Cu, and Rh^{III}, Pt^{II}, Pd^{II} and Ru^{IV}, respectively. However, chelation assisted chromatography is a cumbersome process leading to additional complicated equilibria involving derivatization of the PGMs prior to anylsis.[71] The abovementioned ion-pairing HPLC methods focused on the fractionation of PGMs from each other. Separation of individual species resulting from a single PGM using ion-pairing chromatography is limited to a recent study in which the $[RhCl_n(H_2O)_{6-n}]^{3-n}$ (n = 0 - 6) species were separated.[44] No chelation derivatization step was necessary and quantification of the relevant species was achieved by hyphenation to ICP-MS.

This method represents a significant improvement on earlier ion-pairing methods and served as the initial inspiration for the methods developed in this thesis.

1.4 Research objectives and thesis outline

The aim of the research compiled in this thesis is the development of methods for the separation, quantification and characterization of platinum complexes present at low concentrations (<50 mM) in acidic, halide rich (Cl^- and Br^-) solutions of interest to the PGMs recovery industry. Depending on the halide concentration and solution pH several mixed ligand species such as $[PtCl_{6-n}(H_2O)_n]^{n+2-}$ (n = 0 – 6), $[PtCl_{6-n}(OH)_n]^{2-}$ (n = 0 – 6), $[PtCl_{6-n}Br_n]^{2-}$ (n = 0 – 6), $[PtCl_{5-n}Br_n(H_2O)]^-$ (n = 0 – 5) and $[PtCl_{4-n}Br_n(H_2O)_2]$ (n = 0 – 4) may exist in solution in varying quantities. Using the methods proposed in the literature (section 1.3) will not meet the necessary requirements. It is in this regard that a simple and robust ion-pairing RP-HPLC method capable of analyzing such complex solutions is developed. This method is at the core of an analytical technique exploiting the detection capabilities of high resolution ^{195}Pt NMR, UV-Vis, ICP-MS/OES and high resolution electrospray ionization quadrupole time-of-flight mass spectrometry (ESI-Q-TOF-MS).

Therefore the specific objectives of this study are:

i. To develop an ion-pairing chromatographic method for the separation, characterization and quantification of mixed chlorido-bromido $Pt^{II/IV}$ anionic complexes, $[PtCl_{6-n}Br_n]^{2-}$ (n = 0 – 6) and $[PtCl_{4-n}Br_n]^{2-}$ (n = 0 – 4), in dilute solutions for which ^{195}Pt NMR spectroscopy is not sufficiently sensitive.

ii. To investigate ion-pairing chromatography coupled to ICP-OES as a method to characterize and quantify the mixed chlorido-bromido Pt^{IV} complexes, $[PtCl_{6-n}Br_n]^{2-}$ (n = 0 – 6), by directly determining the metal to halide ratios of separated species.

iii. To extend this chromatographic method to the separation and characterization of the mono-aquated $[PtCl_{5-n}Br_n(H_2O)]^-$ (n = 0 – 5) complexes, which are evident in the ^{195}Pt NMR spectra of concentrated solutions, by using the high sensitivity of ESI-Q-TOF-MS.

iv. To investigate the associated thermodynamic parameters, in particular the relative stepwise equilibrium constants, for the $[PtCl_{6-n}Br_n]^{2-}$ (n = 0 – 6) complexes using the developed ion-pairing chromatographic method.

In **Chapter 2** the development of an ion-pairing RP-HPLC method using tetrabutylammonium chloride (TBA^+Cl^-) is outlined and its successful application to the separation of the $[PtCl_{6-n}Br_n]^{2-}$ (n = 0 – 6) and $[PtCl_{4-n}Br_n]^{2-}$ (n = 0 – 6) complex anions, including the stereoisomers , is described. ^{195}Pt NMR of more concentrated solutions ($[Pt]_T$ = 0.1 M) is used to validate the chromatographic peak assignments, particularly in the case of the Pt^{II} and Pt^{IV} chlorido-bromido stereoisomer species. Hyphenation of the developed ion-pairing HPLC method to ICP-MS/OES enables the quantification of all the above mentioned species.

The difficulty associated with synthesizing individual mixed-halide Pt species suggests that the resulting product will most likely contain a mixture of two or more species.[27] The use of 'standard solutions' in an attempt to identify elution bands observed in a chromatogram is thus problematic. On the other hand, separation of complexes and subsequent fraction collection in order to be analyzed in an off-line capacity is time consuming. Previous studies[26,28] have shown that high resolution ^{195}Pt NMR is highly effective for the *in situ* analysis of several mixed-ligand Pt complexes, but this method requires relatively concentrated Pt solutions (>50 mM) and is limited to NMR-active nuclei. Furthermore, unknown species present in low concentrations can go undetected by this method. A method that can be used to characterize and quantify such complexes in dilute solutions is thus necessary. In **Chapter 3** the development of a novel method by which the metal to halide ratios of separated species is directly determined by means of HPLC-ICP-OES is introduced. This allows for unambiguous characterization of mixed-halide Pt species. The $[PtCl_{6-n}Br_n]^{2-}$ (n = 0 – 6) anionic complexes are analyzed as a proof-of-concept study using the capabilities of the Spectro Arcos ICP-OES, which is capable of detecting the most intense spectral lines for chlorine and bromine in the vacuum ultraviolet range (125-180 nm). The quantification of individual ligands and metals comprising a coordination complex after its separation from similar species represents a novel manner in which to characterize such complexes.

The use of metal to halide ratios to characterize peaks observed in a chromatographic separation were shown to be effective.[93] However, the relatively low sensitivity of the Cl

(134.742 nm) and Br (148.845 nm) emission lines (limits of detection for Cl and Br, 0.67 and 0.29 mmol L^{-1}, respectively), prevents characterization of species present in low abundance. Furthermore, the destructive nature (in terms of molecular structure) of the plasma (temperature = ±10 000 ºC) used in ICP-OES implies that no further structural information pertaining to the relevant complex can be extracted, negating the ability to characterize compounds. In order to obtain structural data of species present in relatively low abundance, such as the mono-aquated $[PtCl_{5-n}Br_n(H_2O)]^-$ (n = 0 – 5) and di-aquated $[PtCl_{4-n}Br_n(H_2O)]$ (n = 0 – 4) anionic complexes, mass spectrometry can be used as detection method. In **Chapter 4** the modification of the developed ion-pairing LC method to facilitate hyphenation to high resolution ESI-Q-TOF-MS is introduced. This entails the use of the volatile ion-pairing reagent, tributylamine, and the chromatographic efficiency of ultra high performance LC (UHPLC). The optimized UHPLC-ESI-Q-TOF-MS method is firstly applied to the proof-of-principle study of the $[PtCl_{6-n}Br_n]^{2-}$ (n = 0 – 6) anionic complexes. The UHPLC-ESI-Q-TOF-MS method is then used to characterize the mono-aquated species $[PtCl_{5-n}Br_n(H_2O)]^-$ (n = 0 – 5) at concentrations much lower than would be possible using ligand to metal ratios. The overarching objective of eventual quantification of the $[PtCl_{5-n}Br_n(H_2O)]^-$ (n = 0 – 5) species by means of HPLC-ICP-OES using the 214.423 nm Pt emission line forms part of future work.

The scope of the study is then widened in **Chapter 5** as the stepwise equilibrium constants (Diagram 1.1) of the $[PtCl_{6-n}Br_n]^{2-}$ (n = 0 – 6) anionic complexes are determined using the developed ion-pairing RP-HPLC method. These experimentally obtained and validated stepwise equilibrium constants are used to elucidate the thermodynamic driving force for the stepwise substitution of Cl^- in $[PtCl_6]^{2-}$ by Br^- to ultimately yield $[PtBr_6]^{2-}$ in aqueous solutions.

This work is compiled in a manuscript[95] in conjunction with quantum computational chemistry (wave functional theory (WFT) and density functional theory (DFT)) calculations performed by the co-authors, Dr. W. J. Gerber and D. M. E. van Niekerk. Herein the aim is to evaluate whether current quantum computational calculations can accurately determine Gibbs free energies, ΔG^o_{rxn}, for the $[PtCl_{6-n}Br_n]^{2-}$ (n = 0 – 6) anionic complexes with the objective of applying these techniques to experimentally more challenging or unobtainable systems for e.g. the $[PtI_{6-n}Br_n]^{2-}$ (n = 0 – 6) anionic complexes.

The work in certain chapters in this thesis (**Chapters 2 and 3**)[92,93] has already been published whilst that in others have been submitted for publication (**Chapters 4 and 5**).[94,95]

1.5 References

1. T. Naldrett, J. Kinnaird, A. Wilson, G. Chunnett, *Earth Science Frontiers*, **2008**, 15(5): 264.
2. R. G. Cawthorn, *Platinum Metals Review*, **2010**, *54*, 205.
3. J. M. Ryder, K. Dymock, *Recycling of metalliferrous materials*, IMM, London, **1990**, p. 255.
4. G. Ertl, H. Knözinger, F. Schüth, J. Weitkamp, *Handbook of Heterogeneous Catalysis*, Wiley-VCH, Weinheim, 2nd edn, **2008**, pp. 37-56.
5. J. Smidt, W. Hafner, R. Jira, J. Sedlmeier, R. Sieber, H. Kojer, R. Rüttinger, *Angewandte Chemie*, **1959**, *71*, 176.
6. G. L. Selman, R. W. Rushforth, *Platinum Metals Review*, **1971**, *18*, 84.
7. F.A Lewis, *Platinum Metals Review*, **1982**, *26*, 20.
8. F.A Lewis, *Platinum Metals Review*, **1982**, *26*, 70.
9. F.A Lewis, *Platinum Metals Review*, **1982**, *26*, 121.
10. R. A. Grant, F. L. Bernardis, D. C. Sherrington, *Reactive & Functional Polymers*, **2005**, *65*, 205.
11. O. Balaj, I. Balteanu, T. Rossteucher, M. Beyer, V. Bondybey, *Angewandte Chemie, International Edition*, **2004**, *43*, 6519.
12. Platinum series, Johnson Matthey, London, UK, Published annually since **1985**.
13. S. Hann, E. Helmers, K. Hoppstock, G. Koellensperger, S. Parry, S. Rauch, M. Rossbach, *Nuclear Analytical Methods for Platinum Group Metals*, ISBN 92-0-102405-3, **2005.**
14. D. Jollie, *Platinum 2010*, Johnson Matthey PLC, Royston, UK, **2010**, p. 54.
15. R.J. Seymore, J.I. O'Farrelly, L.C. Potter, (**1998**). *Encyclopedia of Chemical Technology* (fourth ed.)New York, John Wiley & Sons.
16. H. Zhang, M. Jin, Y. Xia, *Chemical Society Reviews*, **2012**, DOI: 10.1039/c2cs35173k.
17. S. Gambarini. "*Continued SA labour troubles keep Platinum in focus*" BulliomStreet. Ed. P. J. George. 2012. Commodity Online India Limited. 23 August 2012. <http://www.bullionstreet.com/news>
18. R. Clough, L. R. Drennan-Harris, C. F. Harrington, S. J. Hill, J. F. Tyson, *Journal of Analytical Atomic Spectrometry*, **2012**, *27*, 1185.
19. W.C. Wolsey, C.A Reynolds, Kleinberg, *Journal of Inorganic Chemistry*, **1963**, *2*, 463.
20. L. I. Elding, A. Groning, *Chemica Scripta*, **1977**, *11*, 8.
21. L. I. Elding, L. Gustafson, *Inorganica Chimica Acta*, **1976**, *19*, 31.
22. L. I. Elding, L. Gustafson, *Inorganica Chimica Acta*, **1977**, *22*, 201.
23. L. I. Elding, L. Drougge, *Inorganica Chimica Acta*, **1986**, *121*, 175.
24. L. I. Elding, *Inorganica Chimica Acta*, **1978**, *28*, 255.
25. W. Robb, G. M. Harris, *Journal of the American Chemical Society*, **1965**, *87*, 4472.
26. K. R. Koch, J. Kramer, *Inorganic Chemistry*, **2006**, *45*, 7843.
27. G. Peters, W. Preetz, D. Bublitz, *Chemical Reviews*, **1996**, *96*, 977.
28. K. R. Koch, M. R. Burger, J. Kramer, A. N. Westra, *Dalton Transactions*, **2006**, *27*, 3277.
29. O. Gröning, L. I. Elding, Inorganic Chemistry, **1989**, *28*, 3366.
30. S. J. S. Kerrison, P. J. Sadler, *Journal of the Chemical Society, Dalton Transactions*, **1982**, *12*, 2363.
31. K. R. Koch, J. Kramer, *Inorganic Chemistry*, **2007**, *46*, 7466.

32. W. J. Gerber, P. Murray, K. R. Koch, *Dalton transactions*, **2008**, 4113.
33. N. S. Mokgalaka, T. Wondimu, R. I. McCrindle, *Journal of Analytical Atomic Spectrometry*, **2004**, *19*, 1493.
34. J. S. Becker, D. Becker, D. Bellis, I. Staton, C. W. McLeod, J. Dombovari, J. S. Becker, *Fresenius Journal of Analytical Chemistry*, **2000**, *368*, 490.
35. A. R. Timerbaev, *Chemical Reviews*, **2012**, Advanced Article.
36. W.R.L. Cairns, L. Ebdon, S.J. Hill, *Analytical Proceedings Including Analytical Communications*, **1994**, *31*, 295.
37. W. A. J. De Waal, F. J. M. J. Maesssen, J. C. Kraak, *Journal of chromatography*, **1987**, *407*, 253.
38. S. Hann, Zs. Stefánka, K. Lenz, G. Stingeder, *Analytical and Bioanalytical Chemistry*, **2005**, *381*, 405.
39. D. Klueppel, N. Jakubowski, J. Messerschmidt, D. Stuewer, D. Klockow, *Journal of Analytical Atomic Spectrometry*, **1998**, *13*, 255.
40. V. Nischwitz, B. Michalke, A. Kettrup, *Journal of Chromatography A*, **2003**, *1016*, 223.
41. S. Lustig, B. Michalke, W. Beck, P. Schramel, *Fresenius Journal of Analytical Chemistry*, **1998**, *360*, 18.
42. Q. Tu, T. Wang, C. J. Welch, P. Wang, X. Jia, C. Raab, X. Bu, D. Bykowski, B. Hohenstaufen, M. P. Doyle, *Analytical Chemistry*, **2006**, *78*, 1282.
43. Q. Tu, T. Wang, C. J. Welch, *Journal of Pharmaceutical and Biomedical Analysis*, **2010**, *51*, 90.
44. W. J. Gerber, K. R. Koch, H. E. Rohwer, E. C. Hosten, T. E. Geswindt, *Talanta*, **2010**, *82*, 348.
45. G.F. Kirkbright, A. F. Ward, T. S. West, *Analitica Chimica Acta*, **1972**, *62*, 241.
46. D. R. Heine, J. S. Babis, M. B. Denton, *Applied Spectrscopy*, **1980**, *34*, 595.
47. T. Hayakawa, F. Kikui, S. Ikeda, *Specrtochimica Acta*, **1982**, *37B*, 1069.
48. T. Uehiro, M. Morita, K. Fuwa, *Analytical Chemistry*, **1985**, *57*, 1079.
49. O. Schulz, P. Heitland, *Fresenius Journal of Analytical Chemistry*, **2001**, *371*, 1070.
50. I. B. Brenner, A. T. Zander, *Spectrochimica Acta Part B*, **2000**, *55*, 1195.
51. K. Krengel-Rothensee, U. Richter, P. Heitland, *Journal of Analytical Atomic Spectrometry*, **1999**, *14*, 699.
52. J. Naozuka, M. A. Mesquita Silva da Veiga, P. Vitoriano Oliveira, E. de Oliveira, *Journal of Analytical Atomic Spectrometry*, **2003**, *18*, 917.
53. W. Henderson, J. S. McIndoe, (2005). *Mass Spectrometry of Inorganic, Coordination and Organometallic Compounds: Tools-Techniques-Tips*. John Wiley & Sons.
54. J. A. Loo, H. R. Udseth, R. D. Smith, J. H. Futrell, *Rapid Communications in Mass Spectrometry*, **1988**, *2*, 207.
55. P. L. Mauri, L. Lemoli, C. Gardana, P. Riso, P. Simonetti, M. Porrini, P. G. Pietta, *Rapid Communications in Mass Spectrometry*, **1999**, *13*, 924.
56. S. F. Wong, C. K Meng, J. B. Fenn, *Journal of Physical Chemistry*, **1988**, *92*, 546.
57. H. Wang, J. Metzger, *Organometallics*, **2008**, *27*, 2761.
58. D. Harakat, J. Muzart, J. Le Bras, *RSC Advances*, **2012**, *2*, 3094.
59. D. Agrawal, D. Schröder, C. M. Frech, *Organometallics*, **2011**, *30*, 3579.
60. H. Wang, Y. Li, R. Zhang, K. Jin, D. Zhao, C. Duan, *The Journal of Organic Chemistry*, **2012**, *77*, 4849.
61. M. Galanski, B. K. Keppler, *Inorganica Chimica Acta*, **2000**, *300*, 783.

62. K. G. Samper, C. Vicente, V. Rodríguez, S. Atrian, N. Cutillas, M. Capdevila, J. Ruiz, Ò. Palacios, *Dalton transactions*, **2012**, *41*, 300.

63. A. Zayed, G. D. D. Jones, H. J. Reid, T. Shoeib, S. E. Taylor, A. L. Thomas, J. P. Wood, B. L. Sharp, *Metallomics*, **2011**, *3*, 991.

64. E. Rosenberg, *Journal of Chromatography A*, **2003**, *1000*, 841.

65. S. Mowaka, M. Ziehe, D. Mohamed, U. Hochkirch, J. Thomale, M. W. Lincheid, *Journal of Mass Spectrometry*, **2012**, *47*, 1282.

66. M. Cui, Z. Mester, *Rapid Communications in Mass Spectrometry*, **2003**, *17*, 1517.

67. R. B. Burns, R. W. Burton, S. P. Albon, L. Embree, *Journal of Pharmaceutical and Biomedical Analysis*, **1996**, *14*, 367.

68. B. K. Leung, M.J. Hudson, *Solvent Extraction and Ion Exchange*, **1992**, *10*, 173.

69. E. Benguerel, G.P. Demopoulos, *Hydrometallurgy*, **1996**, *40*, 135.

70. T. M. Buslaeva, S.A. Simanova, *Russian Journal of Coordination Chemistry*, **1999**, *25*, 151.

71. R. Vlasankova, L. Sommer, *Chromatographia*, **2000**, *52*, 692.

72. B. Baraj, A. Sastre, M. Martínez, K. Spahiu, *Analytica Chimica Acta*, **1996**, *319*, 191.

73. S.S. Aleksenko, A.P. Gumenyuk, S.P. Mushtakova, L.F. Kozhina, A.R. Timerbaev, *Talanta*, **2003**, *61*, 195.

74. S.S. Aleksenko, A.P. Gumenyuk, S.P. Mushtakova, L.F. Kozhina, A.R. Timerbaev, *Journal of Analytical Chemistry*, **2002**, *57*, 215.

75. S.S. Aleksenko, A.P. Gumenyuk, S.P. Mushtakova, A.R. Timerbaev, *Fresenius Journal of Analytical Chemistry*, **2001**, *370*, 865.

76. M. Hidalgo, J.M. Sánchez, J. Havel, V. Salvadó, *Talanta*, **2002**, *56*, 1061.

77. J.M Sànchez, V. Salvadó, J. Havel, *Journal of Chromatography A*, **1999**, *834*, 329.

78. M. Lederer, E. Leipzig-Pagani, *Analytica Chimica Acta*, **1999**, *391*, 315.

79. M. Lederer, E. Leipzig-Pagani, *Analytica Chimica Acta*, **1997**, *350*, 203.

80. M. Lederer, E. Leipzig-Pagani, T. Lumini, *Analytica Chimica Acta*, **1998**, *371*, 279.

81. D. Nachtigall, S. Artelt, G. Wunsch, *Journal of Chromatography A*, **1997**, *775*, 197.

82. H. Müller, P. Bekk, *Fresenius Journal of Analytical Chemistry*, **1983**, *314*, 758.

83. P. Obergfell, H. Müller, *Fresenius Journal of Analytical Chemistry*, **1987**, *328*, 242.

84. W. Preetz, Z. Erlhofer, *Naturforsch*, **1989**, *44b*, 1185.

85. J. Doležal, L. Sommer, *Collection of Czechoslovak Chemical Communications*, **1997**, *62*, 1029.

86. E. M. Basova, L. G. Bondareva, V. M. Ivanov, *Zhurnal Analiticheskoi Khimii*, **1992**, *47*, 1712.

87. E. M. Basova, V. M. Ivanov, L. G. Bondareva, *Zhurnal Analiticheskoi Khimii*, **1996**, *51*, 954.

88. E. M. Basova, L. G. Bondareva, V. M. Ivanov, *Zhurnal Analiticheskoi Khimii*, **1997**, *52*, 36.

89. E. M. Basova, T. A. Bol'shova, E. N. Shapovalova, V. M. Ivanov, *Zhurnal Analiticheskoi Khimii*, **1991**, *45*, 1947.

90. Q. Liu, H, Zhang, J. Cheng, *Talanta*, **1991**, *38*, 669.

91. E. N. Shapovalova, I. V. Mishenina, E. M. Basova, T. A. Bol'shova, O. A. Shpigun, *Zhurnal Analiticheskoi Khimii*, **1991**, *46*, 1503.

92. P-H. Van Wyk, W. J Gerber, K. R. Koch, *Analytica Chimica Acta*, **2011**, *704*, 154.

93. P-H. Van Wyk, W. J Gerber, K. R. Koch, *Journal of Analytical Atomic Spectrometry*, **2012**, *27*, 577.

94. P-H. Van Wyk, W. J Gerber, K. R. Koch, A. de Villiers, M. A. Stander, J. B. van Dyk, *Submitted For Publication*.

95. P-H. Van Wyk, W. J Gerber, K. R. Koch, D. M. E. van Niekerk, *Submitted For Publication*.

2

A robust method for the speciation, separation and photometric characterization of all $[PtCl_{6-n}Br_n]^{2-}$ (n = 0 - 6) and $[PtCl_{4-n}Br_n]^{2-}$ (n = 0 - 4) complex anions by means of ion-pairing RP-HPLC coupled to ICP-MS/OES, validated by high resolution ^{195}Pt NMR spectroscopy

---

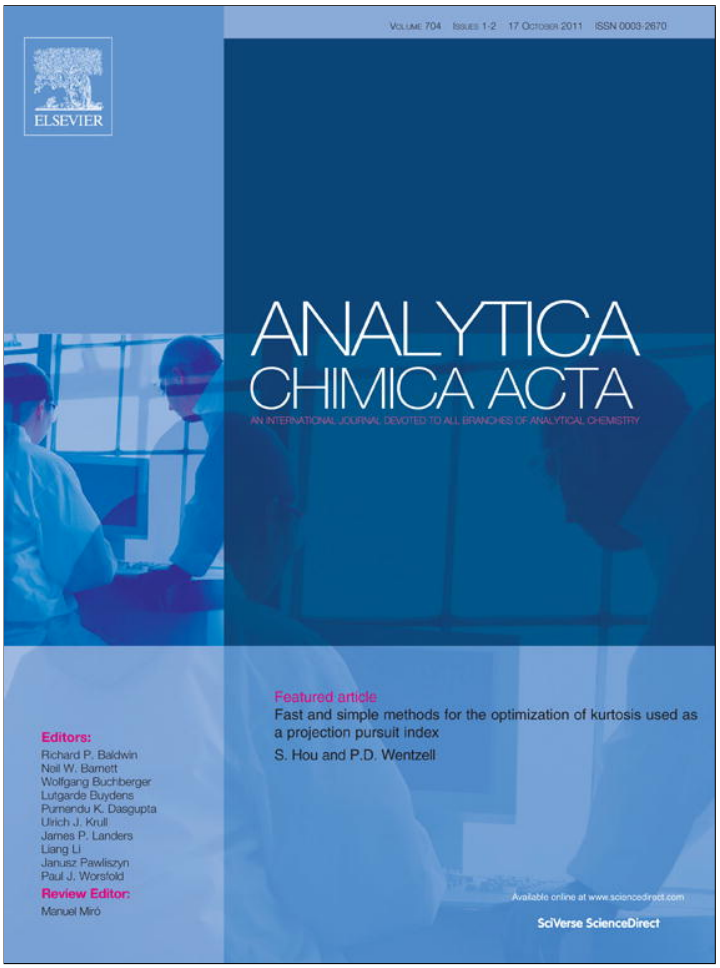

Analytica Chimica Acta 704 (2011) 154–161

Contents lists available at ScienceDirect

Analytica Chimica Acta

journal homepage: www.elsevier.com/locate/aca

A robust method for speciation, separation and photometric characterization of all $[PtCl_{6-n}Br_n]^{2-}$ (n = 0–6) and $[PtCl_{4-n}Br_n]^{2-}$ (n = 0–4) complex anions by means of ion-pairing RP-HPLC coupled to ICP-MS/OES, validated by high resolution ^{195}Pt NMR spectroscopy

Pieter-Hugo van Wyk, Wilhelmus J. Gerber, Klaus R. Koch*

Platinum Metals Chemistry Research Group, Department of Chemistry and Polymer Science, Stellenbosch University, Private Bag XI, Matieland 7602, South Africa

ARTICLE INFO

Article history:
Received 10 May 2011
Received in revised form 10 July 2011
Accepted 21 July 2011
Available online 28 July 2011

Keywords:
Speciation of $[PtCl_{6-n}Br_n]^{2-}$ (n = 0–6) and $[PtCl_{4-n}Br_n]^{2-}$ (n = 0–4) complex anions
Ion-pair Reversed Phase-HPLC coupled Inductively Coupled Plasma-Mass Spectrometry/Optical Emission Spectroscopy
^{195}Pt Nuclear Magnetic Resonance molar absorptivities of $[PtCl_{6-n}Br_n]^{2-}$ (n = 0–6) and $[PtCl_{4-n}Br_n]^{2-}$ (n = 0–4) complexes

ABSTRACT

A robust reversed phase ion-pairing RP-HPLC method has been developed for the unambiguous speciation and quantification of all possible homoleptic and heteroleptic octahedral platinum^{IV} $[PtCl_{6-n}Br_n]^{2-}$ (n = 0–6) as well as the corresponding platinum^{II} $[PtCl_{4-n}Br_n]^{2-}$ (n = 0–4) complex anions using UV/Vis detection. High resolution ^{195}Pt NMR in more concentrated solutions of these Pt$^{II/IV}$ complexes (≥50 mM) served to validate the chromatographic peak assignments, particularly in the case of the possible stereoisomers of Pt$^{II/IV}$ complex anions. By means of IP-RP-HPLC coupled to ICP-MS or ICP-OES it is possible to accurately determine the relative concentrations of all possible Pt$^{II/IV}$ species in these solutions, which allows for the accurate determination of the photometric characteristics (λ_{max} and ε) of all the species in this series, by recording of the UV/Vis absorption spectra of all eluted species, using photo-diode array, and quantification with ICP-MS or ICP-OES. With this method it is readily possible to separate and estimate the concentrations of the various stereoisomers which are present in these solutions at sub-millimolar concentrations, such as *cis*- and *trans*-$[PtCl_4Br_2]^{2-}$, *fac*- and *mer*-$[PtCl_3Br_3]^{2-}$ and *cis*- and *trans*-$[PtCl_2Br_4]^{2-}$ for Pt^{IV}, and *cis*- and *trans*-$[PtCl_2Br_2]^{2-}$ in the case of Pt^{II}. All mixed halide Pt^{II} and Pt^{IV} species can be separated and quantified in a single IP-RP-HPLC experiment, using the newly obtained photometric molar absorptivities, ε, determined herein at given wavelengths.

1. Introduction

Worldwide production of the platinum group metals (PGM) has increased greatly in the last decade, with a gross demand for 7.04×10^6 oz for platinum in 2009; of the total annual production of 5.92×10^6 oz of platinum in that year, *ca* 76.5% of this originated from South Africa [1]. The amount of PGM recycled has also steadily increased over the last decade, accounting for some 20% of the worldwide Pt demand in 2009. In this context, the detailed understanding of the chemistry of these metals in the form of their chlorido-complexes [2] leading ultimately to the production of pure platinum-group metal, plays an indispensible role. The methods of large scale separation of the PGMs as their chlorido-complexes have recently been reviewed [3], the success and efficiency of which depend amongst other factors, critically on the chemical speciation [4] of the chlorido-complexes in acidic aqueous solutions. In their paper Bernardis et al. [3] however somewhat oversimplify the chemical speciation of *inter alia* platinum$^{II/IV}$ in "aqueous chloride media" referring only to $[PtCl_4]^{2-}$ or $[PtCl_6]^{2-}$, which is only strictly true in the presence of a *large excess* of Cl^- ions (usually as hydrochloric acid), relative to the PGM in solution. In the case of Pt^{IV}, being the usual oxidation state of this metal in which it is commercially separated, ^{195}Pt NMR has proven to be a powerful method with which to study the chemistry and speciation of for example the relatively kinetically inert mixed halide $[PtCl_{6-n}Br_n]^{2-}$ (n = 0–6) complexes as first described for very concentrated solutions by von Zelewsky more than four decades ago [5]. More recently Preetz et al. extensively examined the series $[PtX_{6-n}F_n]^{2-}$, X = Cl, Br and $[PtCl_{6-n}Br_n]^{2-}$ (n = 0–6) complexes *inter alia* by means of ^{195}Pt NMR [6]. We demonstrated recently that ^{195}Pt NMR chemical-shift "trend analysis" is a powerful tool for the rapid and unambiguous identification of *all* the possible $[PtCl_{5-n}Br_n(H_2O)]^-$ (n = 0–5) species in perchloric acid, which result as minor species due to the aquation of $[PtCl_{6-n}Br_n]^{2-}$ (n = 0–6) anions [7]. A subsequent ^{195}Pt NMR study extended to all possible, kinetically inert $[PtCl_{6-m-n}Br_m(OH)_n]^{2-}$ (m, n = 0–6)

* Corresponding author. Tel.: +27 21 808 3020; fax: +27 21 808 3342.
E-mail address: krk@sun.ac.za (K.R. Koch).

0003-2670/$ – see front matter © 2011 Elsevier B.V. All rights reserved.
doi:10.1016/j.aca.2011.07.037

complex anions including stereoisomers in alkaline solution, confirms the utility of ^{195}Pt NMR to solutions of potential commercial interest [8]. Based on the observable ^{35}Cl/^{37}Cl isotope effects in the ^{195}Pt NMR resonance of $[PtCl_6]^{2-}$ at higher magnetic fields (>9.4 T) first reported in 1978 by Sadler et al. [9], we recently developed a novel method for the rapid unambiguous identification of $[PtCl_n(H_2O)_{6-n}]^{4-n}$ (n = 4–6) complexes utilizing the unique *isotopologue* and *isotopomer* ^{195}Pt NMR shielding resolved for each individual species at high magnetic field, which serve as a unique ^{195}Pt NMR "fingerprint" for each chloride containing complex $[PtCl_n(H_2O)_{6-n}]^{4-n}$ (n = 4–6) [10]. Unfortunately, the relatively low absolute sensitivity (receptivity[1]) of ^{195}Pt NMR spectroscopy limits this direct spectroscopic method for speciation practically to total platinum complex concentrations of ~50 mM (~9.75 g Pt L^{-1}) or higher, particularly if minor species are the target of investigation. There is thus a need for a means of quantitative chemical speciation in more dilute solutions of Pt^{IV} complex anions in the sub-mM (≤500 mg Pt L^{-1}) concentration ranges. The actual concentrations in process solutions can vary widely depending on their origin, anywhere between 0.02 and >0.35 M, while effluent concentrations are significantly smaller by a factor of 10^2–10^3 or more.

Capillary zone electrophoresis (CZE) has been used for several PGM separation and speciation studies, which includes for example the separation of $[PtCl_6]^{2-}$ from $[PdCl_4]^{2-}$ [11], while Havel et al. have separated several Ir$^{III/IV}$ aqua chlorido-complexes by CZE [12].Capillary zone electrophoresis as a means of speciation of Rh^{III} complexes present in several acidic matrices *viz* HCl, HNO_3 and H_2SO_4 illustrates the existence of numerous Rh^{III} complexes, which were however difficult to assign unambiguously by means of their CZE characteristics alone [13–16]. Müller and Bekk succeeded in separating the hexabromido–chlorido complexes of osmium^{III} and rhenium^{III} utilizing columns packed with DEAE-silica gel, although the stereoisomers of all mixed $[MCl_{6-n}Br_n]^{2-}$ (M = Os, Re) and (n = 0–6) complexes eluted as a single peak [17]. Subsequently, Müller and Obergfell reported the separation of $[OsF_{6-n}Cl_n]^{2-}$ (n = 0–6) complexes using a Nucleosil-10 anion exchange column in a high performance liquid chromatographic (HPLC) system, including their possible stereoisomers [18]. The assignment of the latter stereoisomers by Müller and Obergfell must however be considered to be tentative, since this was based on the expectation that stereoisomers follow an elution order similar to systems such as $[PtCl_{6-n}F_n]^{2-}$ (n = 0–6) [19], an assumption which has been shown to be unreliable when comparing the variable elution order for stereoisomers of the $[OsI_{6-n}Cl_n]^{2-}$ (n = 0–6) and $[PtCl_{6-n}F_n]^{2-}$ (n = 0–6) complex anions using DEAE cellulose, as reported by Preetz et al. [20].

In this paper we report the development of a simple and robust ion-pairing reverse phase high-performance liquid chromatographic (IP-RP-HPLC) method with which the separation, characterization and quantification of all mixed halide complex anions of both $[PtCl_{4-n}Br_n]^{2-}$ (n = 0–4) and $[PtCl_{6-n}Br_n]^{2-}$ (n = 0–6) are easily achieved. Notably this includes the separation of all possible pairs of stereoisomers of these complexes. Detection of the eluted Pt^{II} and Pt^{IV} complex anions can be achieved routinely by means of UV–Vis absorption at 262 and 315 nm, or alternatively using a photo-diode array (PDA) detection system to enable the recording of the individual UV/Vis absorption characteristics (λ_{max} and ε) of all individual $[PtCl_{6-n}Br_n]^{2-}$ (n = 0–6) and $[PtCl_{4-n}Br_n]^{2-}$ (n = 0–4) complexes for the first time. Post-column coupling of the IP-RP-HPLC system to an inductively coupled plasma mass or optical emission spectrometer (ICP-MS/ICP-OES), allows for the accurate measurement of the concentration of all eluted platinum containing species, resulting in the estimation of reliable molar absorptivity, ε, values for all separable complex species not available in the literature. The unambiguous identification of all these species was validated by means of high resolution ^{195}Pt NMR in equilibrated solutions of higher concentration (100 mM in Pt), with particular attention to the stereoisomers *cis*- and *trans*-$[PtCl_4Br_2]^{2-}$, *fac*- and *mer*-$[PtCl_3Br_3]^{2-}$ and *cis*- and *trans*-$[PtCl_2Br_4]^{2-}$ for Pt^{IV} as reported previously [7,8], as well as the *cis*- and *trans*-$[PtCl_2Br_2]^{2-}$ isomers for Pt^{II} complexes.

2. Experimental

2.1. Reagents

HPLC grade acetonitrile was obtained from Merck (608-001-00-3). All aqueous solutions were prepared using ultrapure Milli-Q water (>18 MΩ). Analytical grade purity tetrabutyl-ammonium chloride (TBA^+Cl^-), sodium acetate and glacial acetic acid were obtained from Sigma–Aldrich.

Mobile phases were prepared by the addition of acetonitrile to stock solutions of 0.05 M tetrabutyl-ammonium chloride and 0.1 M acetate buffer (pH = 4.6) to give 48% (v/v) CH_3CN:H_2O solutions. All mobile phases were filtered through 0.45 μm HV filters (Millipore Corporation, HVLP04700) under vacuum and degassed for 15 min in an ultrasonic bath before use. $Na_2PtCl_6{\cdot}2H_2O$ (Johnson Matthey PLC, Precious Metals Division) was of analytical reagent grade quality and was dried in vacuo and stored in a desiccator prior to use.

2.2. High-performance liquid chromatography, with dual wavelength UV–Vis detection

Chromatographic separations were accomplished with a Varian Prostar liquid chromatograph equipped with a binary 210 solvent delivery module, a 410 auto-sampler with a 345 UV–Vis dual wavelength detector. The flow rate was set at 0.8 mL min^{-1} and the absorbance was measured at two fixed wavelengths at 262 and 315 nm. The column used throughout this study was a Microsorb C_{18}, 250 mm × 4.6 mm i.d., 5 μm particles. Column efficiency was tested by the injection of a solution comprising of acetophenone, phenol, aniline, caffeine, uracil, pyridine, benzene and 30% by volume acetonitrile. Column conditioning comprised of mobile phase passage through the column for 45 min prior to analysis followed by a 45 min post-analysis wash with pure acetonitrile.

Optimization of IP-RP-HPLC chromatographic separation conditions showed that the most important factors which influence the retention time (t_r) of anionic analytes in this ion-pair RP-HPLC chromatographic separation are the concentration of the ion pairing agent (TBA^+Cl^-) in the mobile phase and the eluent composition as the CH_3CN:H_2O (v/v) ratio. At a constant mobile phase composition (as CH_3CN:H_2O (v/v) ratio), increasing the TBA^+Cl^- concentration results presumably in an increased amount of ion pairing reagent partitioned into the stationary phase [21], leading to an approximately linear increase in capacity factor (k') [22] for all 10 $[PtCl_{6-n}Br_n]^{2-}$ (n = 0–6) species as shown in Fig. S-1a (supplementary data). We used acetonitrile as "organic modifier" in this separation, since methanol is known to result in the reduction of Pt^{IV} to Pt^{II} complexes [23,24]. As expected increasing the relative volume percentage of acetonitrile in the mobile phase from 33 to 55%, at a constant TBA^+Cl^- concentration of 9.0 mM, results in a decrease in capacity factor (k') for all 10 species shown in Fig. S-1b (supplementary data). In order to maintain a balance between analysis time and resolution, an optimum mobile phase composition of 9.0 mM TBA^+Cl^- and 48% (v/v) acetonitrile/water with a 0.01 M sodium acetate buffer (pH = 4.6) was chosen unless otherwise indicated.

[1] ^{195}Pt NMR receptivity is *ca* 19.1 normalized to ^{13}C NMR [7].

2.3. HPLC with photo-diode array detection

Electronic absorption spectra of each $Pt^{II/IV}$ chlorido–bromido complex anion were obtained using a Hewlett-Packard 1050 high performance liquid chromatographic system consisting of a quaternary pump, auto-sampler equipped with a photo-diode array detection system. The flow rate was set to 0.8 mL min^{-1} and the UV–Vis spectrum was recorded in the wavelength region of 200–750 nm.

2.4. HPLC coupled to inductively coupled plasma mass spectrometry detection

An Agilent 1100 HPLC system, comprising of a de-gasser, binary pump, column compartment and manual injector coupled to an Agilent 7500ce ICP-MS. The HPLC mobile phase flow rate was set to 0.8 mL min^{-1}, with the analyte sample being transferred to the nebulizer by PEEK tubing with internal diameter equal to 0.12 mm. Due to the relatively high concentration of acetonitrile (~43%, v/v) in the mobile phase, certain modifications had to be made to avoid plasma extinction. The flow rate into the ICP-MS nebulizer was set at a low 0.1 mL min^{-1}, the excess HPLC feed solution being sent to waste. The carrier gas flow rate was set to 0.8 L min^{-1} Ar, with make-up flow of 0.41 L min^{-1} Ar/O_2 (80/20) introduced via a T-junction into the gas stream before it reached the ICP torch, to assist the oxidation of excess carbon in the plasma. The RF torch power was set to 1550 W and possible molecular–ion interferences were eliminated via a collision-reaction cell using He gas.

2.5. High-performance liquid chromatography coupled to ICP-OES detection

Chromatographic separations were accomplished with a Varian *Prostar* liquid chromatograph equipped with a binary 210 solvent delivery module and a 410 autosampler operating at an optimized flow rate of mobile phase of 0.8 mL min^{-1}. Detection of Pt emissions at 265.945 nm was performed using a SPECTRO *Arcos* ICP-OES spectrometer operating with a RF power set to 1550 W using Burgener T2002 nebulizer and cyclonic spray chamber. The sample was transferred directly from the column to the nebulizer by PEEK tubing with internal diameter equal to 0.12 mm. The nebulizer flow rate was set at 0.6 mL min^{-1}, auxiliary gas flow rate was set to 2 L min^{-1} and coolant flow rate to 16 L min^{-1}.

2.6. ^{195}Pt NMR spectroscopy

All ^{195}Pt NMR spectra were recorded at 303 K using a Varian INOVA 600 MHz (14.1 T) spectrometer at 129 MHz for ^{195}Pt, using a 5 mm broad-band probe, with conditions as described elsewhere [7,8]. A 1 mm coaxial insert tube containing a $[PtCl_6]^{2-}$ solution (500 mg mL^{-1} $H_2PtCl_6{\cdot}H_2O$ in 30% v/v D_2O/ 1 M HCl) was inserted into 5 mm NMR tubes as internal reference, arbitrarily assigned to $\delta(^{195}Pt) = 0.0$ ppm; this corresponds to a chemical shift of approximately 4522 ppm relative to ^{195}Pt at $\Xi = 21.4$ MHz.

3. Results and discussion

Of the 10 possible octahedral complexes $[PtCl_{6-n}Br_n]^{2-}$ (n = 0–6) obtained on mixing solutions of $[PtCl_6]^{2-}$ and $[PtBr_6]^{2-}$ two may be classified as *homoleptic*, $[PtCl_6]^{2-}$ and $[PtBr_6]^{2-}$, together with eight *heteroleptic* $[PtCl_{6-n}Br_n]^{2-}$ (n = 1–5) species, which for convenience will be designated by a shorthand notation consisting of three numerals (m, n, o), where m, n, o = 0–6 and m, n and o represent the number of Cl^- ions, the number of Br^- ions and number of water molecules respectively, coordinated to the Pt^{IV} as suggested by Drews and Preetz [20,25]. Thus the two homoleptic $[PtCl_6]^{2-}$ and $[PtBr_6]^{2-}$ complexes are represented as (600) and (060), while the $[PtCl_4Br_2]^{2-}$ anion, which can exist as the *cis*- and *trans*-$[PtCl_4Br_2]^{2-}$ complexes are designated as (4^c2^c0) and (4^t2^t0) respectively, while the monoaquated anions $[PtCl_5(H_2O)]^-$ and $[PtBr_5(H_2O)]^-$ are denoted as (501) and (051), etc. We demonstrated previously that ^{195}Pt NMR is a powerful technique by which all possible octahedral complexes $[PtCl_{6-n}Br_n]^{2-}$ (n = 0–6) could be spectroscopically identified by means of $\delta(^{195}Pt)$ chemical-shift-trend analysis, including notably the stereoisomers *cis*- and *trans*-$[PtCl_4Br_2]^{2-}$, *fac*- and *mer*-$[PtCl_3Br_3]^{2-}$ and *cis*- and *trans*-$[PtCl_2Br_4]^{2-}$ [8]. This is illustrated in Fig. 1a by a ^{195}Pt NMR spectrum of an equilibrated (aged for ±2.2 years) solution of H_2PtCl_6 and H_2PtBr_6 ($[Pt]_t$ = 0.1 M) in a 0.1 M $HClO_4$ matrix, which is practically identical to a previously published spectrum [8], showing all ten $[PtCl_{6-n}Br_n]^{2-}$ (n = 0–6) anionic complexes; significantly nine signals of low peak intensity due to the mono-aquated species $[PtCl_{5-n}Br_n(H_2O)]^-$ (n = 0–5) are also detected, which occur in these solutions as a result of the relatively small extent of aquation of these Pt^{IV} complexes, due to the negligible unbound (free) halide-ion (Cl^-/Br^-) concentrations. The accurate measurement of the concentration of platinum complex species by means of ^{195}Pt NMR is limited, in view of the large spectral width 200–250 kHz necessary to detect all the ^{195}Pt NMR resonances in one spectrum, as a result of a somewhat non-uniform radio-frequency excitation over such large spectral widths; nevertheless the relative ^{195}Pt NMR resonance intensities of the peaks in Fig. 1a are proportional to the analytical concentrations of all the Pt containing species, to within an estimated 5–10% relative accuracy.

Fig. 1b shows the IP-RP-HPLC chromatographic separation with photometric detection (λ = 262 and 315 nm) under optimized separation conditions of an equilibrated solution used for the ^{195}Pt NMR spectrum, but diluted by a factor of 10^2 with 1.0 mM acetate buffer to give $[Pt]_{total} \approx 1$ mM at pH ~ 4.6, followed by immediate injection into the IP-RP-HPLC[2]. It is clear that an excellent separation into all the complex species is achieved, the species with elution times ranging from 12 to 35 min most likely being due to the 10 octahedral complexes $[PtCl_{6-n}Br_n]^{2-}$ (n = 0–6), while those peaks in the 4–10 min elution time range are tentatively ascribed to the mono-aquated $[PtCl_{5-n}Br_n(H_2O)]^-$ (n = 0–5) species (Fig. S-2, supplementary data), which have been shown to be present in small amounts in water solutions of higher Pt concentration by ^{195}Pt NMR [7]. In the presence of an excess of Cl^- and/or Br^- ions, the formation of mono-aquated species $[PtCl_{5-n}Br_n(H_2O)]^-$ (n = 0–5) is suppressed and the $[PtCl_{6-n}Br_n]^{2-}$ (n = 0–6) species predominate in equilibrated solutions, as illustrated by the IP-RP-HPLC chromatogram in Fig. S-3 (supplementary data). In this paper we will not further discuss the separation of aquated $[PtCl_{5-n}Br_n(H_2O)]^-$ (n = 0–5) species, which is currently under further study.

The assignment of the eluted peaks in the IP-RP-HPLC chromatogram to the homoleptic species (600) and (060) based only on relative retention times is simple, since the corresponding pure salts are commercially available. By contrast the unambiguous assignment of the chromatographic peaks in Fig. 1b to specific heteroleptic species is more difficult, since the synthesis of such complexes as single reaction products is impossible [20], so that comparison of retention times to known species is not an option. Moreover, there is no *a priori* rule for the reliable assignment of these species based on relative retention times, as highlighted by the interchangeable elution orders of stereoisomers present in the mixed-halide series $[OsI_{6-n}Cl_n]^{2-}$ and $[PtCl_{6-n}F_n]^{2-}$ (n = 0–6)

[2] Rapid ligand redistribution in these species does not occur for these kinetically inert complexes under these conditions, in the absence of light and the time scale of the separation.

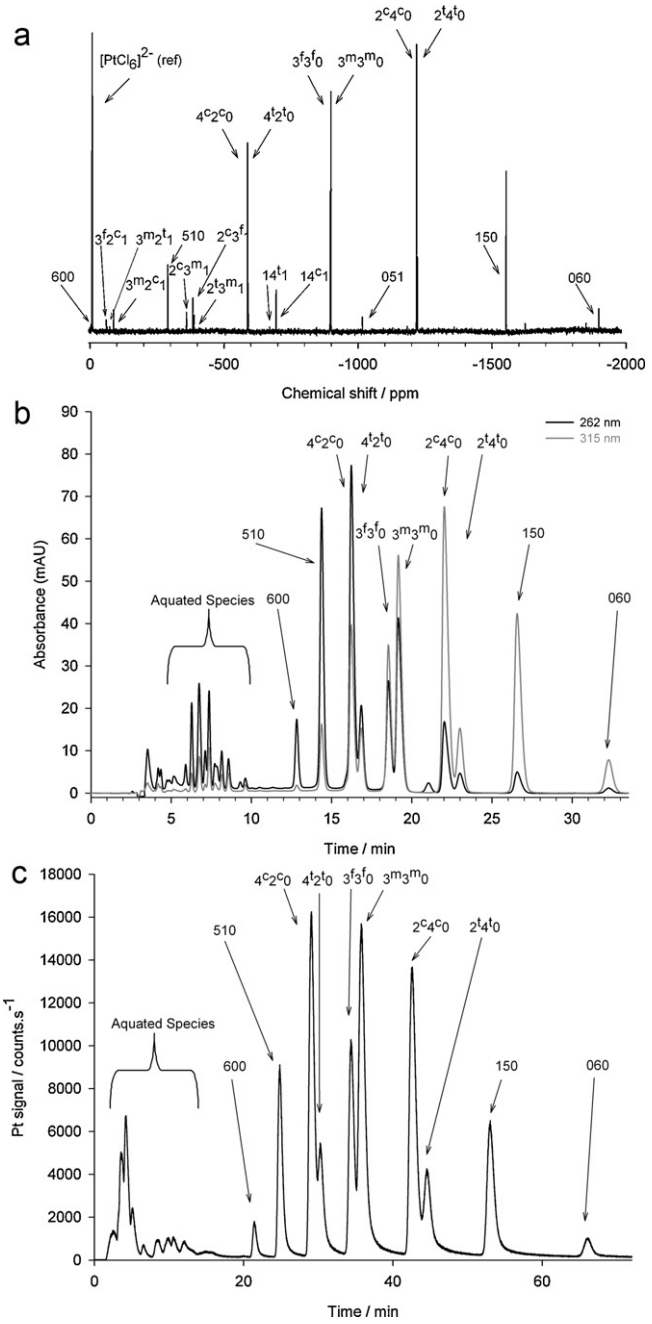

Fig. 1. (a) ^{195}Pt NMR spectrum of a solution containing equimolar amounts of H_2PtCl_6 and H_2PtBr_6 ($[Pt]_t = 0.1$ M) in a 0.1 M $HClO_4$ matrix. (b) The chromatogram obtained upon injection of the solution after 100 fold dilution onto a C_{18} reversed phase column and a mobile phase CH_3CN:H_2O (v/v) ratio of 48% and 9.0 mM TBA^+Cl^- utilizing UV/Vis detection at 262 and 315 nm, and (c) ICP-MS as detection system. The mobile phase composition was decreased to 43% (v/v) CH_3CN:H_2O to avoid plasma extinction.

as reported by Preetz et al. [20]. However a qualitative comparison of the IP-RP-HPLC chromatogram of a 1 mM $[Pt]_{total}$ solution (Fig. 1b) with that of the 100 mM $[Pt]_{total}$ solution investigated by means of ^{195}Pt NMR (Fig. 1a) shows excellent correlation between the number and approximate concentration of the possible heteroleptic $[PtCl_{6-n}Br_n]^{2-}$ ($n = 1$–5) complex anions (as estimated respectively by the chromatographic peak intensities determined photo-metrically at 262 nm and 315 nm, and the relative ^{195}Pt NMR resonance peak intensities). The satisfactory semi-quantitative correlation of the speciation of $[PtCl_{6-n}Br_n]^{2-}$ ($n = 0$–6) anionic complexes between two completely independent techniques in solutions differing in concentration by two orders of magnitude thus obtained, validates the peak assignment of the IP-RP-HPLC separation by a direct ^{195}Pt NMR structure-sensitive spectroscopic technique. However, since the molar absorptivities (ε) of all the fractionated species by means of IP-RP-HPLC are not known, the relative concentration of the platinum containing species eluted in the chromatogram (Fig. 1b) is not accurately determinable at the given detection wavelengths.

Unambiguous chromatographic quantification and characterization of all the heteroleptic species $[PtCl_{6-n}Br_n]^{2-}$ ($n = 1$–5) in the separation shown in Fig. 1b was achieved by coupling the IP-RP-HPLC system to a photodiode array (PDA) detector to record the complete UV/Vis spectrum of each eluted species, and subsequently to a ICP-MS or ICP-OES spectrometer as detectors, by which the accurate Pt concentration could be determined. Thus injection of a 20 μl aliquot of freshly diluted (100 fold) equilibrated solution containing a mixture of H_2PtCl_6 and H_2PtBr_6 ($[Pt]_t = 0.1$ M) in 0.1 M $HClO_4$ with 1 mM acetate buffer into IP-RP-HPLC coupled to an ICP-MS spectrometer as detection system with optimized eluent composition of 43% (v/v) (CH_3CN:H_2O, 9.0 mM TBA^+Cl^-) yielded the ICP-MS detected chromatogram shown in Fig. 1c. The IP-RP-HPLC chromatogram obtained by coupling to the ICP-MS shows somewhat lower resolution and differing retention times, as a result of the necessity of lowering the acetonitrile concentration to 43% (v/v) in the mobile phase composition, use of reduced chromatographic eluent flow rate, together with a post-column splitter to enable di-oxygen gas feed to achieve a stable plasma or prevent plasma extinguishing, given the high carbon content of the mobile phase entering the plasma.

From Fig. 1c it is clear that apart from a slight loss of resolution due to the lower acetonitrile concentration in the mobile phase and reduced flow rate when using ICP-MS as detection system, a very similar chromatogram to Fig. 1b was obtained with photometric detection. Nevertheless, accurate platinum concentrations of all separable Pt^{IV} complex species could be obtained for each eluted peak using ICP-MS. Quantification was achieved by integration and summation of the total platinum ion count at m/e of 194.965 of each eluted species, from which the relative fraction of each individual species could be calculated from the total known platinum concentration injected into the IP-RP-HPLC-ICP-MS.

Inspection of Fig. 1b and c, shows that species which elute as distinct "peak pairs" ($t_r \approx 16.5$, 19 and 22.5 min) are most likely attributable to the stereoisomer pairs *cis*-/*trans*-$[PtCl_2Br_4]^{2-}$ (2^c4^c0 and 2^t4^t0), *fac*-/*mer*-$[PtCl_3Br_3]^{2-}$ (3^f3^f0 and /3^m3^m0) and *cis*-/*trans*-$[PtCl_4Br_2]^{2-}$ (4^c2^c0 and 4^t2^t0). In order to unambiguously assign and quantify these stereoisomers, we compared the relative peak ratios from the ^{195}Pt NMR spectrum of these pairs obtained for the equilibrated 100-fold more concentrated solutions, to the chromatographic peak area ratios as obtained from the IP-RP-HPLC-ICP-MS from freshly diluted platinum complex solutions. Despite the somewhat poorer chromatographic resolution between peak pairs due to stereoisomers of the (4^c2^c0) and (4^t2^t0) species accurate estimates of relative concentrations were obtained by the use of a least squares de-convolution of peak areas protocol using the exponentially modified Gaussian (EMG) equation recommended by Foley et al. [26,27] and Papas et al. [28]. A representative chromatogram is shown in Fig. S-4 (supplementary data), confirming that the predominant (4^c2^c0) complex elutes somewhat before its more symmetrical (4^t2^t0) isomer, and consistent with the ^{195}Pt NMR data. A similar protocol applied to the (3^f3^f0/3^m3^m0) and (2^c4^c0/2^t4^t0) pairs of stereoisomers, allows for acceptably accurate concentration ratios for these isomers. Table 1 shows good agreement between the relative concentration ratios of the 2^c4^c0/2^t4^t0, 4^c2^c0/4^t2^t0 and 3^t3^t0/3^m3^m0 stereoisomer pairs as determined by ^{195}Pt NMR and IP-RP-HPLC within experimental error, confirming the consistency and acceptable accuracy in the quantification

Table 1
Stereoisomer ratios expected on a statistical basis and those determined from the ^{195}Pt NMR spectrum and HPLC-ICP-MS chromatogram.

Stereoisomer pairs	Stereoisomer ratios determined		
	^{195}Pt NMR	HPLC-ICP-MS	Statistical ratio[a]
cis:*trans*-$[PtCl_4Br_2]^{2-}$	4.1:1	3.8:1	4:1
fac:*mer*-$[PtCl_3Br_3]^{2-}$	2:3.9	2:3.7	2:3
cis:*trans*-$[PtCl_2Br_4]^{2-}$	3.4:1	3.2:1	4:1

[a] Ref. [30].

of these isomeric platinum species using this approach. The good agreement between these peak ratios is consistent with previous ^{195}Pt NMR assignments [8], as well as the expected relatively higher thermodynamic stability of the (4^c2^c0) over (4^t2^t0) and (2^c4^c0) over (2^t4^t0) isomers, given the higher *trans* influence of the bromido over the chlorido ligand bound to Pt^{IV} [29]. Interestingly the relative concentration ratios determined for the stereoisomer pairs ($4^c2^c0/4^t2^t0$) and ($2^c4^c0/2^t4^t0$) compare reasonably well with the expected *statistical* ratios (statistical considerations only take into account the relative probability for stepwise ligand substitutions at the Pt^{IV} metal centre in which the coordination number remains constant throughout the series in question, but does not necessarily reflect the relative thermodynamic stabilities of these species) [30]. Notably our experimentally determined value for the ratio of ($3^f3^f0/3^m3^m0$) differs from the statistical ratio of 2:3 [30], suggesting appreciable thermodynamic stability differences between the (3^f3^f0) and (3^m3^m0) stereoisomer pair. To our knowledge, this is the first time that reliable direct estimates of the actual concentrations of these isomers (presumably at thermodynamic equilibrium) present in the series $[PtCl_{6-n}Br_n]^{2-}$ (n = 0–6) of complex anions in such solutions have been possible.

The significant advantage of the IP-RP-HPLC coupled to an ICP-MS as detector is that it allows for an accurate estimate of the actual concentration of all separable Pt^{IV} containing species eluting from the column, which in turn allows for the determination of the UV/Vis absorption characteristics (λ_{max} and ε) for all 10 octahedral $[PtCl_{6-n}Br_n]^{2-}$ (n = 0–6) species, something not previously possible (apart from the trivial $[PtCl_6]^{2-}$ and $[PtBr_6]^{2-}$ species). Thus for a separation as in Fig. 1b with a PDA detection system it is easy to record the entire UV/Vis spectrum of each eluted individual species, resulting in determination of the λ_{max} and calculation of the corresponding molar absorptivities, ε, at any wavelength for all the separable species listed in Table 2. Our experimentally obtained molar absorptivities of the homoleptic species $[PtCl_6]^{2-}$ and $[PtBr_6]^{2-}$ compare well to those few available from the literature [31,32], generally validating our data in Table 2 as far as is possible.

Illustrated in Fig. 2 are the individual UV/Vis absorption spectra of the 10 possible species, the sum of which would correspond the experimental absorption spectrum of a mixture of all $[PtCl_{6-n}Br_n]^{2-}$ (n = 0–6) complex anions present at these concentrations. Given the so obtained molar absorptivities ε_n of all the $[PtCl_{6-n}Br_n]^{2-}$ (n = 0–6) complex anions, this allows for the possibility of accurate quantification of each of these complexes by means of IP-RP-HPLC with conventional UV/Vis detection (at λ = 262 nm), thus avoiding the use of the more costly and somewhat complicated use of an ICP-MS detection mode not necessarily widely available. The good mass-balance demonstrated (Table S1, supplementary data) between the total amount of Pt_{tot} injected into the HPLC system (as concentration 1 mM) and that subsequently obtained from the measured peak areas of the various species in the resulting chromatogram, adequately confirms the UV/Vis molar absorptivity data in Table 2, and thus the veracity of this methodology. The photometric absorption data shown for all the $[PtCl_{6-n}Br_n]^{2-}$ (n = 0–6) complex anions in Fig. 2 is consistent with the expected bathochromic shift in absorption maxima expected for the ligand-to-metal charge-transfer (LMCT) bands in the UV/Vis spectra of this series of complexes, as a consequence of the stepwise substitution of chlorido by bromido ligands bound to the Pt^{IV}. Similar photometric trends have been observed by Preetz et al. for complexes such as $[MCl_{6-n}Br_n]^{2-}$ (M = Re, Os, Ir and Ru) (n = 0–6) [20].

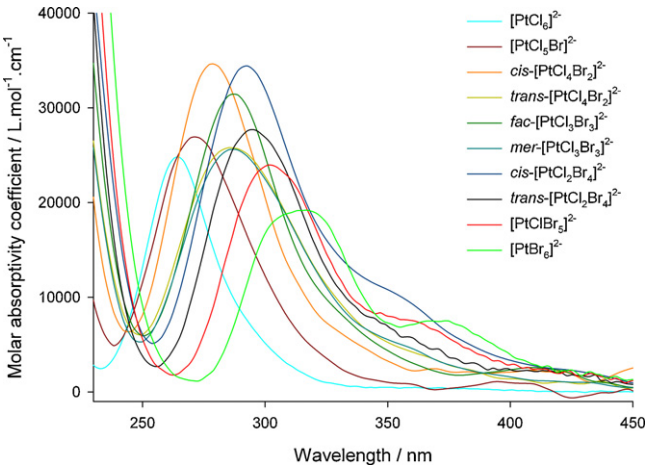

Fig. 2. The UV/Vis absorption spectra, shown as molar absorptivity (ε/L mol^{-1} cm^{-1}) versus λ for each of the 10 individual $[PtCl_{6-n}Br_n]^{2-}$ (n = 0–6) species, calculated from the UV/Vis absorption spectra obtained for each individual $[PtCl_{6-n}Br_n]^{2-}$ (n = 0–6) species by means of PDA detection, and knowledge of individual platinum concentration in 48% (v/v) CH_3CN:H_2O with 9.0 mM TBA^+Cl^-.

It is also possible to study the stepwise substitution of Cl^- by Br^- in $[PtCl_6]^{2-}$ using the IP-RP-HPLC method developed here, as shown in Fig. 3 by way of example. A series of solutions were prepared in which $[Pt^{IV}]_t$ = 10 mM with variable Cl^- and Br^- concentrations at constant ionic strength, by maintaining the total free halide concentration ($[Cl^-] + [Br^-]$) at 1.0 M, and the $[H^+]_t$ at 0.2 M at 294 K; these were injected into the IP-RP-HPLC, each sample with

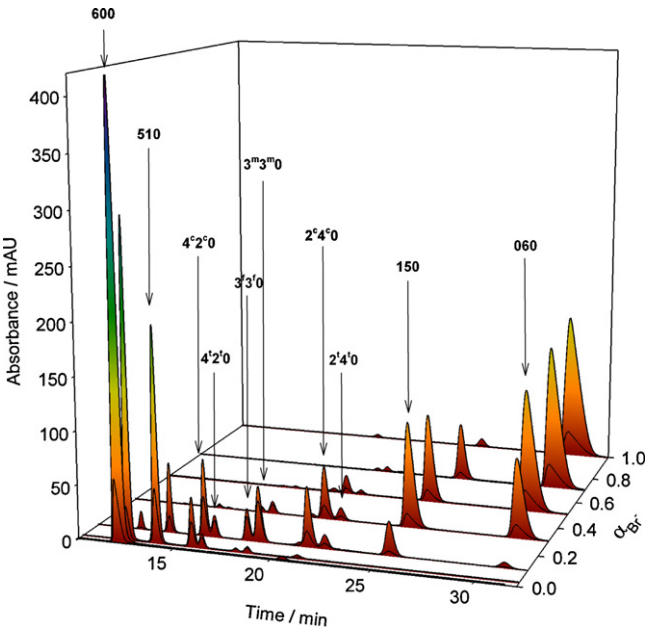

Fig. 3. Chromatograms depicting the stepwise substitution of Cl^- by Br^- in $[PtCl_6]^{2-}$ as a function of increasing Br^- mole fraction (Cl^-/Br^-) from 0 to 0.98, by the formation of the series of anions $[PtCl_{6-n}Br_n]^{2-}$ (n = 0–6) complex from initially only $[PtCl_6]^{2-}$ to $[PtBr_6]^{2-}$. Each chromatogram was obtained using a mobile phase 48% (v/v) CH_3CN:H_2O with 9.0 mM TBA^+Cl^-.

Table 2
Molar absorptivities for the $[PtCl_{6-n}Br_n]^{2-}$ (n = 0–6) and $[PtCl_{4-n}Br_n]^{2-}$ (n = 0–4) complex anions estimated at λ_{max} and measured at 262 nm.

Species	λ_{max} (nm)	$\varepsilon_{expt.}$ (L mol^{-1} cm^{-1}) (at λ_{max})	$\varepsilon_{expt.}$ (L mol^{-1} cm^{-1}) (at 262 nm)	$\varepsilon_{lit.}$ (L mol^{-1} cm^{-1}) (λ in parentheses)[a]
Pt^{IV}				
600	262	24 370 ± 483	24 370 ± 483	24 500 (262)
510	271	26 992 ± 2015	23 208 ± 374	–
4^c2^c0	278	34 600 ± 2948	20 847 ± 924	–
4^t2^t0	286	25 960 ± 2849	16 250 ± 889	–
3^f3^f0	287	31 530 ± 2753	11 237 ± 873	–
3^m3^m0	287	25 604 ± 1925	9919 ± 857	–
2^c4^c0	292	27 615 ± 2438	6283 ± 273	–
2^t4^t0	295	34 399 ± 4057	5068 ± 238	–
150	302	24 042 ± 2097	2159 ± 87	–
060	315	19 120 ± 1927	3586 ± 104	19 000 (313)
Pt^{II}				
400	217	12 102 ± 1530	451 ± 13	440 (262)
310	238	11 450 ± 1354	1569 ± 71	2000 (262)
220[b]	246	11 261 ± 1647	6107 ± 265	6750 (262)
130	257	10 508 ± 1153	9982 ± 479	7380 (262)
040	270	9018 ± 1035	6231 ± 302	6200 (262)

[a] References [31–33].
[b] Molar absorptivity of overlapping 2^c2^c0 and 2^t2^t0 isomers which are not resolved under these conditions.

a defined mole fraction of Br^- to Cl^- to ranging from 0 to 0.98. Initially, for a solution containing no bromide ions, only $[PtCl_6]^{2-}$ is eluted, but increasing the mole fraction of Br^- from 0 to 0.98 results in the formation of the various $[PtCl_{6-n}Br_n]^{2-}$ (n = 1–6) species, which appear and disappear again from successive chromatograms in a "stepwise" manner, as the bromide ions displace the chloride ions from the Pt^{IV} complex. Moreover, the relative kinetic inertness of the $[PtCl_{6-n}Br_n]^{2-}$ (n = 0–6) anionic complexes with regard to the time-frame of a single chromatographic run permits a semi-qualitative kinetic investigation into the rate of chlorido by bromido ligand substitution in these complexes. Thus the ability to quantify the $[PtCl_{6-n}Br_n]^{2-}$ (n = 0–6) species by IP-RP-HPLC facilitates an in-depth study of the thermodynamic stabilities of these complexes and kinetics of ligand exchange, something we are currently exploring further.

3.1. Speciation of Pt^{II} chlorido–bromido complex anions

The convenient IP-RP-HPLC speciation of the octahedral Pt^{IV} complexes, suggests thus a similar study to include the analogous stable square-planar Pt^{II} species. We thus examined the mixed Pt^{II} $[PtCl_{4-n}Br_n]^{2-}$ (n = 0–4) species, with the objective of developing a simultaneous separation of the $[PtCl_{6-n}Br_n]^{2-}$ (n = 0–6) and $[PtCl_{4-n}Br_n]^{2-}$ (n = 0–4) complex anions in a single chromatographic run.

Fig. 4a shows a ^{195}Pt NMR spectrum recorded at 294 K of all 6 possible $[PtCl_{4-n}Br_n]^{2-}$ (n = 0–4) complex anions present in an equilibrated solution with $[Pt^{II}]_t$ = 0.1 M, 0.2 M in $[H_3O^+]_t$ and free halide ion concentration adjusted to $[Cl^-]$ = 0.85 M and $[Br^-]$ = 0.15 M with $[Na^+]_t$ = 0.8 M. The ^{195}Pt NMR assignments of all signals were carried out by means of chemical shift trend-analysis similar to that of Pt^{IV} complexes [6,7], and compared well with the limited data available from the literature as reported by von Zelewski et al. [5] and Elding et al. [33]. Fig. 4b shows the IP-RP-HPLC chromatogram obtained by injection of a 20 μl aliquot of a freshly 100 fold diluted sample of the concentrated Pt^{II} solution with 1.0 mM acetate buffer (pH ∼ 4.6) in water onto a 25.0 cm C_{18} reversed phase column under the same experimental conditions used before for Pt^{IV} with standard photometric UV/Vis detection at 262 and 315 nm. Under these conditions (9.0 mM TBA^+Cl^- and 48% (v/v) acetonitrile/water with a 0.01 M sodium acetate buffer), only 5 of the expected 6 peaks were observed in the chromatogram. The "central" peak ($t_r \approx 8$ min) is due to the two stereoisomers (2^t2^t0) and (2^c2^c0), which co-elute as a result of only small retention time differences under these conditions. This was verified by decreasing the acetonitrile concentration in the mobile phase to 26% (v/v) CH_3CN:H_2O, which results in partial chromatographic resolution of peaks due to the (2^c2^c0) and (2^t2^t0) isomers, albeit at the expense of rather long retention times and broad peaks, as shown by the insert in Fig. 4b. The partial chromatogram of such a separation with mobile phase of 26% (v/v) CH_3CN:H_2O is shown in Fig. S-5 (supplementary data).

As described for the octahedral Pt^{IV} anions above, easy quantification of the $[PtCl_{4-n}Br_n]^{2-}$ (n = 0–4) complex anions by IP-RP-HPLC coupled to an ICP-OES spectrometer as detector is achieved as shown in Fig. 4c. Owing to the necessity of post column modification when using an ICP-MS system as detector to reduce the risk of plasma extinction using mobile phases with high organic modifier compositions, we found the use of a conventional ICP-OES spectrometer with a radial plasma torch more robust and convenient as detector. The use of a radial torch configuration, with the plasma power output set to 1550 W and using a Burgener T2002 nebulizer connected to a cyclonic spray-chamber, gives rise to a stable plasma, with adequate Pt detection limits to allow for the platinum concentration in all eluted peaks from the chromatographic system. An additional advantage of using an ICP-OES detection mode is that no addition of di-oxygen as auxiliary gas to argon is necessary; moreover the passage of analyte directly from column to nebulizer leads to improved chromatographic peak shapes and resolution. Fig. 4c shows a chromatogram of all $[PtCl_{4-n}Br_n]^{2-}$ (n = 0–4) anionic complexes, obtained with a mobile phase 48% (v/v) CH_3CN:H_2O using ICP-OES as detector, including an unresolved peak due to (2^c2^c0)/(2^t2^t0) isomers; the insert in Fig. 4c shows a section of the chromatogram recorded with a 26% (v/v) CH_3CN:H_2O mobile phase composition, in which the (2^c2^c0)/(2^t2^t0) isomers are partially separated, from which the isomer (2^c2^c0)/(2^t2^t0) ratio could be determined by means of deconvolution analysis (Fig. S-6, supplementary data). The measured (2^c2^c0)/(2^t2^t0) isomer ratios by ^{195}Pt NMR (Fig. 4a), and chromatographically with ICP-OES (Fig. 4c), compared to the statistically expected ratios [30] are respectively 1.85:1, 1.91:1 and 2:1, satisfactorily validating these relative ratios as well as the correct chromatographic assignments.

Similar to the methodology followed for the Pt^{IV} species above, the individual UV/Vis spectra of each separable $[PtCl_{4-n}Br_n]^{2-}$ (n = 0–4) complex anion and their corresponding molar absorptivities, ε, of all individual complexes $[PtCl_4]^{2-}$, $[PtCl_3Br]^{2-}$, $[PtClBr_3]^{2-}$ and $[PtBr_4]^{2-}$ together with the unresolved UV/Vis spectrum of the (2^c2^c0) and (2^t2^t0) isomers can be easily obtained, as shown in Fig. 5 and listed in Table 2.

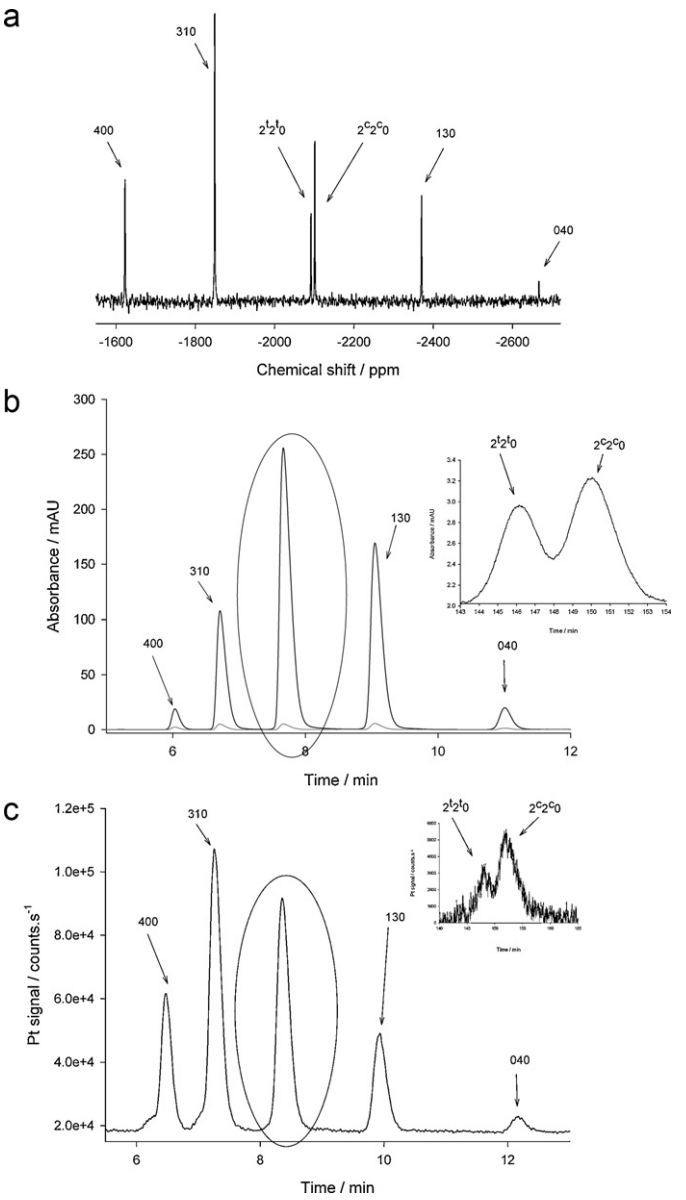

Fig. 4. (a) ^{195}Pt spectrum of the 6 $[PtCl_{4-n}Br_n]^{2-}$ (n = 0–4) complex anions detected in solution ($[Pt]_t$ = 0.1 M) in which the total halide concentration ($[Cl^-]$ = 0.85 M] + $[Br^-]$ = 0.15 M]$)_t$ = 1.0 M, the $[H_3O^+]_t$ = 0.2 M and the $[Na^+]_t$ = 0.8 M. (b) Chromatogram recorded by UV/Vis detection of the same sample used in (a) upon 100 fold dilution and injection. The insert shows a partial chromatogram recorded using a mobile phase of a 26% (v/v) CH_3CN/H_2O giving a partial separation of the (2^t2^t0) and (2^c2^c0) isomers. (c) Injection of a 1.25 mM $[PtCl_{4-n}Br_n]^{2-}$ (n = 0–4) sample using a mobile phase CH_3CN:H_2O (v/v) ratio of 48% with ICP-OES detection, with a corresponding partial chromatogram of the (2^t2^t0)/(2^c2^c0) pair at 26% (v/v) CH_3CN:H_2O shown as in the insert.

The bathochromic shift of the electronic absorption maxima in the LMCT region of the spectra observed for $[PtCl_{6-n}Br_n]^{2-}$ (n = 0–6) species is similarly observed for the $[PtCl_{4-n}Br_n]^{2-}$ (n = 0–4) series. Comparison of molar absorptivities, ε, of the various Pt^{II} species with data available from the literature is satisfactory, although it is reasonable to expect data obtained by our method is likely to be more accurate.

3.2. Simultaneous separation of Pt^{II} and Pt^{IV} complexes

Finally, the differences in partition ratio between aqueous and non-aqueous solvents of the six-coordinate octahedral Pt^{IV} compared to the square-planar four-coordinate Pt^{II} complex anions,

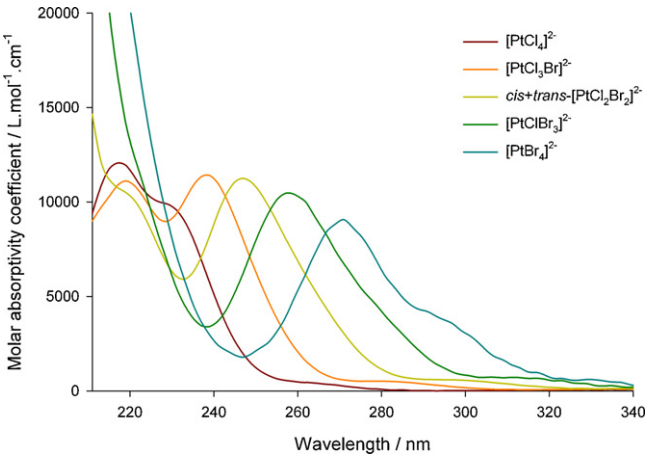

Fig. 5. The UV/Vis absorption spectra of $[PtCl_4]^{2-}$, $[PtCl_3Br]^{2-}$, $[PtClBr_3]^{2-}$, $[PtBr_4]^{2-}$ and the combined stereoisomer species (2^c2^c0) + (2^t2^t0), as a function of molar absorptivity, ε/(L mol^{-1} cm^{-1}) against λ determined as described in the text and figure, for the Pt^{II} in 48% (v/v) CH_3CN:H_2O with 9.0 mM TBA^+Cl^-.

being significantly more favourable for octahedral Pt^{IV} complexes [2], suggests that the former are likely to have longer retention times compared to the Pt^{II} complexes in the IP-RP-HPLC mode.

As may be seen from the IP-RP-HPLC chromatogram shown in Fig. 6, it is readily possible to achieve a rapid separation and thus unambiguous speciation of mixtures of both $[PtCl_{4-n}Br_n]^{2-}$ (n = 0–4) and $[PtCl_{6-n}Br_n]^{2-}$ (n = 0–6) complex anions in aqueous solutions with $[Pt]_t \sim 1.5$ mM, in the presence of an excess of Cl^- and Br^- anions ($[Cl^-]$ = 0.85 M and $[Br^-]$ = 0.15 M).

The various Pt^{II} complex species elute in the range 6–10.5 min while Pt^{IV} complex anions elute in the 11.5–28 min range, with in most cases, excellent resolution. The last Pt^{II} species (040) to elute is separated by only 1 min from the first Pt^{IV} species (600) to elute under these chromatographic conditions, within total chromatographic elution time of approximately 30 min, using standard C_{18} reversed phase columns. Knowledge of the molar absorptivities (ε) at various wavelengths in the 220–320 nm range from this study allows for the ready quantification of such complexes at the mM and sub-mM total [Pt] concentrations. In our experience the

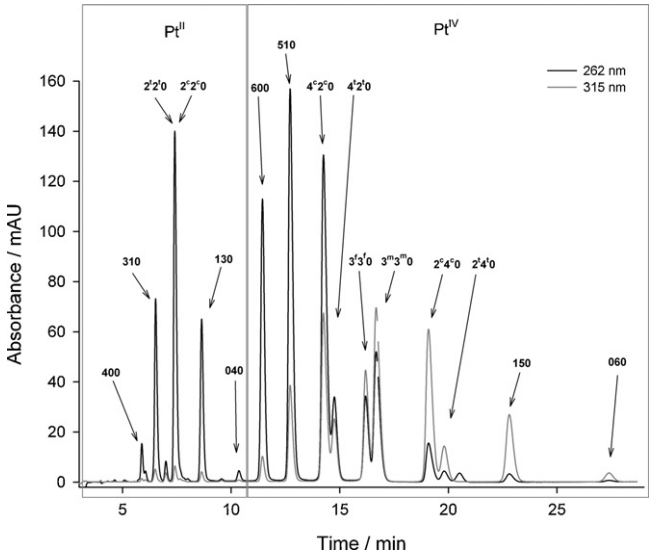

Fig. 6. UV/Vis recorded chromatogram depicting the simultaneous separation of the mixed chlorido–bromido $Pt^{II/IV}$ species, i.e. $[PtCl_{4-n}Br_n]^{2-}$ (n = 0–4) and $[PtCl_{6-n}Br_n]^{2-}$ (n = 0–6) complex anions using a mobile phase 48% (v/v) CH_3CN:H_2O at 9.0 mM TBA^+Cl^-.

columns used, retain their separation efficiency for more than a year if properly flushed after use, despite the somewhat chemically aggressive nature of the solutions in which the $Pt^{II/IV}$ complex anions occur, particularly in a commercial context. As indicated at the beginning of this paper the opportunity to use this technique for the speciation of the aquated $Pt^{II/IV}$ complex anions possibly present in process solutions, is an interesting prospect which we are actively exploring at present. The use of the speciation technique described here to other kinetically inert PGM metal complexes in various relevant matrices is also currently being studied in our laboratory.

4. Conclusions

We have developed a robust ion-pairing RP-HPLC method for the unambiguous speciation and quantification of all possible homoleptic and heteroleptic octahedral $[PtCl_{6-n}Br_n]^{2-}$ ($n = 0$–6) as well as the corresponding $[PtCl_{4-n}Br_n]^{2-}$ ($n = 0$–4) complex anions using UV/Vis detection. High resolution ^{195}Pt NMR which in more concentrated solutions of these $Pt^{II/IV}$ complexes ($\geq$50 mM), served to validate our assignments particularly in the case of the possible stereoisomers of $Pt^{II/IV}$ complex anions, something not achieved before. By means of IP-RP-HPLC coupled to ICP-MS or ICP-OES it is possible to accurately determine the relative concentration of all possible $Pt^{II/IV}$ species in these solutions, which allows for in conjunction with photo-diode array recording of the UV/Vis absorption spectra of all eluted species, the determination of the photometric characteristics (λ_{max} and ε) of all possible species in this series, much of this data not being available in the literature. With this data it becomes possible to readily carry out practical speciation studies of such $Pt^{II/IV}$ complex anions, where relevant using standard analytical equipment. We estimate the limit of detection (LOD) and quantification (LOQ) of the IP-RP-HPLC method (with UV/Vis detection at 262 nm) for the various Pt containing species to be in the range 0.17–0.30 and 0.6–1.1 mg L^{-1} respectively, based on the $[PtCl_6]^{2-}$ species, taking into account small adjustments due to the differences of molar absorptivities (Table 1) of the various species at this wavelength. By means of this technique it is also possible to investigate more fundamental mechanistic aspects of the deceptively simple chemistry of related $Pt^{II/IV}$ complexes in aqueous solutions as relevant to many areas in which $Pt^{II/IV}$ metallo-halogenates are involved such as "precursor" substances, or in process streams and other applications.

Acknowledgements

Financial support from the University of Stellenbosch and Angloplatinum Ltd., is gratefully acknowledged. We appreciate assistance of Ms. Riana Coetzee with the HPLC interface with the ICP-MS of the Central Analytical Facility of Stellenbosch University, as well as thank Dr. A. J. de Villiers for helpful discussions and the use of HPLC equipped with a PDA detector.

Appendix A. Supplementary data

Supplementary data associated with this article can be found, in the online version, at doi:10.1016/j.aca.2011.07.037.

References

[1] D. Jollie, Platinum 2010, Johnson Matthey PLC, Royston, UK, 2010, p. 54.
[2] G.J. Berfeld, A.J. Bird, R.I. Edwards, Gmelin Handbook of Inorganic Chemistry, 8th ed., Springer-Verlag, Berlin, 1986, pp. 8–30.
[3] R.A. Grant, F.L. Bernardis, D.C. Sherrington, Reactive & Functional Polymers 65 (2005) 205–217.
[4] D.M. Templeton, F. Ariese, R. Cornelis, L.G. Danielsson, H. Muntau, H.P. van Leeuwen, R. Loinski, Pure Applied Chemistry. 72 (2000) 1453–1470.
[5] A. Von Zelewsky, Helvetica Chimica Acta 51 (1968) 803–807.
[6] E. Peters, G. Parzich, W. Preetz, Zeitschrift fuer Naturforschung 48 (1993) 1169–1174.
[7] J. Kramer, K.R. Koch, Inorganic Chemistry 45 (2006) 7843–7855.
[8] J. Kramer, K.R. Koch, Inorganic Chemistry 46 (2007) 7466–7476.
[9] F.M. Ismail, S.J.S. Kerrison, P.J. Sadler, Chemical Communication 23 (1980) 1175–1176.
[10] W.J. Gerber, P. Murray, K.R. Koch, Dalton Transactions 31 (2008) 4113–4117.
[11] B. Baraj, A. Sastre, M. Martínez, K. Spahiu, Analytica Chimica Acta 319 (1996) 191–197.
[12] J.M. Sànchez, V. Salvadó, J. Havel, Journal of Chromatography A 834 (1999) 329–340.
[13] S.S. Aleksenko, A.P. Gumenyuk, S.P. Mushtakova, L.F. Kozhina, A.R. Timerbaev, Talanta 61 (2003) 195–202.
[14] S.S. Aleksenko, A.P. Gumenyuk, S.P. Mushtakova, L.F. Kozhina, A.R. Timerbaev, Journal of Analytical Chemistry 57 (2002) 215–220.
[15] S.S. Aleksenko, A.P. Gumenyuk, S.P. Mushtakova, A.R. Timerbaev, Fresenius Journal of Analytical Chemistry 370 (2001) 865–871.
[16] M. Hidalgo, J.M. Sánchez, J. Havel, V. Salvadó, Talanta 56 (2002) 1061–1071.
[17] H. Müller, P. Bekk, Fresenius Journal of Analytical Chemistry 314 (1983) 758–759.
[18] P. Obergfell, H. Müller, Fresenius Journal of Analytical Chemistry 328 (1987) 242–243.
[19] W. Preetz, Z. Erlhofer, Naturforsch 44b (1989) 412–418.
[20] G. Peters, W. Preetz, D. Bublitz, Chemical Reviews 96 (1996) 977–1026.
[21] R. Vlasankova, L. Sommer, Chromatographia 52 (2000) 692–702.
[22] D.J. Barkley, L. Giroux, Canadian Journal of Chemistry 72 (1994) 269–273.
[23] I.V. Khmelinski, V.P. Grivin, V.F. Plyusnin, Journal of Photochemistry and Photobiology A: Chemistry 51 (1990) 379–389.
[24] I.V. Khmelinski, V.P. Grivin, V.F. Plyusnin, Journal of Photochemistry and Photobiology A: Chemistry 51 (1990) 371–377.
[25] H.H. Drews, W. Preetz, Naturrforsch B 51 (1996) 1563–1570.
[26] J.P. Foley, Analytical Chemistry 59 (1987) 1984–1987.
[27] J.P. Foley, M.S. Jeansonne, Journal of Chromatography 594 (1992) 1–8.
[28] A.N. Papas, T.P. Tougas, Analytical Chemistry 62 (1990) 234–239.
[29] A. Von Zelewsky, The stereochemical course of reactions of metal complexes, in: G. Meyer, A. Nakamura, J.D. Woollins (Eds.), Stereochemistry of Coordination Compounds, Wiley, Chichester, U.K., 1996, pp. 202–206.
[30] A. Wilkinson, G. Cotton, Advanced Inorganic Chemistry, 5th ed., John Wiley & Sons, New York, 1988, p. 44.
[31] V. Balzani, F. Manfrin, L. Moggi, Inorganic Chemistry 6 (1966) 354–358.
[32] L.E. Cox, D.G. Peters, E.L. Wehry, Journal of Inorganic Nuclear Chemistry 34 (1972) 297–305.
[33] L.I. Elding, A. Groning, Chemica Scripta 11 (1977) 8–16.

Supporting Information

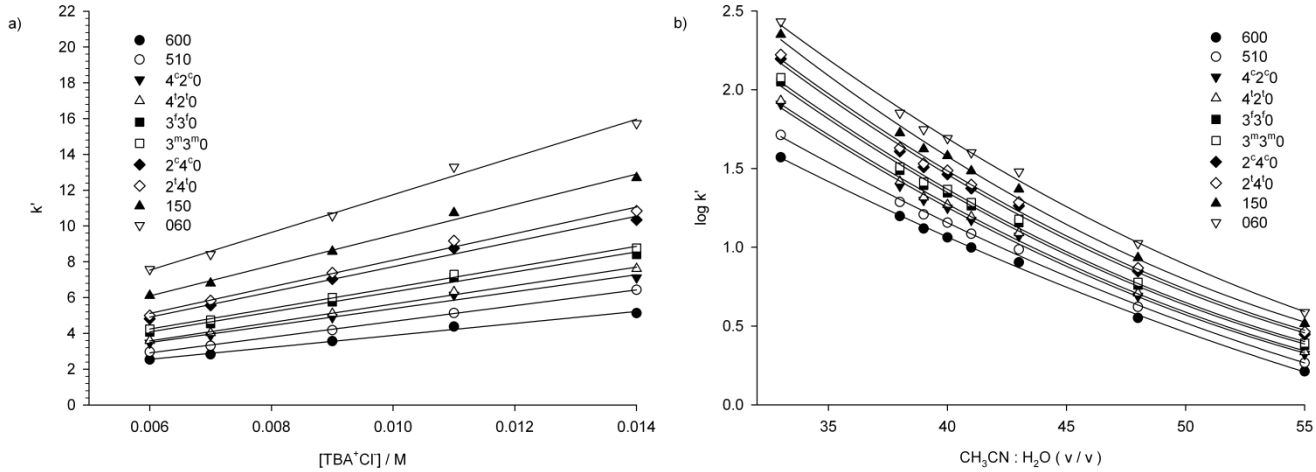

Figure S-1. The influence of (a) varying TBA^+Cl^- concentration on k' and (b) varying the volume percent of acetonitrile on log k' values of the 10 $[PtCl_{6-n}Br_n]^{2-}$ (n = 0 – 6) complex anions. The notation used for the 10 species is as described in the text. $[Pt]_t$ = 10 mM.

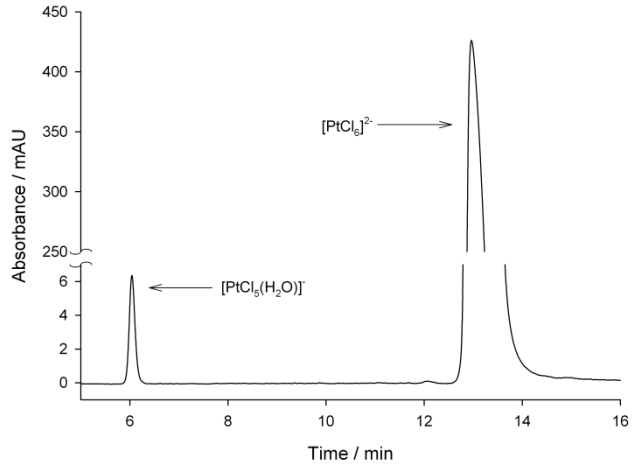

Figure S-2. Chromatogram displaying the presence of a single aquated species, $[PtCl_5(H_2O)]^-$ using a mobile phase CH_3CN:H_2O (v/v) ratio of 48% and 9.0 mM TBA^+Cl^-. This solution was prepared by dissolving the Na_2PtCl_6 salt in ultrapure Milli-Q water only such as to allow aquation of the $[PtCl_6]^{2-}$ complex anion.

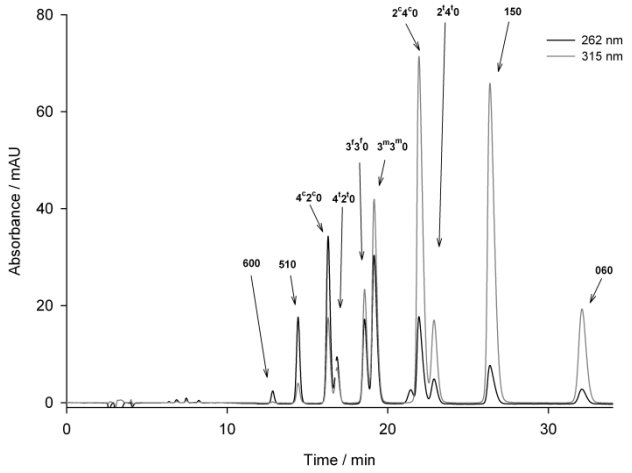

Figure S-3. Chromatogram displaying only the $[PtCl_{6-n}Br_n]$ (n = 0 - 6) species obtained using a mobile phase CH_3CN:H_2O (v/v) ratio of 48% and 9.0 mM TBA^+Cl^-. 'Aquation' of the complex anions is suppressed by a high halide (Cl^- + Br^- = 1.0 M) concentration.

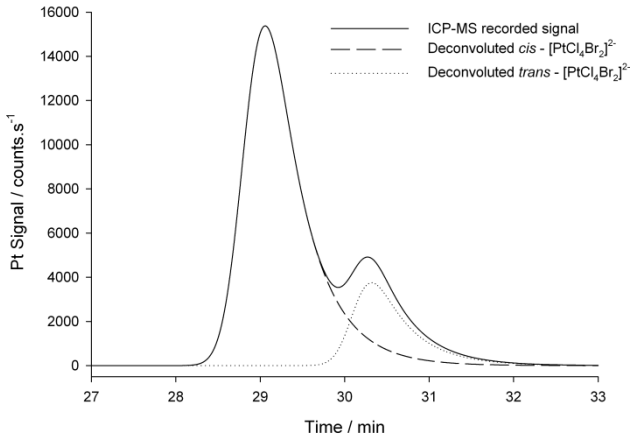

Figure S-4. De-convolution of a typical chromatogram of the *cis*- and *trans*-$[PtCl_4Br_2]^{2-}$ (4^c2^c0 and 4^t2^t0) stereoisomers detected by ICP-MS uing the exponentially modified Gaussian function (eqn.1 in text)

Table S1. Mass balance for the $[PtCl_{6-n}Br_n]^{2-}$ (n = 0 - 6) and $[PtCl_{4-n}Br_n]^{2-}$ (n = 0 – 4) complex anions corresponding to the injection of 7.9 and 4.4 mM solutions, respectively.

Species	Absorbance area at 262 nm / mAU^2	Concentration / mM
Pt^{IV}		
600	4.008	0.182
510	17.19	0.804
4^c2^c0	21.55	1.213
4^t2^t0	6.741	0.488
3^f3^f0	7.171	0.817
3^m30	14.08	1.430
2^c4^c0	6.153	1.309
2^t4^t0	2.178	0.515
150	1.713	0.735
060	0.174	0.060
Total		7.554[b]
Pt^{II}		
400	0.214	0.527
310	1.880	1.331
220[a]	8.060	1.466
130	7.218	0.803
040	1.147	0.205
Total		4.332[b]

[a] Overlapping 2^c20 and 2^t20 isomers which are not resolved under these conditions

[b] The discrepancies observed between the injected and detected amount is attributed to the presence of mono-aquated Pt species in small quantities.

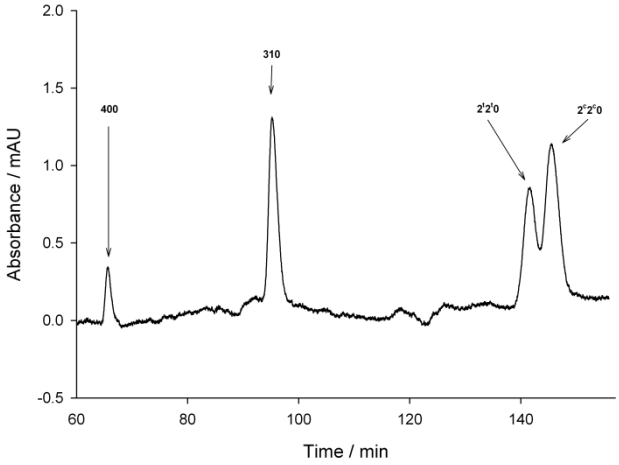

Figure S-5. Chromatogram recorded with UV-Vis detection (262 nm) showing the separation of the stereoisomer species, *trans*-and *cis*-$[PtCl_2Br_2]^{2-}$, using a mobile phase CH_3CN:H_2O (v/v) ratio of 26% and 9.0 mM TBA^+Cl^-.

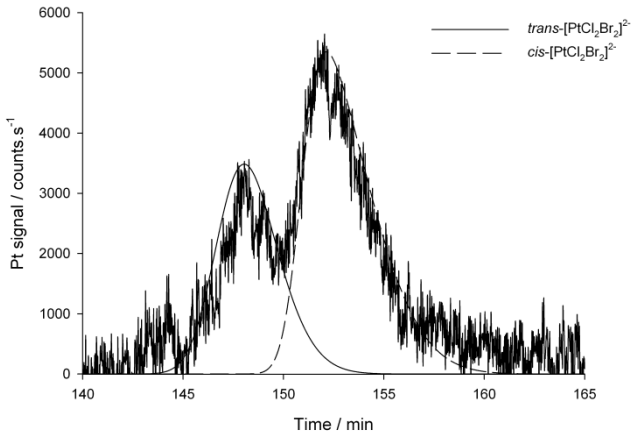

Figure S-6. Deconvolution the chromatogram as detected by ICP-OES of the partially separated *cis*- and *trans*-$[PtCl_2Br_2]^{2-}$ isomers, to estimate the relative concentrations of these species using a mobile phase CH_3CN:H_2O (v/v) ratio of 26% and 9.0 mM TBA^+Cl^-.

3

Direct determination of metal to halide mole ratios in platinum complex anions $[PtCl_{6-n}Br_n]^{2-}$ (n = 0 - 6) by means of HPLC-ICP-OES using Cl, Br and Pt emissions emissions of all separated species

---

JAAS

Cite this: DOI: 10.1039/c2ja10342g

www.rsc.org/jaas

COMMUNICATION

Direct determination of metal to halide mole ratios in platinum complex anions $[PtCl_{6-n}Br_n]^{2-}$ (n = 0–6) by means of HPLC-ICP-OES using Cl, Br and Pt emissions of all separated species†

Pieter-Hugo van Wyk, Wilhelmus J. Gerber and Klaus R. Koch*

Received 29th November 2011, Accepted 30th January 2012
DOI: 10.1039/c2ja10342g

A hyphenated HPLC-ICP-OES method for the direct determination of the metal to ligand mole ratios for the series of individually separated $Pt^{II/IV}$ chlorido–bromido $[PtCl_4]^{2-}$, $[PtCl_6]^{2-}$ and $[PtCl_{6-n}Br_n]^{2-}$ (n = 0–6) species by simultaneous monitoring of the Pt (177.708 nm), Cl (134.724 nm) and Br (148.845 nm) ICP emissions leads to a novel and unambiguous method of chemical speciation of such $Pt^{II/IV}$ complexes in acidic aqueous solutions.

Ion-pairing RP-HPLC coupled to ICP-OES is a powerful tool for the speciation of the platinum group metals (PGMs) in highly acidic, chloride rich solutions of considerable interest to the PGM recovery and refining industry.[1] In such solutions, for example $Pt^{II/IV}$ and Rh^{III} exist as relatively kinetically inert complex halide anions, which can readily be fractionated by chromatographic means into all $[PtCl_{4-n}Br_n]^{2-}$ (n = 0–4), $[PtCl_{6-n}Br_n]^{2-}$ (n = 0–6)[1] and $[RhCl_n(H_2O)_{6-n}]^{3-n}$ (n = 0–6)[2] species, as described recently. The need for unambiguous chemical speciation and the ability to unambiguously quantify the individual complex species containing the same metal centre but with variable ligand to metal ratios is of considerable importance in many diverse fields of application such as in homogeneous catalysis,[3] heavy metal toxicity concerns[4,5] and platinum group metals refining[6,7] to mention but a few. Specifically in the PGM refining industry, the high value of Pt, Rh and associated metals requires maximum recovery efficiencies, so that knowledge and control of chemical speciation of complexes in solutions is of utmost importance to both the primary and secondary PGM refining industry.[1,2,7] The most challenging aspect regarding speciation methods of metal complexes[8] (usually by fractionation coupled to some form of spectroscopic detection system) is the unambiguous assignment of an eluted band(s) of metal complexes. Typical strategies to solve this problem include (i) injection of a solution containing known metal complex species, although this is of limited use since in solution some metal complexes may undergo ligand exchange reactions,[9] such as aquation[1,2,9] and/or hydrolysis equilibria; (ii) exploitation of stepwise ligand exchange reaction kinetics (where known) for species assignment *e.g.* the stereo-specific substitution of successive aquation reactions of the $[RhCl_6]^{3-}$ complex;[10] and (iii) the time-consuming separation and fraction collection, followed by ligand to metal ratio determination using an 'off-line' methodology.[11] To our knowledge no direct method of chemical speciation of PGM complexes in halide rich acidic solutions based on the determination of the metal : ligand (M : L) ratios has been described in the literature.

In this proof-of-concept study we selected the homoleptic $[PtCl_4]^{2-}$, $[PtCl_6]^{2-}$, $[PtBr_6]^{2-}$ and the series of heteroleptic chlorido–bromido Pt^{IV} species $[PtCl_{6-n}Br_n]^{2-}$ (n = 1–5), in which we report a novel hyphenated HPLC-ICP-OES technique with which we directly determine the ligand to metal (L : M) mole ratio of a given complex anion as it elutes from the IP-RP-HPLC column, so to rapidly and unambiguously determine the chemical speciation of $Pt^{II/IV}$ halide complexes, particularly in aqueous solutions. The $Pt^{II/IV}$ complex anions are kinetically relatively inert towards ligand substitution and so may be readily fractionated by means of optimized ion-pair C_{18} reversed phase chromatographic conditions.[1] Separation of these anions by IP-RP-HPLC coupled to an ICP-OES spectrometer, while simultaneously monitoring the Pt (177.708 nm), Cl (134.724 nm) and Br (148.845 nm) emissions allows for the direct coordinated (halide) ligand to metal (L : M) mole ratio determination of all separated species. As we have alluded to previously, the $[PtCl_{6-n}Br_n]^{2-}$ (n = 0–6) complexes may, under certain conditions, also undergo hydrolysis, and some of the aquated species are also separable,[1] for the purposes of this study we chose conditions in which such hydrolysis is minimized. Further work in this regard is in progress. To our knowledge, this is the first report of a hyphenated on-line speciation analysis in which L : M mole ratios have been directly and quantitatively determined for PGMs.

There are relatively few reports in the literature of the use of ICP-OES for the determination of chlorine and bromine, probably in view of the relatively low emissive sensitivity of the halide atoms. Moreover most non-metal atoms/ions emit in the vacuum ultraviolet range below 190 nm,[12] with halides below 160 nm, a detection range not commonly accessible in many ICP-OES spectrometers. Nevertheless it has been shown that Cl, Br and I can satisfactorily be determined in waste oils[12] and milk[13] by means of ICP-OES. More

Platinum Metals Chemistry Research Group, Department of Chemistry and Polymer Science, Stellenbosch University, Private Bag XI, Stellenbosch, 7602, South Africa. E-mail: krk@sun.ac.za; Fax: +2721 808 2344; Tel: +2721 808 3020

† Electronic supplementary information available: Instruments, agents, experimental procedures and additional chromatograms. See DOI: 10.1039/c2ja10342g

generally, ICP-MS has been successfully used for the speciation of halogens or halogen containing substances in for example humic substances,[14] as well as halogen and oxyhalogenide containing substances.[15,16]

The fractionation and ICP-OES detection of the homoleptic $[PtCl_4]^{2-}$, $[PtCl_6]^{2-}$ and a series of ten possible $[PtCl_{6-n}Br_n]^{2-}$ (n = 0–6) complex anions using IP-RP-HPLC, coupled to an ICP-OES spectrometer while monitoring Pt, Cl and Br emissions at 177.708 nm, 134.724 nm and 148.845 nm respectively are shown in Fig. 1. In order to ensure optimum signal to noise ratios for the weak chloride and/or bromide emissions, it is necessary that excess halide ions are not present in the eluent mobile phase, so that tetrabutylammonium nitrate ($TBA^+NO_3^-$) is used as the ion pairing agent in place of the corresponding chloride salt (TBA^+Cl^-) as previously described.[1] For the injection of only homoleptic $[PtCl_4]^{2-}$ and $[PtCl_6]^{2-}$ complexes, the expected two elution bands are observed in both the 177.708 nm Pt and 134.724 nm Cl chromatographic traces (Fig. 1a).

Any uncoordinated or 'free' Cl^- and Br^- anions possibly present in the sample matrix are relatively weakly retained by the C_{18} column, thus elute within approximately 3.5 minutes, well before the $Pt^{II/IV}$ complex anions (ESI, Fig. S1†). Fig. 1b shows all nine possible $[PtCl_{6-n}Br_n]^{2-}$ (n = 0–5) complex anions[1] mostly separately resolved as observed in the 177.708 nm Pt chromatogram. Due to the absence of a Br^- ion in the $[PtCl_6]^{2-}$ (11.5 min) complex or a Cl^- ligand in the $[PtBr_6]^{2-}$ (24 min) complex only 7 and 8 peaks respectively are detected in the 134.724 nm Cl and the 148.845 nm Br emission detected chromatograms (Fig. 1b). Although baseline separation of the *cis*/*trans*-$[PtCl_4Br_2]^{2-}$, *fac*/*mer*-$[PtCl_3Br_3]^{2-}$ and *cis*/*trans*-$[PtCl_2Br_4]^{2-}$ stereoisomers is possible,[1] for the purposes of this study complete separation of the stereoisomers is unnecessary,‡ so that chromatographic conditions were selected to allow for the shortest overall elution times of the individual species; under these conditions, the stereoisomers virtually co-elute, shown by the poorly resolved peaks at $t_r \approx$ 14, 16 and 18 minutes in Fig. 1b. Nevertheless a well-resolved chromatogram of all the $[PtCl_{6-n}Br_n]^{2-}$ (n = 0–5) species is possible under optimized conditions (ESI, Fig. S2†), demonstrating also that the replacement of TBA^+Cl^- by $TBA^+NO_3^-$ has no marked effect on their separation efficiency. The relative differences in emissive sensitivity of the Pt, Cl and Br lines chosen together with the fractionation of the heteroleptic Pt^{IV} complex anions by the IP-RP-HPLC however necessitated injection of relatively concentrated samples ($Pt_T \approx$ 3.8 mmol L^{-1}) to obtain reasonable *S*/*N* ratios when using the Cl and Br ICP emissions; moreover we used the least sensitive Pt 177.708 nm emission line§ in these experiments.

In order to obtain quantitative Cl/Br : Pt mole ratios of the individual species, the following strategy was followed: (i) the total Pt, Cl and Br emission intensities, and hence $[Pt]_T$, $[Cl^-]_T$ and $[Br^-]_T$ concentrations in a sample, were determined by direct ICP-OES analysis without separation (please refer to ESI†); subsequently, (ii) two independent aliquots of a known quantity of either homoleptic or heteroleptic $Pt^{II/IV}$ complexes were injected into the hyphenated system, one by-passing the separation column to give only a single transient emission peak representing the total amount of Pt and Cl/Br present in this aliquot, followed by a second injection *via* the separation column while recording the Pt and Cl/Br emissions of the separated bands. The various transient emission signals recorded were integrated using the PeakFit® v4.12 software package. The experimentally obtained Pt, Cl^- and Br^- concentrations of each

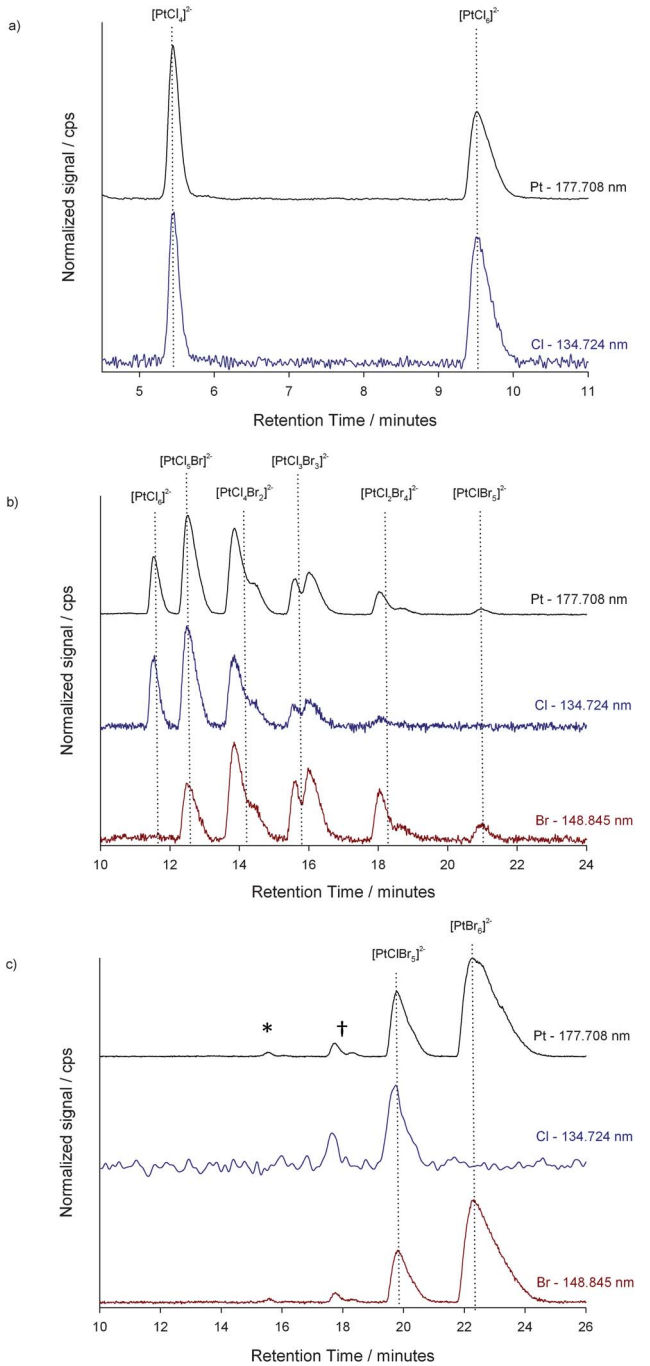

Fig. 1 Normalized chromatograms depicting the elution bands as monitored by 177.708 nm Pt, 134.724 nm Cl and 148.845 nm Br emissions as indicated in (a) $[PtCl_4]^{2-}$ and $[PtCl_6]^{2-}$ species after injection into a C_{18} reversed phase column using a mobile phase $CH_3CN : H_2O$ (v/v) ratio of 55% and 9.0 mM $TBA^+NO_3^-$. (b) shows a total of 9 peaks due to the $[PtCl_{6-n}Br_n]^{2-}$ (n = 0–5) species, although three set at ~14, 16 and 18.5 min are poorly resolved, these being due to stereoisomers using a mobile phase $CH_3CN : H_2O$ (v/v) ratio of 55% and 18.0 mM $TBA^+NO_3^-$. (c) A sample with Cl : Br ratio adjusted (see text) to show mainly the $[PtClBr_5]^{2-}$ and $[PtBr_6]^{2-}$ species using the same mobile phase as in (b). Peaks * and † observed in (c) at ~15.5 and 17.5 min are the isomers of $[PtCl_3Br_3]^{2-}$ and $[PtCl_2Br_4]^{2-}$ respectively (small differences in retention times between (b) and (c) are due to column overload effects).

Table 1 Experimental Pt, Cl^- and Br^- concentrations as determined by means of IP-RP-HPLC-ICP-OES from which the experimental Cl/Br : Pt mole ratios for the $[PtCl_4]^{2-}$, $[PtCl_6]^{2-}$ and $[PtCl_{6-n}Br_n]^{2-}$ ($n = 0$–6) species were determined as compared to the expected ratios[b]

	Experimental concentration/mmol L^{-1}			Expt. L : Pt mole ratio	
	Pt	Cl	Br	Cl/Pt	Br/Pt
$[PtCl_4]^{2-}$ and $[PtCl_6]^{2-}$					
$[PtCl_4]^{2-}$	0.336 ± 0.005	1.39 ± 0.087	—	4.2 ± 0.25	—
$[PtCl_6]^{2-}$	0.388 ± 0.005	2.42 ± 0.152	—	6.2 ± 0.40	—
$[PtCl_{6-n}Br_n]^{2-}$ ($n = 0$–5)					
$[PtCl_6]^{2-}$	1.330 ± 0.018	7.96 ± 0.500	—	6.0 ± 0.38	—
$[PtCl_5Br]^{2-}$	3.289 ± 0.046	16.94 ± 1.060	3.46 ± 0.154	5.1 ± 0.33	1.0 ± 0.05
$[PtCl_4Br_2]^{2-}$	3.720 ± 0.052	14.83 ± 0.924	7.36 ± 0.330	4.0 ± 0.25	2.0 ± 0.09
$[PtCl_3Br_3]^{2-}$	2.224 ± 0.031	7.26 ± 0.455	6.59 ± 0.295	3.2 ± 0.21	2.9 ± 0.14
$[PtCl_2Br_4]^{2-}$	0.836 ± 0.011	—[a]	3.47 ± 0.155	—[a]	4.1 ± 0.19
$[PtClBr_5]^{2-}$	0.167 ± 0.002	—[a]	0.87[b] ± 0.039	—[a]	5.2 ± 0.24
$[PtCl_{6-n}Br_n]^{2-}$ ($n = 5$–6)					
$[PtClBr_5]^{2-}$	2.965 ± 0.042	3.33 ± 0.085	14.70 ± 0.657	1.1 ± 0.07	5.0 ± 0.23
$[PtBr_6]^{2-}$	8.828 ± 0.124	—	55.38 ± 2.475	—	6.2 ± 0.29

[a] Concentrations below the LOD (3σ). [b] Concentrations between LOD (3σ) and LOQ (10σ); LOQs calculated for Pt, Cl^- and Br^- were 9.8×10^{-3}, 2.24 and 0.97 mmol L^{-1}.

complex, Table 1, were determined by relating the total Pt, Cl^- and Br^- emission intensities ($[Pt]_T$, $[Cl^-]_T$ and $[Br^-]_T$) of each injected sample to the mole-fraction of Pt, Cl^- and Br^- attributable to each individual complex in that sample (Fig. 1a–c). Thus to determine the chlorido ligand concentration $[Cl^-]$, bound to a given complex, *e.g.* $[PtCl_5Br]^{2-}$, the equation $[Cl^-]_{[PtCl_5Br]^{2-}} = [Cl^-]_T \frac{A_{Cl^-}}{A_{\text{Total Cl}^-}}$ was used where $[Cl^-]_T$ is the total Cl^- concentration in solution, A_{Cl-} is the area of the elution band of the $[PtCl_5Br]^{2-}$ anion in the 134.724 nm Cl chromatographic trace; $A_{\text{Total Cl}-}$ is obtained from the transient emission peak when by-passing the column resulting in the total Cl concentration present in this aliquot. The corresponding total $[Pt]_T$, $[Cl^-]_T$ and $[Br^-]_T$ concentrations determined by ICP-OES directly give typical limits of detection (LOD, 3σ) for Pt, Cl and Br of 0.88, 67.1 and 8.26 μmol L^{-1} respectively, with good reproducibility. By contrast, the corresponding LODs obtained when using HPLC-ICP-OES are considerably higher at 2.97×10^{-3}, 0.67 and 0.29 mmol L^{-1} for Pt, Cl and Br respectively, as may be expected due to the fractionation of the complex species and some chromatographic band-broadening before detection. Nevertheless this approach is suitable for the determination of the Cl/Br : Pt mole ratio of these complexes at sub-millimolar concentrations as confirmed in Table 1.

The halide (Cl^-, Br^-) to Pt mole ratios calculated from the elemental concentrations agree remarkably well with those expected for the authentic separated complex species, as confirmed in Table 1. Although the concentrations of some complex species were present at, or below, the limits of detection/quantification (LOD/Q) of Cl^- or Br^-, Table 1, this problem can be circumvented by preparing a sample with a higher free Br^- concentration in order to alter the $[PtCl_{6-n}Br_n]^{2-}$ ($n = 0$–6) species distribution, Fig. 1c. The alternative of injecting more concentrated samples was not done, since signs of column overload were already evident (Fig. 1b and c), which results in further loss of resolution.

In conclusion, successful direct determination of the L : Pt mole ratios for $[PtCl_4]^{2-}$ and the series of $[PtCl_{6-n}Br_n]^{2-}$ ($n = 0$–6) complexes using HPLC-ICP-OES based on the Pt and Cl/Br emissions as a means of quantitative detection is readily possible with this hyphenated technique. This is a simple new method for the unambiguous chemical speciation of such complexes based on the determination of the Pt : halide mole ratio of individually separated species, which is not dependent on their relative chromatographic retention times, which may not always be entirely reliable.

Moreover the potential application of this methodology for the identification of other relevant species such as for example the *aquated* and/or *hydrolyzed* chlorido–bromido $Pt^{II/IV}$ species of relevance to efficient PGM recovery and refining, as well as separable PGM complexes containing ligands with donor atoms such as S, P and N, is currently being actively studied by us.

Acknowledgements

Financial support from Angloplatinum Ltd., the University of Stellenbosch and the NRF is gratefully acknowledged.

Notes and references

‡ These stereoisomers have the same numerical Cl/Br : Pt mole ratios.
§ We chose deliberately a less sensitive Pt emission line to match the relatively weak emission intensity of Cl and Br which require larger integration times to obtain good S/N ratios and avoid detector saturation observed for the more intense Pt lines using these settings. In Fig. S2, we chose a more intense Pt emission line at 214.423 nm.

1 P.- H. Van Wyk, W. J. Gerber and K. R. Koch, *Anal. Chim. Acta*, 2011, **704**, 154–161.
2 W. J. Gerber, K. R. Koch, E. C. Hosten and T. E. Geswindt, *Talanta*, 2010, **82**, 348–358.
3 H. Chen, R. Tagore, G. Olack, J. S. Vrettos, T. Weng, J. Penner-Hahn, R. H. Crabtree and G. W. Brudvig, *Inorg. Chem.*, 2007, **46**, 34–43.
4 D. P. Persson, T. H. Hansen, P. E. Holm, J. K. Schjoerring, H. C. B. Hansen, J. Nielsen, I. Cakmak and S. Husted, *J. Anal. At. Spectrom.*, 2006, **21**, 996–1005.
5 Y. Jya-Jyun and M. Wai, *Anal. Chem.*, 1991, **36**, 842–845.
6 G. J. Berfeld, A. J. Bird and R. I. Edwards, in *Gmelin Handbook of Inorganic Chemistry*, Springer-Verlag, Berlin, 8th edn, 1986, Suppl. vol. A1, pp. 8–30.
7 R. A. Grant, F. L. Bernardis and D. C. Sherrington, *React. Funct. Polym.*, 2005, **65**, 205–217.
8 D. M. Templeton, F. Ariese, R. Cornelis, L. G. Danielsson, H. Muntau, H. P. van Leeuwen and R. Loinski, *Pure Appl. Chem.*, 2000, **72**, 1453–1470.

9 G. Peters, W. Preetz and D. Bublitz, *Chem. Rev.*, 1996, **96**, 977–1026.
10 M. J. Pavelich and G. M. Harris, *Inorg. Chem.*, 1973, **12**, 423–431.
11 E. E. Mercer, W. M. Campbell and R. M. Wallace, *Inorg. Chem.*, 1964, **3**, 1018–1024.
12 K. Krengel-Rothensee, U. Richter and P. Heitland, *J. Anal. At. Spectrom.*, 1999, **14**, 699–702.
13 J. Naozuka, M. A. Mesquita Silva da Veiga, P. V. Oliveira and E. de Oliveira, *J. Anal. At. Spectrom.*, 2003, **18**, 917–921.
14 G. Rädlinger and K. G. Heumann, *Fresenius J. Anal. Chem.*, 1997, **359**, 430–433.
15 Z. L. Chen, M. Megharaj and R. Naidu, *Chromatographia*, 2007, **65**, 115–118.
16 M. Pantsar-Kallio and P. K. G. Manninen, *Anal. Chim. Acta*, 1998, **360**, 161–166.

Supporting Information

Experimental

HPLC grade acetonitrile was obtained from Merck (608-001-00-3). All aqueous solutions were prepared using ultrapure Milli-Q water (› 18MΩ). Analytical grade purity tetrabutylammonium nitrate ($TBA^+NO_3^-$), sodium acetate and glacial acetic acid were obtained from Sigma-Aldrich. Mobile phases were prepared by the addition of acetonitrile to stock solutions of 0.05 M tetrabutylammonium nitrate and 0.1 M acetate buffer (pH = 4.6) to give 55% (v/v) CH_3CN:H_2O solutions. All mobile phases were filtered through 0.45 μm HV filters (Millipore Corporation, HVLP04700) under vacuum and degassed for 15 min in an ultrasonic bath before use. $Na_2PtCl_6 \cdot 2H_2O$ (Johnson Matthey PLC, Precious metals division) was of analytical reagent grade quality and was dried in vacuo and stored in a desiccator prior to use.

ICP-OES

Determination of the samples Pt, Cl^- and Br^- concentrations was accomplished with a SPECTRO Arcos ICP-OES spectrometer operating with a RF power set to 1400 W using a Burgener T2002 nebulizer and cyclonic spray chamber. The nebulizer flow rate was set at 0.8 $mL.min^{-1}$, auxiliary gas flow rate was set to 1 $L.min^{-1}$ and coolant flow rate to 13 $L.min^{-1}$. Pt standard solutions were prepared from a 1000 ppm ± 3 ppm stock solution in a 500 mL 10% HCl matrix obtained from De Bruyn Spectroscopy (Ultraspec). Cl^- and Br^- standard solutions were prepared from NaCl and NaBr (puriss; 99 %) obtained from Sigma-Aldrich, respectively. NaCl and NaBr was dried at 60ºC for 1 day and cooled in a vacuo desiccator prior to preparation of the relevant standard solutions. Matrix matching was strictly upheld throughout the preparation of all the standard solutions (Pt, Cl^- and Br^-). The Pt, Cl^- and Br^- concentrations obtained by means of ICP-OES for the samples 1, 2 and 3 used to obtain Figures 1a, b and c respectively, shown in Table S1.

IP-RP-HPLC-ICP-OES

The column used throughout this study was a Gemini C18, 250 mm x 4.6 mm i.d., 5 µm particles. Column conditioning comprised of mobile phase passage through the column for 45 minutes prior to analysis followed by a 45 minute post-analysis wash with pure acetonitrile. Platinum samples, Table S1, were prepared in an HCl matrix. The bromido Pt^{IV} species was obtained by the addition of appropriate amounts of NaBr, Table S1. Prior to injection each Pt sample was diluted 3 times and injected as a 40µl aliquot onto the C18 reversed phase column unless stated otherwise. The HPLC hyphenated ICP-OES setup comprised of a Varian *Prostar* liquid chromatograph equipped with a binary 210 solvent delivery module and a 410 autosampler operating at an optimized flow rate of mobile phase of 0.8 $mL.min^{-1}$ connected to the same SPECTRO *Arcos* ICP-OES spectrometer mentioned above, operating with a RF power set to 1600 W using a Burgener T2002 nebulizer and cyclonic spray chamber. The nebulizer flow rate was set to 0.6 $mLmin^{-1}$, auxiliary gas flow to 2 $L.min^{-1}$, and coolant flow rate to 17 $L.min^{-1}$. The aliquot was transferred directly from the column to the nebulizer *via* PEEK tubing with internal diameter equal to 0.12 mm.

Table S1. Total experimental Pt, Cl^- and Br^- concentrations as determined by means of ICP-OES directly for the 3 samples used in this study. Samples were prepared by the addition of 2.0 M stock solutions containing appropriate quantities of HCl and NaBr to weighed amounts of Na_2PtCl_6 to give a known [Pt] ~ 10 mM in 5 ml. These samples were diluted three times with the relevant mobile phase before injection.

Sample	Experimental concentration of samples prepared prior to injection (mol L^{-1})		
	Pt	Cl^-	Br^-
1	0.0127 ± 0.0002	0.1550 ± 0.0053	–
2	0.0125 ± 0.0002	0.1580 ± 0.0054	0.0246 ± 0.0002
3	0.0160 ± 0.0002	0.0840 ± 0.0033	0.2362 ± 0.0021

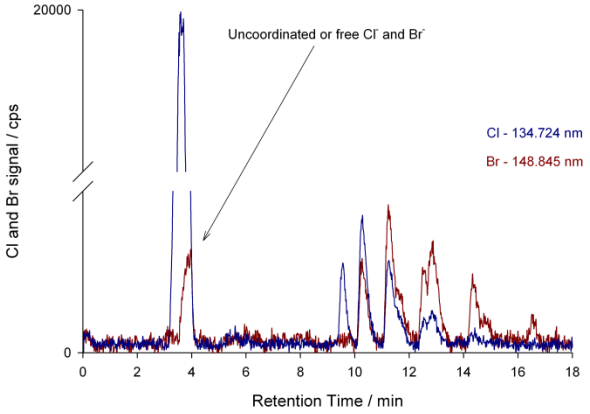

Figure S1. Chromatograms depicting the elution bands of the uncoordinated or free Cl^- and Br^- in the sample matrix, as well as the 9 $[PtCl_{6-n}Br_n]^{2-}$ (n = 0 – 6) species as monitored by 134.724 nm Cl and 148.845 nm Br emissions. Both chromatograms were obtained after injection of the relevant sample onto a C_{18} RP column using a mobile phase CH_3CN:H_2O (v/v) ratio of 55% and 9.0 mM $TBA^+NO_3^-$.

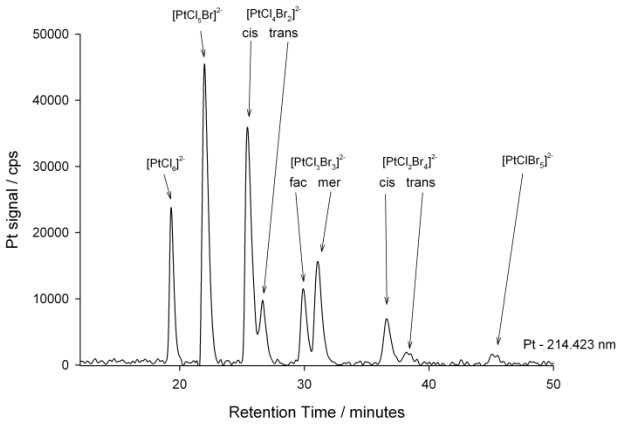

Figure S3. Chromatogram of the 9 $[PtCl_{6-n}Br_n]^{2-}$ (n = 0 – 5) species as monitored by the 214.423 nm Pt ICP emission after injection of a 20 µl aliquot sample onto a C_{18} RP column using a mobile phase CH_3CN:H_2O (v/v) ratio of 55% and 18.0 mM $TBA^+NO_3^-$.

4 An ion-pairing reversed phase UHPLC-ESI-Q-TOF-MS method for the characterization of $[Pt^{IV}Cl_{6-n}Br_n]^{2-}$ (n = 0 – 6) and mono-aquated $[Pt^{IV}Cl_{5-n}Br_n(H_2O)]^-$ (n = 0 – 5) species at the sub parts per million range

An ion-pairing reversed phase UHPLC-ESI-Q-TOF-MS method for the characterization of $[Pt^{IV}Cl_{6-n}Br_n]^{2-}$ (n = 0 – 6) and mono-aquated $[Pt^{IV}Cl_{5-n}Br_n(H_2O)]^{-}$ (n = 0 – 5) species at the sub parts per million range

Introduction

The ability of platinum to facilitate both oxidation and reduction reactions[1] makes it an important constituent of many catalysts, as exemplified by the automotive emission control device (catalytic converter) which simultaneously oxidizes CO to CO_2 and H_2O and reduces NO_x to N_2.[2] Approximately 10 g of platinum group metals (PGMs)[3] are used in each converter which accounts for over 50% of the world's Pt demand in recent years.[4] These applications have stimulated a large number of studies focused on the synthesis of Pt nanocrystals and their morphological control using $[PtCl_6]^{2-}$ as a precursor.[5-8] Yu *et al* have shown that Pt nanocrystal morphology differs significantly when the precursor changes from $[PtCl_6]^{2-}$ to a mixture of $[PtCl_6]^{2-}$ and $[PtCl_5H_2O]^{-}$.[9] As a case in point, recently the formation of Pt-Pd bimetallic nanocrystals through a bromide-induced galvanic replacement reaction has been described.[10] However, in this study Xia *et al* somewhat simplified the formation of the $[PtBr_6]^{2-}$ species from the $[PtCl_6]^{2-}$ precursor by neglecting the stepwise ligand exchange reactions that furnish several mixed-ligand chlorido-bromido Pt^{IV} species.[4] Depending on the solution pH, ionic strength and the concentration of halide ligands, several mixed ligand Pt^{IV} species such as $[PtCl_{6-n}(H_2O)_n]^{n+2-}$ (n = 0 – 6), $[PtCl_{6-n}(OH)_n]^{2-}$ (n = 0 – 6), $[PtCl_{6-n}Br_n(OH)]^{2-}$ (n = 0 – 6), $[PtCl_{6-n}Br_n]^{2-}$ (n = 0 – 6) and $[PtCl_{5-n}Br_n(H_2O)]^{-}$ (n = 0 – 5) may be present in solution in varying quantities.[11,12] The characterization and quantification of such species, typically at sub parts per million (ppm) concentration range,[8,9] is critical in order to evaluate which Pt^{IV} species, or combination of species, are transformed to a particular bimetallic or Pt nanocrystal morphology.

High resolution ^{195}Pt NMR is a proven technique for species assignment and in some cases structural information of individual species can be deduced, e.g. stereoisomers such as *cis*- and *trans*-$[PtCl_4(H_2O)_2]$.[11-16] However, the low receptivity of the ^{195}Pt nucleus limits these analyses to relatively concentrated Pt solutions (> 50 mM). We have recently reported an ion-pairing reversed phase high performance liquid chromatography-inductively coupled plasma-optical

emission spectroscopy (HPLC-ICP-OES) method capable of the separation, characterization and quantification of $Pt^{II/IV}$ chlorido-bromido complexes in well-defined acidic solutions at much lower concentrations than is possible by ^{195}Pt NMR.[17] Characterization was performed by determining metal-to-ligand ratios of separated species.[17] However, apart from the good limits of quantification (LOQs) obtained for the Pt emission line (177.708 nm, 1.9 ppm), the relatively low sensitivity of the Cl (134.742 nm) and Br (148.845 nm) emission lines (LOQ's of 79 and 77 ppm, respectively) prevents characterization of Pt^{IV} species at low or sub ppm levels. Moreover, ligands containing elements that are also present in the mobile phase could not be quantified using this approach due to high background noise.

For example, Schramel *et al*[18] reported the direct infusion electrospray ionization mass spectrum for a Cu^{II} chlorido complex and found that the parent ions undergo extensive fragmentation. However, the relatively high sensitivity of the latest generation of time-of-flight mass spectrometry instruments prompted us to investigate whether characterization of Pt^{IV} aquo-chlorido-bromido species present in relatively low abundance (*vide infra*) would be possible using this technique. Moreover, to achieve our overarching objective of eventual quantification of all the Pt^{IV} species mentioned above, by means of LC-ICP-OES using the 214.423 nm Pt emission line, prohibits the use of direct infusion ESI-MS. In this manuscript we therefore describe the development of an ion-pairing ultra high pressure liquid chromatography ESI-quadrupole-TOF mass spectrometry (UHPLC-ESI-Q-TOF-MS) method and apply it first in a proof-of-principle study to characterize the $[PtCl_{6-n}Br_n]^{2-}$ (n = 0 – 6) anionic complexes by means of comparison of the high resolution mass spectra of isotopologue[‡] intensities with those theoretically calculated. The UHPLC-ESI-Q-TOF-MS method was then used to characterize the aquated series of species $[PtCl_{5-n}Br_n(H_2O)]^-$ (n = 0 – 5), that contain several stereoisomer pairs (Reaction scheme 1) present in well-defined solutions at low abundance. To the best of our knowledge this is the first speciation method that can separate and characterize these inorganic complexes at the sub-ppm range.

[‡] Isotopologue refers to chemical species that differ only in isotopic composition of their molecules or ions. Isotopomers are isomers with the same amount of each isotopic atom, differing in their position in the molecule or ion.[19]

Experimental

Reagents

Acetonitrile and methanol (Romil far UV grade) were supplied by Microsep (Johannesburg, South Africa), analytically pure formic acid and tributylamine (TriBA) were acquired from Sigma-Aldrich (Johannesburg, South Africa). All aqueous solutions were prepared using ultrapure Milli-Q water (>18MΩ) (Millipore Corporation, Millford, MA, USA). The $Na_2PtCl_6 \cdot 2H_2O$ and K_2PtBr_6 salts (Johnson Matthey PLC, Precious Metals Division) were of analytical reagent grade quality and stored in a desiccator prior to use.

Liquid chromatographic separation

All LC-ESI-MS analyses were performed on a Waters Acquity ultra performance liquid chromatograph (UPLC) fitted with a photodiode array (PDA) detector and autosampler. Separation was achieved at room temperature on a Waters Acquity BEH C18 column (2.1 x 100 mm) packed with 1.7 µm particles at a flow rate of 0.28 $ml.min^{-1}$. The mobile phase consisted of 18 mM TriBA with 36 mM formic acid as solvent A and methanol as solvent B. TriBA (pKa = 10.7) is protonated under these mobile phase conditions. The gradient started with 30% solvent B for the first 8 minutes followed by a linear gradient over 4 minutes to 45% solvent B and to 100% B over the next minute. The column was re-equilibrated for 3 minutes.

HPLC-UV-Vis analyses were performed on an Agilent 1260 Infinity system fitted with a photodiode array (PDA) detector and autosampler (Agilent Technologies, Waldronn, Germany). Separation was achieved at room temperature on a Gemini (Separations, Johannesburg, South Africa) C18 column (4.6 x 250mm) packed with a 5 µm particle size at a flow rate of 0.8 $ml.min^{-1}$. Chromatographic traces were recorded using the 262 and 315nm wavelengths. The mobile phase consisted of 18 mM TriBA with 36 mM formic acid as solvent A and methanol or acetonitrile as solvent B.

Mass spectrometry

All MS experiments were performed on a Waters Synapt G2 Q-TOF mass spectrometer equipped with an ESI source (Waters, Milford, MA, USA). The mass spectrometer was calibrated with sodium formate and leucine enkephalin was used as lock mass for accurate mass

determinations. A desolvation temperature of 275 ºC and desolvation gas (N_2) flow rate of 650 $l.h^{-1}$ was used. The rest of the MS settings were selected for best sensitivity. Data were acquired in continuum mode over a mass range of 200-1200 amu using a 0.5 second scan time.

All direct infusion experiments were carried out with electrospray ionization applied in the negative mode employing a capillary voltage of 2.5 kV, and varying sample cone voltages (15 - 100 V) as seen in Figure 1.

For all UHPLC-ESI-MS experiments negative mode electrospray ionization was performed using a capillary voltage of 2 kV and sample cone voltage of 5V.

Sample preparation

The $[PtCl_{6-n}Br_n]^{2-}$ (n = 0 – 6) samples were prepared by addition of the $Na_2PtCl_6{\cdot}2H_2O$ and K_2PtBr_6 salts such that $[Pt]_T$ = 10 mM in a sample matrix of 0.2 M $[Br^-]$ and 0.8 M $[Cl^-]$ for the sample shown in Figure 2a and 0.5 M $[Br^-]$ and 0.5 M $[Cl^-]$ for the sample shown in Figure 2b. The $[PtCl_{5-n}Br_n(H_2O)]^-$ (n = 0 – 5) sample was prepared by addition of the $Na_2PtCl_6{\cdot}2H_2O$ and K_2PtBr_6 salts with $[Pt]_T$ = 10 mM in Milli-Q H_2O such that the Cl^-:Br^- mole ratio was 1:1. All samples used in UHPLC-ESI-Q-TOF-MS analyses were diluted 5 fold directly prior to injection and were injected as 5µl aliquots. Samples used in HPLC-UV-Vis analyses were diluted 15 fold prior to injection and were injected as 20 µl aliquots.

Results and Discussion

Upon mixing solutions containing the homoleptic $[PtCl_6]^{2-}$ and $[PtBr_6]^{2-}$ complex anions, ligand exchange occurs and eight additional chlorido-bromido $[PtCl_{6-n}Br_n]^{2-}$ (n = 1 – 5) species forms, Reaction scheme 1, which are classified as the heteroleptic species. In acidic, halide deficient solutions the $[PtCl_{6-n}Br_n]^{2-}$ (n = 0 – 6) species can undergo partial aquation, leading to the formation of at most 12 mono-aquated $[PtCl_{5-n}Br_n(H_2O)]^{-}$ (n = 0 – 5) complex anions, Reaction scheme 1, and several di-aquated $[PtCl_{4-n}Br_n(H_2O)_2]$ (n = 0 – 4) species.

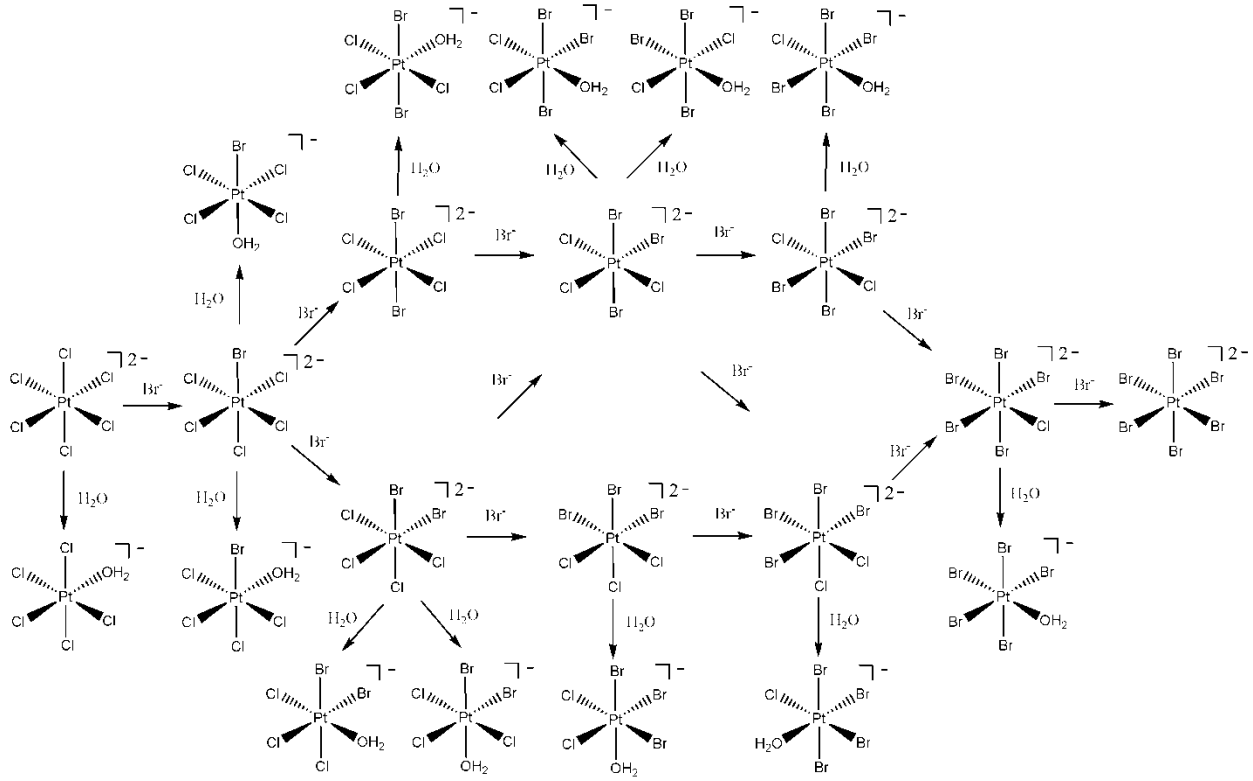

Reaction scheme 1. The stepwise exchange of a Cl^- with a Br^- from $[PtCl_6]^{2-}$ to $[PtBr_6]^{2-}$ resulting in the formation og the $[PtCl_{6-n}Br_n]^{2-}$ (n = 0 – 6) species. Partial aquation of these species results in the formation of the mono-aquated $[PtCl_{5-n}Br_n(H_2O)]^{-}$ (n = 0 – 5) species.

Schramel *et al*[18] have shown that for metal halido complexes, unlike highly covalently bonded organometallic compounds, a high degree of fragmentation occurs during ESI-MS analysis and that the parent ion can be 'directly' observed in the MS at a relatively low cone voltage. In order to ascertain the fragmentation behavior of the $[PtCl_6]^{2-}$ complex anion we performed direct infusion ESI-Q-TOF-MS analysis of a 1 mM Pt solution (11.2 mg $Na_2PtCl_6{\cdot}2H_2O$ dissolved in 20 ml acetonitrile). The cone voltage was varied from 15 to 100 V and the mass spectra obtained are shown in Figure 1. The $[PtCl_6]^{2-}$ complex anion dissociates into several fragments; the extent

of fragmentation increases as the cone voltage is raised.[20] The natural abundances of the stable isotopes of Pt (^{194}Pt, ^{195}Pt, ^{196}Pt) and Cl (^{35}Cl, ^{37}Cl) yield a characteristic isotopologue peak pattern for each charged complex, which in conjunction with high resolution mass spectral data can be used as a 'fingerprint' to identify a given Pt species. Applying this to the set of peaks in the *m/z* range 201.891-206.889 which are separated by half *m/z* units allows for the identification of the doubly charged $[H_2PtCl_6]^{2-}$ anion, Figure 1, and is confirmed by the excellent agreement between the experimental isotopologue peak pattern intensities and *m/z* with those calculated. The same set of peaks, measured on a relatively low mass resolution system, was previously incorrectly assigned to the parent ion, $[PtCl_6]^{2-}$.[20] The parent molecular ion is instead observed as a sodium ion-pair adduct, $[Na+M]^-$, at the exact *m/z* ratios from 426.765 to 434.757 amu. The most intense set of peaks in Figure 1a, *m/z* range 368.808-376.804, correspond to a singly charged anion containing 1 Pt and 5 Cl atoms, $[Pt^{IV}Cl_5]^-$. As the cone voltage is increased, Figures 1b to d, the abundance of this peak decreases and the relative percentage of the lower oxidation state Pt species increase by a 'stepwise' reduction of Pt^{IV} in the gas phase.[20] These Pt species that form in the gas phase range from the rare Pt^{III} and Pt^{I} oxidation states present in the form of $[Pt^{III}Cl_4]^-$, *m/z* 333.838-341.838, and $[Pt^{I}Cl_2]^-$, *m/z* 263.895-269.895, respectively, to the well-known 'stable' (in solution) Pt^{II} oxidation state species, in the form of a $[Pt^{II}Cl_3]^-$, *m/z* 298.840-304.841. A density functional theory (DFT) study is currently in progress to elucidate the structure and reactivity of these species in the gas phase.

When it is taken into consideration that several additional Pt^{IV} species $\{[PtCl_{6-n}(H_2O)_n]^{n+2-}$ (n = 0 – 6), $[PtCl_{6-n}(OH)_n]^{2-}$ (n = 0 – 6) and $[PtCl_{6-n}Br_n]^{2-}$ (n = 0 – 6)$\}$ of similar composition may be present in solution that can yield several overlapping fragment ions, coupled to the fact that some parent ions are not detected (*vide infra*), as well as the inability to quantify individual complexes will decidedly complicate a speciation study in solution using direct infusion ESI-MS. Separation of such complexes prior to analysis by ESI-Q-TOF-MS is thus critical and necessitated the development of a LC-MS for the characterization of these Pt^{IV} complexes.

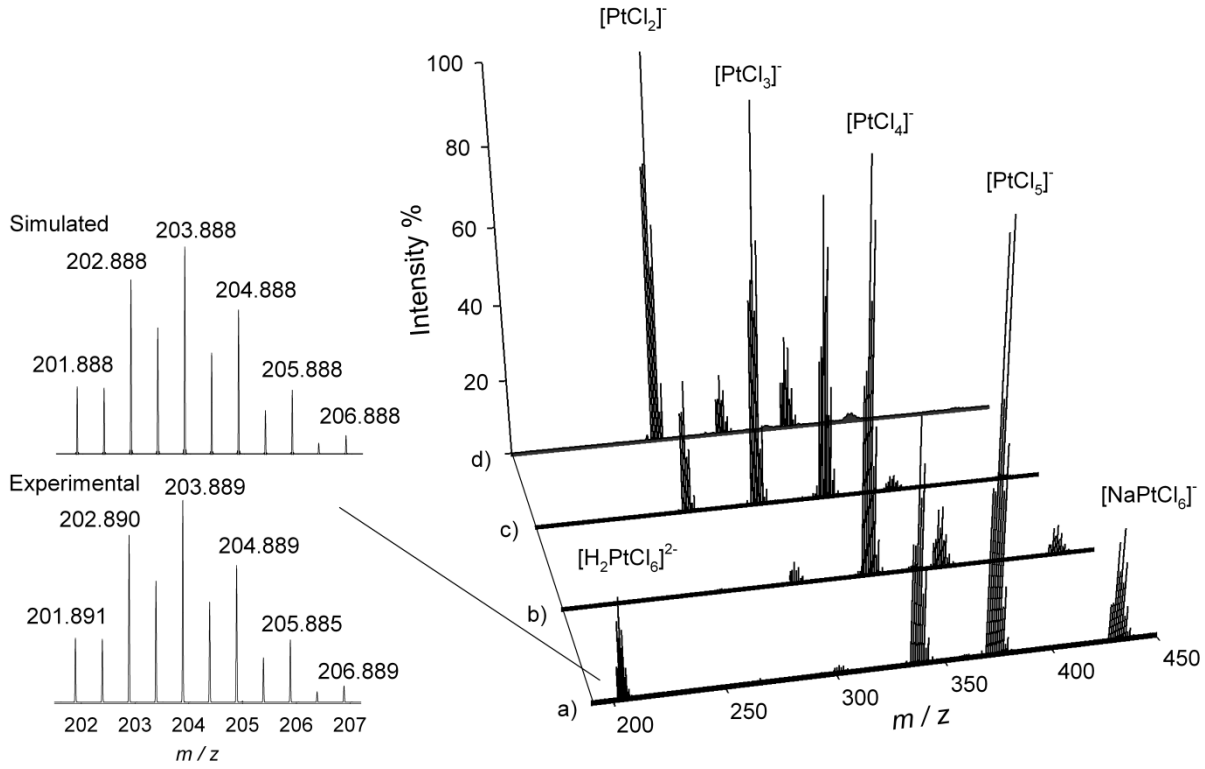

Figure 1. High resolution ESI mass spectra observed for the direct infusion the $[PtCl_6]^{2-}$ species as a function of cone voltage; (a) 15 V, (b) 25 V, (c) 50 V and (d) 100 V. The insert displays the simulated and experimental isotopic distributions and *m/z* values for the $[H_2PtCl_6]^{2-}$ anion.

We have recently developed a hyphenated reversed phase ion-pair HPLC-(UV-Vis)-(ICP-MS)-(ICP-OES) method for the separation and quantification of the $[PtCl_{6-n}Br_n]^{2-}$ (n = 0 – 6) anionic complexes using tetrabutyl ammonium chloride (TBA^+Cl^-) as ion-pairing reagent.[17] However, the incompatibility of such a non-volatile ion-pair reagent with ESI-MS is well documented.[21] In light of this, the abovementioned method was modified to facilitate LC hyphenation to MS by using a 'volatile' ion pairing reagent, tributylamine (TriBA).[21] Moreover, the mobile phase composition of acetic acid/sodium acetate and acetonitrile used previously[4,17] caused high background interference in the ESI-MS, and were replaced by formic acid and methanol, respectively. This change has its own drawbacks, although manageable (*vide infra*). Furthermore, the disparity between the optimal flow rate used in HPLC (0.8 $ml.min^{-1}$) and sample optimal uptake rate into the ESI source (~0.3 $ml.min^{-1}$), means a large portion of the sample is lost to waste by post-column splitting. Decreasing the flow rate used in HPLC as alternative would lead to unwanted band broadening and a loss of sensitivity. In contrast, typical narrow-bore UHPLC columns provide optimal flow rates ideally compatible to MS detection. In

addition, the high efficiency of these columns allows for relatively short columns and analysis times, further improving sensitivity.[22]

Injection of samples containing differing amounts of the individual $[PtCl_{6-n}Br_n]^{2-}$ (n = 0 – 6) complex anions yielded the UV-Vis and total ion chromatographic traces shown in Figures 2a - 2b and 2c - 2d, respectively. The stereoisomer species, *cis*- and *trans*-$[PtCl_4Br_2]^{2-}$/$[PtCl_2Br_4]^{2-}$ and *mer*- and *fac*- $[PtCl_3Br_3]^{2-}$, Scheme 1, are not distinguishable by MS, thus chromatographic conditions were chosen to ensure co-elution of these complexes (t_R = 12.4, 12.7 and 13.0 min, respectively, Fig 2a and b) for optimal signal to noise (S/N) ratios. Experimental conditions were selected to provide relatively high retention times for the $[PtCl_{6-n}Br_n]^{2-}$ (n = 0 – 6) species, Figures 2a to d, taking into consideration the $[PtCl_{5-n}Br_n(H_2O)]^{-}$ (n = 0 – 5) species, which when present elute before the $[PtCl_{6-n}Br_n]^{2-}$ (n = 0 – 6) complex anions (*vide infra*). The total ion chromatograms, Figs. 2c and d, display the 7 elution bands expected for the $[PtCl_{6-n}Br_n]^{2-}$ (n = 0 – 6) complex anions, as well as 3 additional peaks barely visible in the UV-Vis chromatographic traces identified with asterisks. The latter elution bands have not previously been observed in the chromatographic traces of the $[PtCl_{6-n}Br_n]^{2-}$ (n = 0 – 6) series when using a TBA^+Cl^-/acetonitrile/acetate buffer mobile phase and UV-Vis or ICP-MS/OES as detectors and will be discussed later.[4,17]

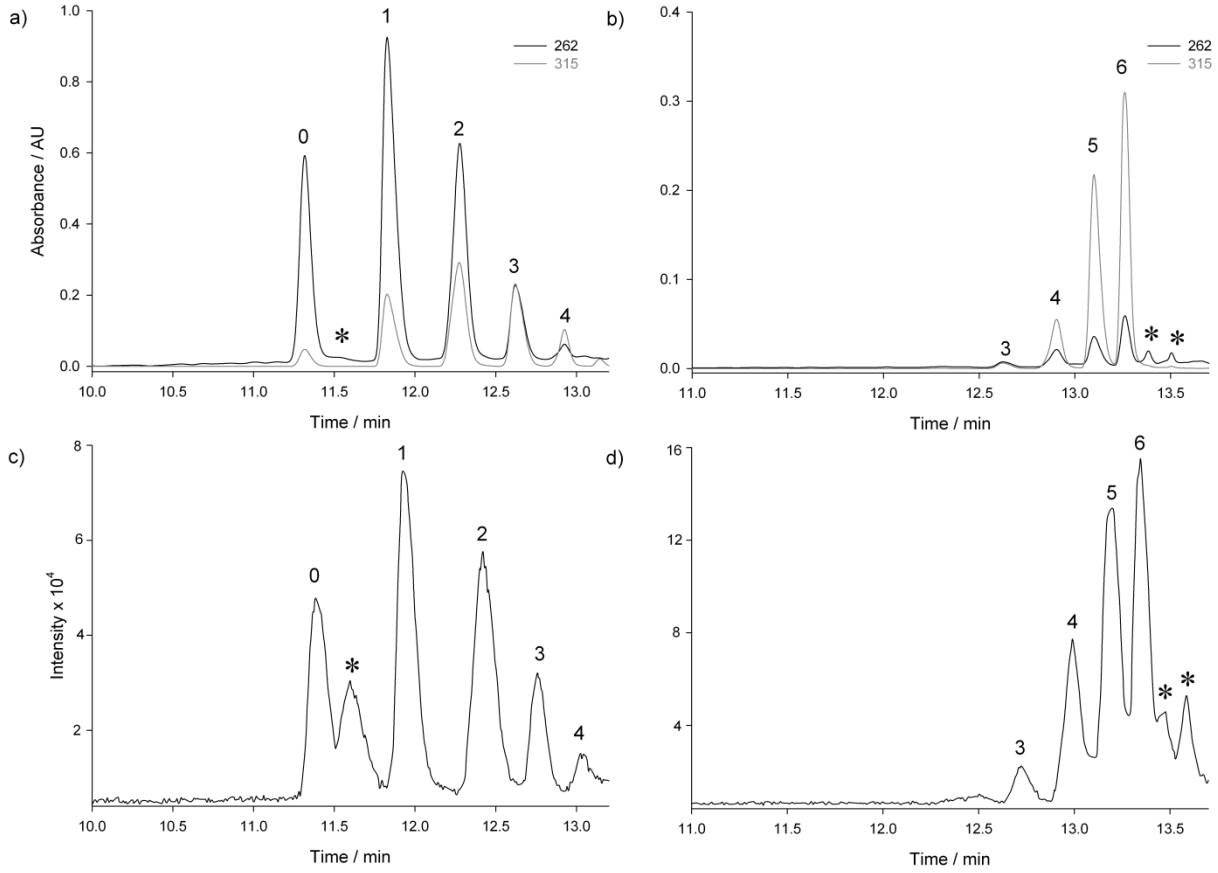

Figure 2. UHPLC-UV chromatograms of (a) the chlorido dominated (262 nm) and (b) bromido dominated (315) $[PtCl_{6-n}Br_n]^{2-}$ (n = 0 – 6) species. The corresponding UHPLC-MS total ion chromatograms are shown in (c) and (d), respectively. Peak numbering corresponds to n in the $[PtCl_{6-n}Br_n]^{2-}$ (n = 0 – 6) formula. (*) denotes on-column reaction products resulting from interaction between the Pt^{IV} complexes and the mobile phase.

The high resolution ESI mass spectrum of the $[PtCl_6]^{2-}$ complex (t_R = 11.4 min, Fig 2a) is shown in Fig. 3a. In contrast to the direct infusion of the $[PtCl_6]^{2-}$ species, Fig. 1a, Na^+ passes through the column without being retained and hence no sodium adduct is detected at *m/z* of 426.765-434.757. However, the high resolution *m/z* data and intensity distribution of peaks observed at *m/z* 589.9948-600.004 are consistent with a singly charged ion containing 1 Pt, 6 Cl atoms and a single protonated TriBA molecule, i.e. an ion-pair adduct $[M+NHC_{12}H_{27}]^-$, Fig 3a. Moreover, the mass spectra of the remaining $[PtCl_{6-n}Br_n]^{2-}$ (n = 1 – 6) anionic complexes all contain the analogues ion-pair adduct $[M+NHC_{12}H_{27}]^-$, Figures 3b to g. The successive substitution of a Cl^- ion by a Br^- ion upon moving from one Pt^{IV} species to the next, Reaction scheme 1, results in a constant incremental change of *m/z* 44 ($^{79/81}Br$ - $^{35/37}Cl$) in the $[M+NHC_{12}H_{27}]^-$ adducts. This observation serves to simplify the characterization of the separated $[PtCl_{6-n}Br_n]^{2-}$ (n = 0 – 6) species. Even if the ion-pair adduct $[M+NHC_{12}H_{27}]^-$ was not

observed, the wealth of information contained in Figures 3a-g can be used for species characterization. For example, the $[PtCl_4Br_2]^{2-}$ species can be assigned on the basis of the following observations: (i) unlike the mass spectra of the $[PtCl_5Br]^{2-}$ and $[PtCl_6]^{2-}$ species, no $[PtCl_5]^-$ fragment was present in its mass spectrum (Table 1) and (ii) of the 5 fragments displaying varying combinations of Cl and Br atoms, a maximum of 4 Cl and/or 2 Br atoms were detected, Table 1. The only species that can account for these findings is the $[PtCl_4Br_2]^{2-}$ complex anion. Several additional noteworthy fragmentation trends are observed in the MS spectra obtained for the homo and heteroleptic species. The most intense set of peaks, *m/z* 333.805-341.801, in the ESI mass spectrum of $[PtCl_5Br]^{2-}$ corresponds to the $[PtCl_4]^-$ ion, Figure 3b, indicating a loss of both Cl^- and Br^-, $[M\text{-}Cl^-\text{-}Br^-]^-$. Inspection of the mass spectra of the remaining heteroleptic species, $[PtCl_{6-n}Br_n]^{2-}$ (n = 2 – 5), reveals this fragmentation path to be the dominant one for all, Fig. 3b-f. Moreover, this fragmentation pathway results in a constant incremental change of *m/z* 44 ($^{79/81}Br$ - $^{35/37}Cl$) in the base peaks of each successive heteroleptic species, Fig. 3b to f, similar to that observed for the $[M+NHC_{12}H_{27}]^-$ ion-pair adduct, Fig. 3a to g. Two additional mixed ligand fragmentation paths are observed resulting in the $[M\text{-}2Cl^-\text{-}Br^-]^-$ ion, detected for all the $[PtCl_{6-n}Br_n]^{2-}$ (n = 1 – 4) species, and the $[M\text{-}Cl^-\text{-}2Br^-]^-$ ion, detected for all the $[PtCl_{6-n}Br_n]^{2-}$ (n = 3 – 5) species, Table 1. Other fragmentation pathways involve the loss of only Cl^- or Br^- ions, Table 1. Individually, the high resolution ESI mass spectra of each $[PtCl_{6-n}Br_n]^{2-}$ (n = 0 – 6) species convey transparency to the chromatographic peak assignment of each respective complex, however, when these spectra are viewed as a series encompassing the trends brought about by the exchange of a Cl^- ion by a Br^- ion upon moving from one Pt^{IV} species to the next, Reaction scheme 1, the full potential of this method to characterize species in solution is revealed. Furthermore, the limit of quantification (LOQ) for this technique is estimated to be 0.1 $mg.L^{-1}$ and is sufficient to characterize the mono-aquated $[PtCl_{5-n}Br_n(H_2O)]^-$ (n = 0 – 5) complex anions present in low abundance.

The high resolution ESI mass spectrum obtained for the elution band (t_R = 11.6) marked by an (*), Figure S1, exhibits several fragmentation components, each characteristic of an ion containing one Pt and multiple Cl atoms. Among these are the $[PtCl_3]^-$ (base peak), $[PtCl_4]^-$ and $[PtCl_5]^-$ fragment ions. The presence of the $[PtCl_5]^-$ ion negates the possibility of an on-column reduction product of Pt^{IV}. Interestingly the set of peaks at *m/z* 326.8795-334.8681 exhibit the exact isotopologue distribution associated with an ion containing 1 Pt and 3 Cl atoms. However,

the observed ion mass is greater by 28 amu, $[PtCl_3$+ 28 amu$]^-$. It should be made clear that only the elution bands marked by an (*) have mass spectra that contain fragments which are heavier by 28 amu. Candidate molecules which can account for this mass discrepancy are limited to CO, C_2H_2, CH_2N and N_2, however, the theoretical *m/z* values and intensities calculated in Masslynx® V4.1 for these molecules do not unambiguously agree with the experimentally observed *m/z* values and intensities. Although the exact identity of this elution band (*) remains unknown, it is most likely a Pt species coordinated to CO originating from formic acid. Considering the changes made to our previous chromatographic method[4,17] in order to facilitate hyphenation of a IP-LC to MS; this elution band (*, t_R = 11.6) and others (*, t_R =13.6 and 13.7) are attributed to on-column reaction products between the Pt^{IV} complexes and the mobile phase (formic acid). While interesting, it should be noted that the presence of these additional species have no significant effect on the characterization of the $[PtCl_{6-n}Br_n]^{2-}$ (n = 0 – 6) species.

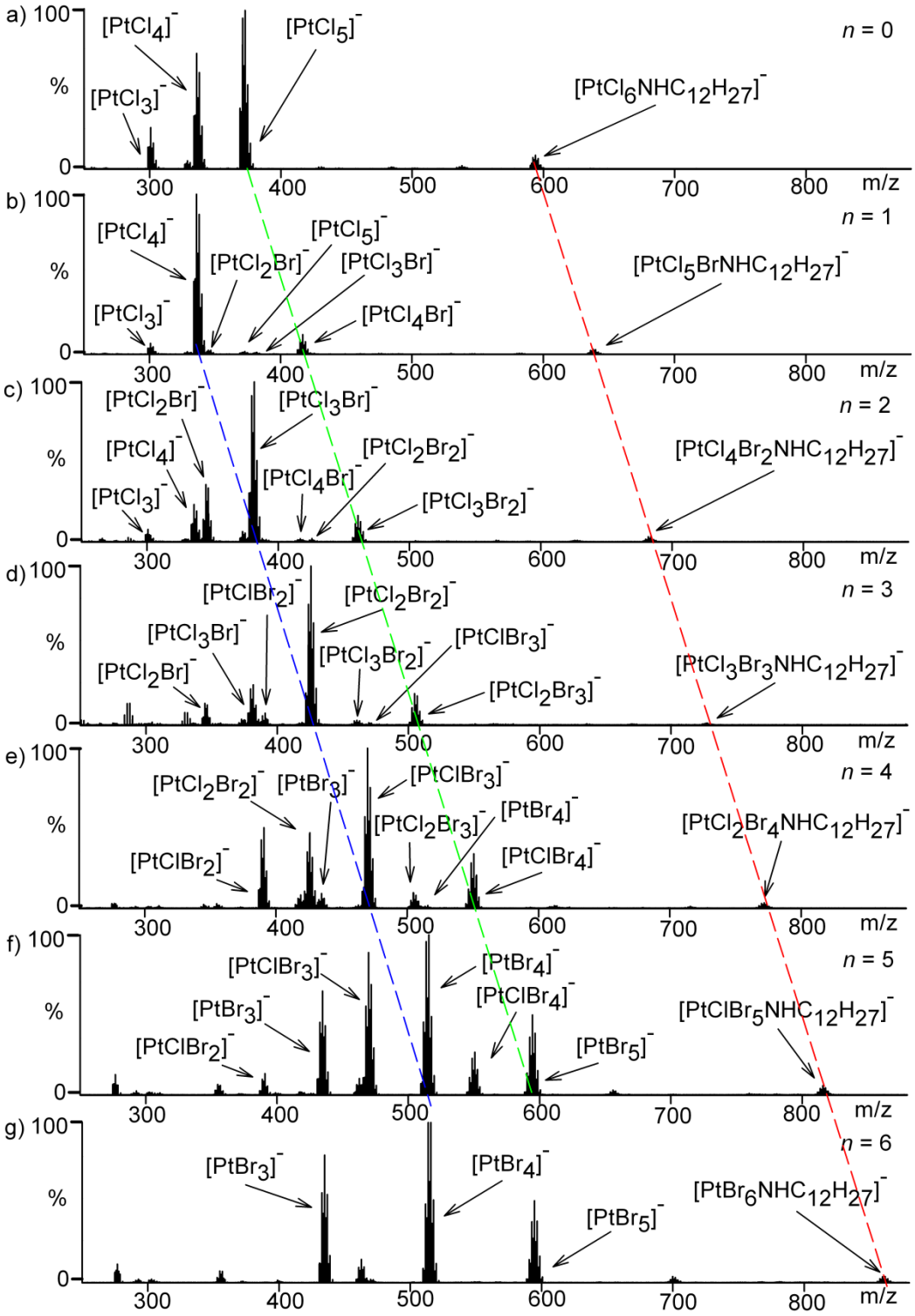

Figure 3a-g. Examples of mass spectra obtained by UHPLC-ESI-Q-TOF-MS analysis of the $[PtCl_{6-n}Br_n]^{2-}$ (n = 0 – 6) complex anions. The constant incremental change of m/z 44 in the mass spectra upon moving from $[PtCl_6]^{2-}$ to $[PtBr_6]^{2-}$ is clearly illustrated in the mass spectra, especially those associated with the $[M+NHC_{12}H_{27}]^-$ (red), $[M\text{-}Cl^-]^-$ (green) and $[M\text{-}Cl^-\text{-}Br^-]^-$ (blue) fragment ions.

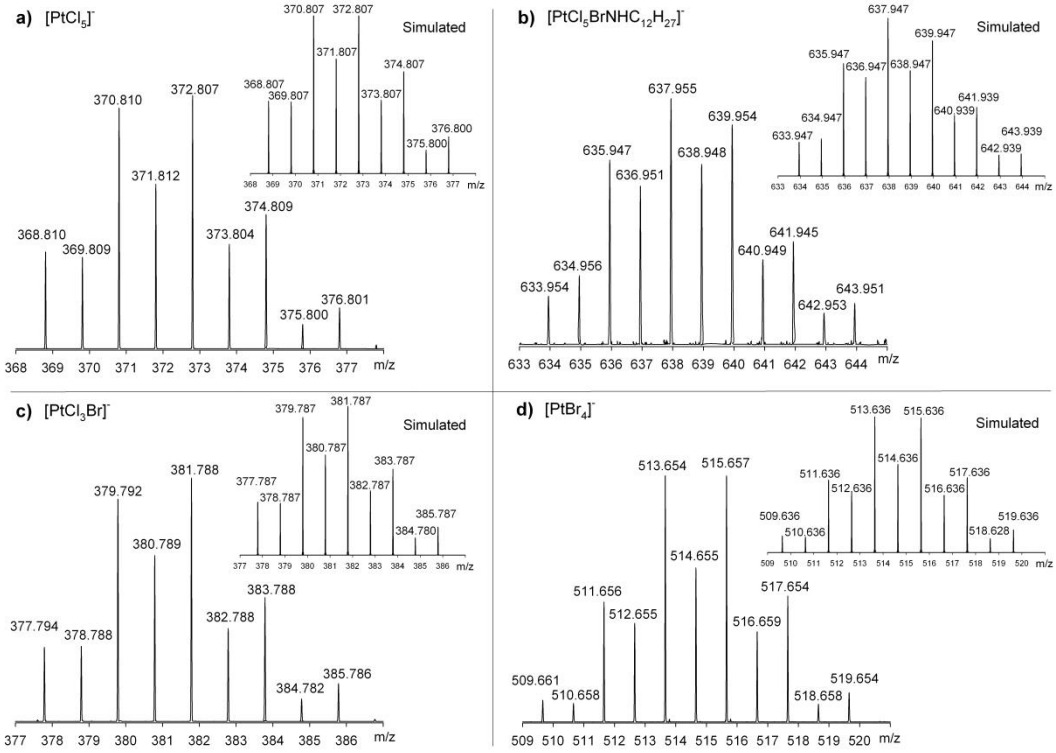

Figure 4. Experimentally obtained mass spectra illustrating the isotopologue distributions for the (a) $[PtCl_5]^-$ (b) $[PtCl_5BrNHC_{12}H_{27}]^-$ (c) $[PtCl_3Br]^-$ and (d) $[PtBr_4]^-$ ions. These compare well to the theoretical isotopologue distributions.

Table 2. The most abundant ions observed for the $[PtCl_{6-n}Br_n]^{2-}$ (n = 0 – 6) complex anions by UHPLC-ESI-MS analysis.

	Fragment ions									
n	$[M\text{-}Cl^-]^-$	$[M\text{-}2Cl^-]^-$	$[M\text{-}3Cl^-]^-$	$[M\text{-}Br^-]^-$	$[M\text{-}2Br^-]^-$	$[M\text{-}3Br^-]^-$	$[M\text{-}Cl^-\text{-}Br^-]^-$	$[M\text{-}2Cl^-\text{-}Br^-]^-$	$[M\text{-}Cl^-\text{-}2Br^-]^-$	$[M+IP]^-$
0	368.8105-376.8002	333.8375-341.8372	298.8664-306.8675	-	-	-	-	-	-	589.9958-600.0045
1	412.7556-422.7501	377.7945-385.7861	342.8248-350.8155	368.8105-376.8003	-	-	333.8375-341.8376	298.8663-306.8673	-	633.9541-643.9513
2	456.7143-466.7052	421.7356-431.7375	386.7744-394.7649	412.7555-422.7509	589.9956-600.0040	-	377.7942-385.7867	342.8246-350.8158	589.9951-600.0042	677.8992-689.9002
3	500.6648-510.6481	465.7047-475.7078	-	456.7147-466.7059	377.7945-385.7860	-	421.7355-431.7372	386.7747-394.7645	342.824-350.8156	721.8377-733.8265
4	544.6335-556.6201	509.6719-519.6345	-	500.6641-510.6482	421.7534-431.7460	342.8242-348.8374	465.7041-475.7071	430.7485-438.7392	386.7747-394.7648	765.8232-777.8302
5	588.5846-600.5712	-	-	544.6335-556.6205	465.7048-475.7079	589.9957-600.0046	509.6512-519.6543	-	430.7489-438.7392	811.7821-821.7865
6	-	-	-	588.5845-600.5711	509.6517-519.6544	430.7485-438.7392	-	-	-	855.7409-865.7288

Table 3. The most abundant ions observed for the $[PtCl_{5-n}Br_n(H_2O)]^-$ (n = 0 – 5) complex anions by UHPLC-ESI-MS analysis.

	Fragment ions					
n	$[M\text{-}H_2O]^-$	$[M\text{-}Cl^-\text{-}Br\text{-}H_2O]^-$	$[M\text{-}Br^-\text{-}H_2O]^-$	$[M\text{-}2Br^-\text{-}H_2O]^-$	$[M\text{-}Cl^-\text{-}H_2O]^-$	$[M\text{-}2Cl^-\text{-}H_2O]^-$
0	368.8108-376.8009	-	-	-	333.8372-341.8377	298.8664-306.8672
1	412.7552-422.7502	298.8667-306.8678	333.8378-341.8376	-	-	-
2	456.7147-466.7059	342.8249-350.8155	377.7942-385.7865	-	-	-
3	500.6643-510.6483	386.7747-394.7645	421.7353-431.7373	-	-	-
4	544.6335-556.6205	430.7482-438.7391	465.7045-475.7073	386.7747-394.7648	-	-
5	588.5847-600.5717		-	430.7482-438.7392	-	-

In addition to the $[PtCl_{6-n}Br_n]^{2-}$ (n = 0 – 6) species characterized above, partial aquation of these complexes also occurs in acidic, halide deficient solutions and can lead to the formation of 12 mono-aquated $[PtCl_{5-n}Br_n(H_2O)]^-$ (n = 0 – 5) species, Scheme 1, as well as several di-aquated chlorido-bromido Pt^{IV} species.[11] In order to investigate these species and to simplify matters initially, $Na_2PtCl_6{\cdot}2H_2O$ ($[Pt]_t$ = 10 mM) was dissolved in Milli-Q water UHPLC-ESI-Q-TOF-MS. The resultant LC-UV and total ion chromatographic traces are shown in Figures 5a and b, respectively. Since the only ligands present in this sample that can coordinate to Pt are Cl^- and H_2O, four of the five peaks were tentatively assigned to the $[PtCl_6]^{2-}$, $[PtCl_5(H_2O)]^-$ and the di-aquated species, *cis*- and *trans*-$[PtCl_4(H_2O)_2]$. The relatively low mobile phase pH of 3.5 prevents the formation of the mono-hydroxido $[PtCl_5OH]^{2-}$ complex.[11] In contrast, the di-aquated species can only be retained if partial/total deprotonation occurs to form a mixture of aquated/hydroxido species (*cis*- and *trans*-$[PtCl_4(H_2O)(OH)]^-$ and $[PtCl_4(OH)_2]^{2-}$) in rapid exchange. The elution band at t_R =11.4 was assigned to the $[PtCl_6]^{2-}$ species based on the retention time and mass spectrum for this complex (Figure 2a and 3a). The mass spectrum obtained for the $[PtCl_5(H_2O)]^-$ species (t_R = 7.5 min), Figure 5b, did not contain any ion-pair adduct as found for the $[PtCl_{6-n}Br_n]^{2-}$ (n = 0 – 6) species. However, the $[PtCl_5]^-$, $[PtCl_4]^-$ (base peak) and $[PtCl_3]^-$ fragment ions are present, Figure 5c, implying that this complex must have had at least 5 Cl atoms in its original molecular make-up, which supports the $[PtCl_5(H_2O)]^-$ assignment. Of the three remaining elution bands in Figure 5a and b two were assigned as the di-aquated *cis*- and *trans*-$[PtCl_4(H_2O)_2]$ complexes with t_R of 2.2 and 2.9 min, respectively. Mass spectra of both elution bands contained the $[PtCl_3]^-$, $[PtCl_3O]^-$ and $[PtCl_4]^-$ fragment ions, Figure 5c. The first peak (*) at a t_R of 1.9 min in Figures 5a and c is attributed to an on-column reaction product for the same reasons as discussed earlier (Figures 2a and b). The above experiment was repeated using a K_2PtBr_6 salt instead of the $Na_2PtCl_6{\cdot}2H_2O$ salt. This sample was left for several days to allow for the formation of aquated $[PtBr_5(H_2O)]^-$ species. The UV-Vis and total ion chromatograms of this sample ($[Pt]_t$ = 10 mM) are shown in Figures 5c and d, respectively. The $[PtBr_6]^{2-}$ species, t_r = 13.3 min, was assigned according to the criteria outlined above. The high resolution mass spectrum obtained for the band eluting at 8.3 min contained the $[PtBr_3]^-$ and $[PtBr_4]^-$ fragment ions, Figure 5d. A relatively low intensity $[PtBr_5]^-$ fragment ion signal was observed (signal/noise ≈ 3). This elution band was therefore assigned to the $[PtBr_5(H_2O)]^-$

complex. The first elution band (*) at 5.6 min in Figures 5c and d is attributed to an on-column reaction product.

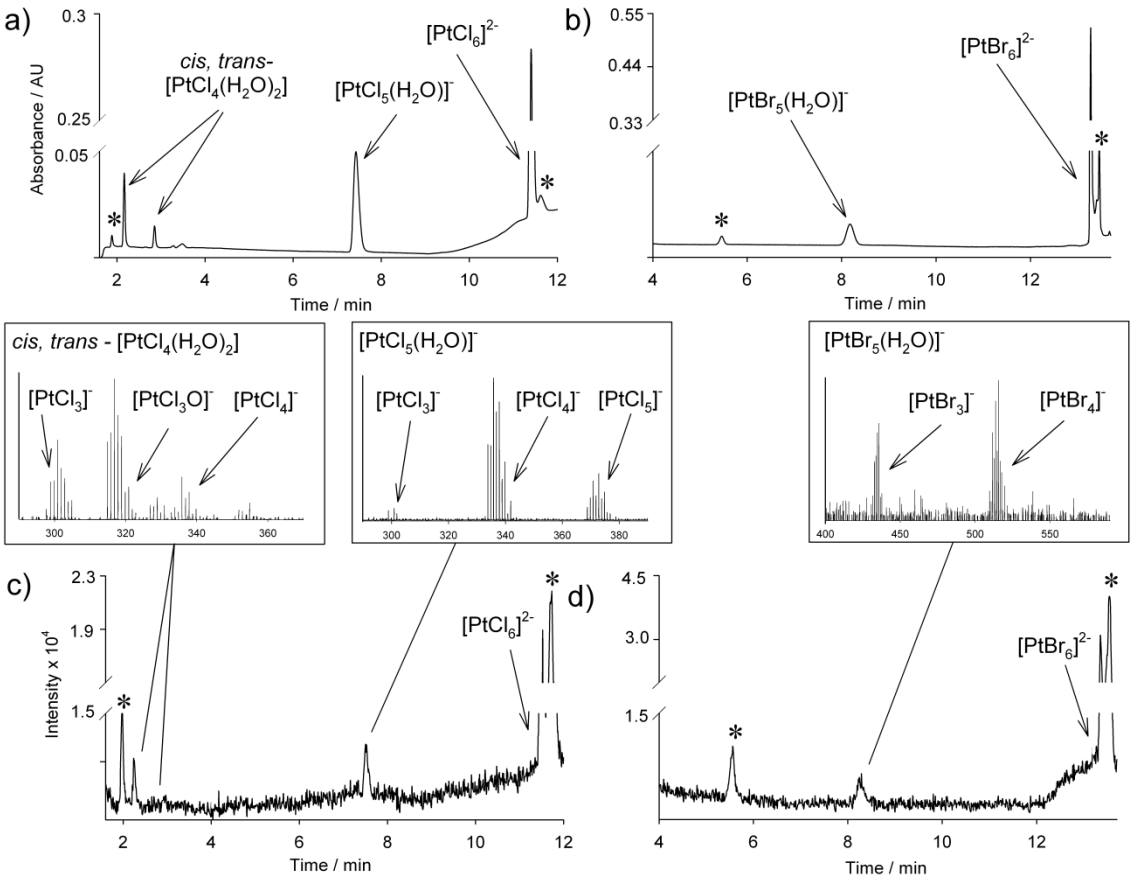

Figure 5. UHPLC-UV chromatograms of (a) the chlorido (262 nm) and (b) bromido aquated (315 nm) species. The corresponding total ion chromatograms are shown in (c) and (d), respectively, with the respective mass spectra of each aquated species. (*) denotes on-column reaction products resulting from interaction between the Pt^{IV} complexes the mobile phase.

The heteroleptic chlorido-bromido Pt^{IV} aquated species were furnished upon addition of equal portions of the above-mentioned aquated chlorido and aquated bromido samples in a 1:1 Cl^- to Br^- mole ratio. The UV-Vis and total ion chromatographic traces of this sample are shown in Figure 6a and b, respectively, with three distinct elution zones identifiable. The first unresolved zone of elution bands (t_R = 1.7-4.4 min) are indicative of the di-aquated species present in relatively low abundance.[11] The second zone of elution bands (t_R = 5.8-10.9 min) corresponds to the mono-aquated $[PtCl_{5-n}Br_n(H_2O)]^-$ (n = 0 – 5) species, and the third (t_R = 11.7-13.50 min) elution zone consists of the predominant species present, namely the $[PtCl_{6-n}Br_n]^{2-}$ (n = 0 – 6)

anionic complexes. The mono-hydroxido Pt^{IV} species are not formed in the relatively low mobile phase pH (3.5).[11] Characterization of the relatively low abundance di-aquated species present is beyond the ambit of the current study and will not be discussed further. The separation and assignment of the mono-aquated $[PtCl_{5-n}Br_n(H_2O)]^-$ (n = 0 – 5) species are expected to be less than trivial due to the presence of 10 stereoisomer species (Scheme 1), for example, the $[PtCl_3Br_2(H_2O)]^-$ configuration alone accounts for 3 nonequivalent complexes. Nonetheless, several well resolved peaks are observed for these species, Figures 6a and b, with the corresponding mass spectra shown in Figures 7a to h. The order in which the mass spectra have been placed coincides with the elution order of the respective peak. The mass spectrum of the first elution band (t_R = 5.8 min) exhibits the $[PtCl_3]^-$, $[PtCl_4]^-$ (base peak) and $[PtCl_4Br]^-$ fragment ions, Figure 7a, and is therefore assigned to the $[PtCl_4Br(H_2O)]^-$ species. The mass spectra obtained for the remaining complexes, Figures 7b to h, and fragment ions, Table 2, were analyzed in an analogues way, resulting in the assignment of all the observed elution bands, Figure 6a and b. Note that the $[PtCl_5(H_2O)]^-$ and $[PtClBr_4(H_2O)]^-$ species co-eluted, and that the relevant fragment ions of both species are present in the mass spectrum, Figure 7d. Further confirmation of these assignments are obtained when considering the fragmentation pathways for these species, namely those that result in the $[M\text{-}Cl^-\text{-}Br^-\text{-}H_2O]^-$, $[M\text{-}H_2O]^-$ and $[M\text{-}Br^-\text{-}H_2O]^-$ fragment ions, indicated in Figures 7a to h by the dashed lines. In each fragmentation pathway a characteristic incremental change of 44 *m/z* in the respective mass spectra is observed, indicative of the substitution of a Cl^- by a Br^- to give rise to the next eluting species. Interestingly, these trends also indicate the presence of 2 distinct elution orders for the mono-aquated stereoisomer species. One set is observed from t_R = 5.8 to 7.5 min, Figures 7a to d and the other from t_R = 8.3 to 10.9 min, Figures 7e to h. In contrast to the $[PtCl_{6-n}Br_n]^{2-}$ (n = 0 – 6) species, the mono-aqua-mixed-halide species does not elute between the $PtCl_5(H_2O)]^-$ (t_R = 7.5 min) and $[PtBr_5(H_2O)]^-$ (t_R = 8.3 min) species.[11]

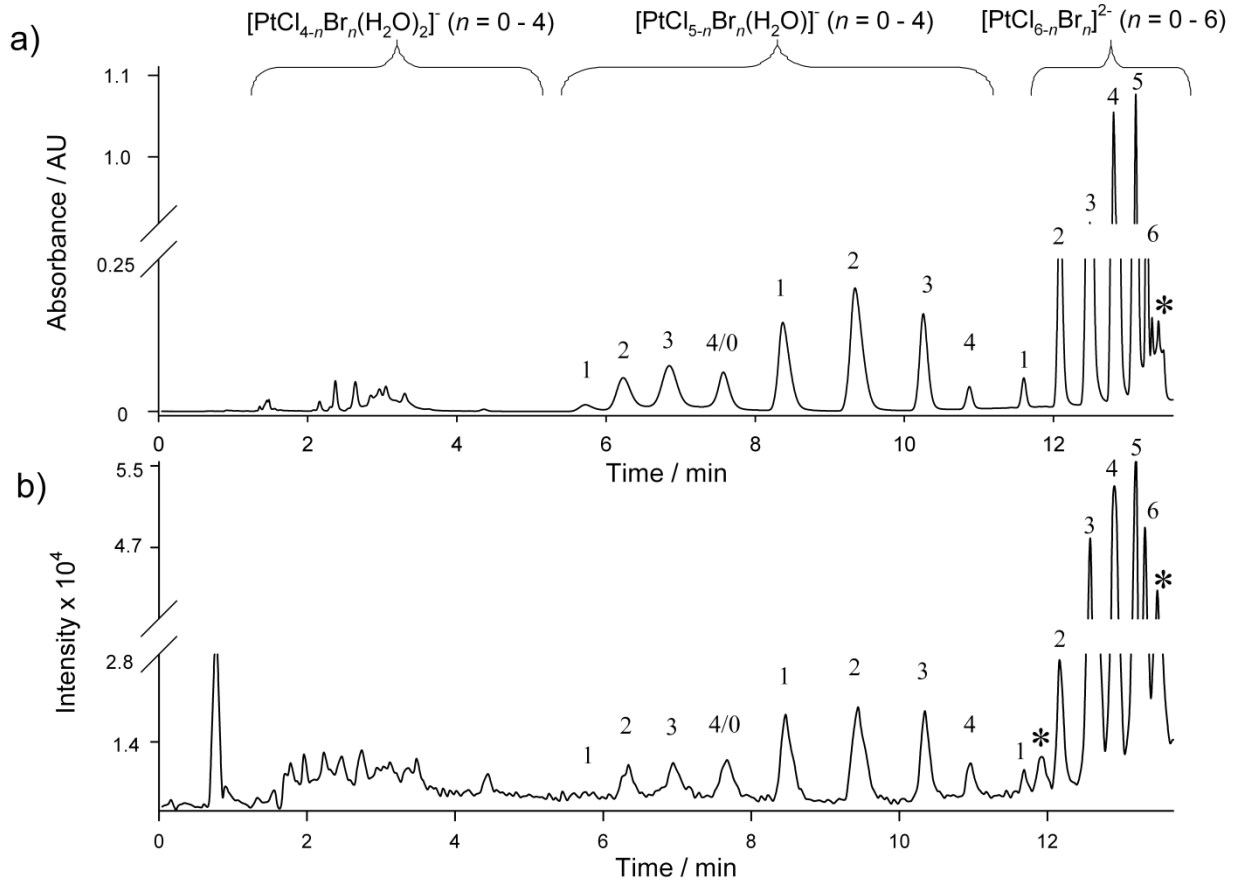

Figure 6. a) UHPLC-UV-Vis recorded chromatogram, 262 nm, and (b) the UHPLC-ESI-Q-TOF-MS total ion chromatogram of the $[PtCl_{4-n}Br_n(H_2O)_2]^-$ (n = 0 – 4), $[PtCl_{5-n}Br_n(H_2O)]^-$ (n = 0 – 4) and $[PtCl_{6-n}Br_n]^{2-}$ (n = 0 – 6) species. Peak numbering corresponds to n in the respective formulae. (*) denotes on-column reaction products resulting from interaction between the Pt^{IV} complexes and the mobile phase.

The use of methanol instead of acetonitrile as organic modifier results in significant changes in retention as well as selectivity, Figures 8a and b. Retention times for $[PtCl_6]^{2-}$ and $[PtBr_6]^{2-}$ species shift from 9.9 to 10.3 min and 13.6 to 17.2 min, Figures 8a and b, when methanol is replaced by acetonitrile as mobile phase organic modifier, respectively. In contrast, retention times for $[PtCl_5(H_2O)]^-$ decreased from 7.2 to 6.5 min and increased for $[PtBr_5(H_2O)]^-$ from 7.6 to 14.8 min in methanol and acetonitrile (Figures 8a and b), respectively. Solvation of the charged mono-aquated species in the mobile phase plays a critical role in their retention behavior and provides some clarification of the 'unusual' retention time trends observed in methanol.

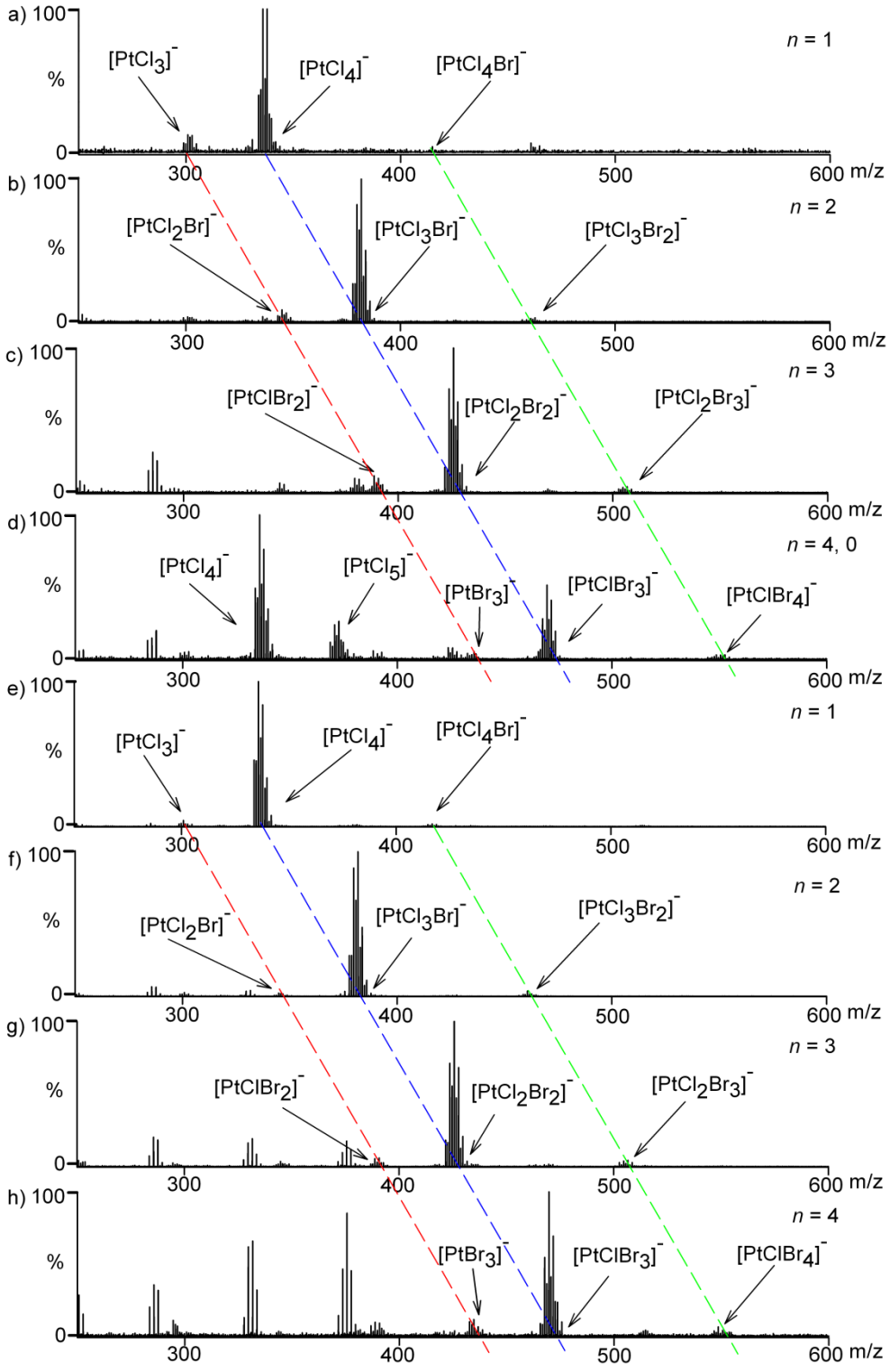

Figure 7a-h. ESI-MS spectra obtained for the $[PtCl_{5-n}Br_n(H_2O)]^-$ (n = 0 – 4) complex anions by UHPLC-ESI-Q-TOF-MS analysis, placed in the order of elution observed in Figure 6. The constant incremental change of *m/z* 44 in the MS is illustrated in the fragmentation pathways, especially those resulting in the $[M\text{-}H_2O]^-$ (green), $[M\text{-}H_2O\text{-}Br^-]^-$ (green) and $[M\text{-}Cl^-\text{-}H_2O\text{-}Br^-]^-$ (blue) fragment ions.

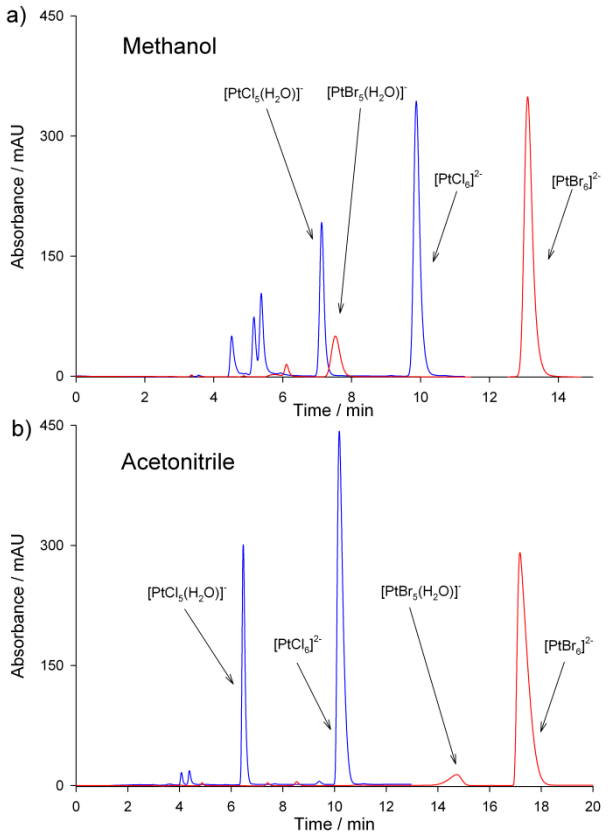

Figure 8a and b. The effect of mobile phase organic modifier is illustrated when using methanol (a) as opposed to acetonitrile (b) in the separation of the $[PtCl_5(H_2O)]^-$ and $[PtCl_6]^{2-}$ species, and the $[PtBr_6]^{2-}$ and $[PtBr_5(H_2O)]^-$ species (obtained using HPLC with PDA detection, a 25 cm column and the same mobile phase composition as earlier; 18 mM TriBA and 36 mM formic acid). This effect is most notable for the $PtCl_5(H_2O)]^-$ and $[PtBr_5(H_2O)]^-$ species due to their solvation in the relevant mobile phase. Detection was performed at 262 nm (blue) and 315 nm (red).

Due to the large influence of solvation on stereoisomer species retention, assignment of these species (*cis*, *trans*, *mer* or *fac*) based on the dipole moment of the relevant species was not attempted. Moreover, the $[PtCl_3Br_2(H_2O)]^-$ and $[PtCl_2Br_3(H_2O)]^-$ complex anions both account for three nonequivalent species, of which two of each are detected in the chromatograms shown in Figures 6a and b. The third unaccounted for stereoisomers are therefore either not present in solution, or more likely, co-eluting with other bands. However, unlike the co-elution of the $[PtCl_5(H_2O)]^-$ and $[PtClBr_4(H_2O)]^-$ species, these co-elutions involve stereoisomers, Figure 7e, which exhibit identical fragmentation patterns. As a result distinguishing between them is not possible, Figures 7a to c and e to h.

Conclusions

With the aid of an ion-pairing C18 reversed phase UHPLC system hyphenated to high resolution ESI-Q-TOF-MS the homoleptic and heteroleptic Pt^{IV} $[PtCl_{6-n}Br_n]^{2-}$ (n = 0 – 6) species in conjunction with the $[PtCl_{5-n}Br_n(H_2O)]^-$ (n = 0 – 5) complex anions could successfully be characterized in well-defined acidic solutions. The ion-pairing reagent tributylamine resulted in sufficient chromatographic resolution for the Pt^{IV} species while its volatility provided low background noise in MS spectra. From the known total Pt concentration injected onto the UHPLC-ESI-Q-TOF-MS system, the limit of quantification (LOQ) for this technique is estimated to be below 0.2 $mg.L^{-1}$. Even though extensive fragmentation of all the complexes occur, the formation of $[PtCl_{6-n}Br_n]^{2-}$ (n = 0 – 6) ion-pair adducts, $[M+NHC_{12}H_{27}]^-$, simplified the assignment of these species. In contrast, no $[M+NHC_{12}H_{27}]^-$ adducts of the $[PtCl_{5-n}Br_n(H_2O)]^-$ (n = 0 – 5) species could be observed. However, the relevant fragmentation pathways exhibit a characteristic incremental change of 44 *m/z* in the respective mass spectra indicating the substitution of a Cl^- by a Br^- to give rise to the next eluting species, allowing for the characterization of the mono-aquated species.

References

1. G. Ertl, H. Knözinger, F. Schüth, J. Weitkamp, *Handbook of Heterogeneous Catalysis*, Wiley-VCH, Weinheim, 2nd edn, **2008**, pp. 37-56.
2. J. Smidt, W. Hafner, R. Jira, J. Sedlmeier, R. Sieber, H. Kojer, R. Rüttinger, *Angewandte Chemie*, **1959**, *71*, 176.
3. P. Millington, A. York, *Platinum Metals Review*, **2012**, *56*, 58.
4. P-H. Van Wyk, W. J Gerber, K. R. Koch, *Analytica Chimica Acta*, **2011**, *704*, 154.
5. Y. Xia, Y. Xiong, B. Lim, S. E. Skrabalak, *Angewandte Chemie International Edition*, **2009**, *48*, 60.
6. J. Chen, B. Lim, E. Lee, Y. Xia, *Nano today*, **2009**, *4*, 81.
7. Z. Peng, H. Yang, *Nano today*, **2009**, *4*, 143.
8. H. Zhang, M. Jin, Y. Xia, *Chemical Society Reviews*, **2012**, DOI: 10.1039/c2cs35173k.
9. Y-T. Yu, J. Wang, J-H. Zhang, H-J. Yang, B-Q. Xu, J-C. Sun, *Journal of Physical Chemistry C*, **2007**, *111*, 18563.

10. H. Zhang, M. Jin, J. Wang, W. Li, P. H. C. Camargo, M. J. Kim, D. Yang, Z. Xie, Y. Xia, *Journal of the American Chemical Society*, **2011**, *133*, 6078.
11. K. R. Koch, J. Kramer, *Inorganic Chemistry*, **2006**, *45*, 7843.
12. K. R. Koch, J. Kramer, *Inorganic Chemistry*, **2007**, *46*, 7466.
13. G. Peters, W. Preetz, D. Bublitz, *Chemical Reviews*, **1996**, *96*, 977.
14. A. Von Zelewsky, *Helvetica Chimica Acta*, **1968**, *51*, 803.
15. E. Peters, G. Parirzich, W. Preetz, *Zeitschrift fuer Naturforschung*, **1993**, *48*, 1169.
16. F. M. Ismail, S. J. S. Kerrison, P. J. Sadler, *Chemical Communications*, **1980**, *23*, 1175.
17. P-H. Van Wyk, W. J Gerber, K. R. Koch, *Journal of Analytical Atomic Spectrometry*, **2012**, *27*, 577.
18. Schramel, O. Michalke, B. Kettrup, A, *Fresenius' Journal of Analytical Chemistry*, **1999**, *363*, 452.
19. W. J. Gerber, P. Murray, K. R. Koch, *Dalton transactions*, **2008**, *31*, 4113.
20. W. Henderson, J. S. McIndoe, (2005). *Mass Spectrometry of Inorganic, Coordination and Organometallic Compounds: Tools-Techniques-Tips*. John Wiley & Sons.
21. M. Holčapek, K. Volná, P. Jandera, L. Kolářová, K. Lemr, M. Exner, A. Círka, *Journal of Mass Spectrometry*, **2004**, *39*, 43.
22. A. de Villiers, F. Lestremau, R. Szucs, S. Gélébart, F. David, P. Sandra, *Journal of Chromatography A*, **2006**, *1127*, 60.

Supporting Information

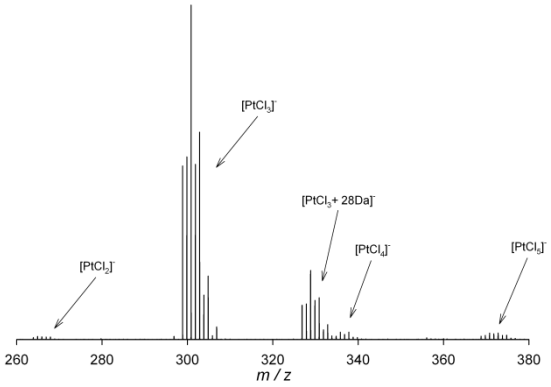

Figure S-1. ESI-MS spectrum obtained for the elution band marked by an (*) in Figure 2a. The $[PtCl_2]^-$, $[PtCl_3]^-$, $[PtCl_4]^-$, $[PtCl_5]^-$ and $[PtCl_3 + 28\ Da]^-$ fragment ions are observed.

5 Thermodynamic Stability of the $[PtCl_{6-n}Br_n]^{2-}$ (n = 0 – 6) Complex Anions in Aqueous Solutions

Thermodynamic Stability of the $[PtCl_{6-n}Br_n]^{2-}$ (n = 0 – 6) Complex Anions in Aqueous Solutions

Introduction

Probably the most extensively studied metal-ligand equilibria across the periodic table are those of metal cation halido complexes.[1] On-going motivation for these investigations include the continued use of halido complexes as synthetic precursors for a large number of applications and the optimization of platinum group metals (PGMs) refining/purification processes which rely critically on the speciation of the different PGMs.[2] Interestingly, when Ahrland scrutinized the available overall formation constants for *p*-, *d*- and *f*- block halido complexes in solution[3-14] he found that metal cations can be divided into two groups.[3] The first group exhibits thermodynamic stability in the order $F^- >> Cl^- > Br^- > I^-$ and in the second group, a triangular 'island of stability', the thermodynamic stability order is the exact opposite. This 'triangular' region of the periodic table mainly contains the PGMs and some metal cations that border the precious metals. In Pearson's hard and soft acid and base (HSAB) proposal the first group of metal cations as defined by Ahrland are classified as class (a) or hard and the second group as class (b) or soft.[15] In addition, HSAB was used to qualitatively rationalize why each metal cation should be classified as (a) or (b) class or 'borderline'. Undeniably HSAB has influenced the thinking of which elements have a larger affinity for each other and in that sense influenced the way how certain reactions or synthesis routes are approached. In a recent paper Mayr *et al*[16] show with detailed examples how HSAB fails in the prediction of ambident reactivity; this raises the question whether HSAB can account for the thermodynamic stability of the 'deceptively simple' metal cation halido complexes. Moreover, in Pearson's initial formulation of HSAB it is stated;[15]

"*Also solvation effects alone would not cause a division into two distinct classes of acids as are found. What solvation does do is to generally destroy class (a) character and enhance class (b) character. The magnitude of the class (a) character in the gas phase will determine if a solvent can cause inversion (...). It is clear then that solvation effects, while of great importance, particularly for ions, do not explain why some acids prefer hard bases and some acids prefer soft*

bases. The explanation for this must come from interactions existing in the acid-base complex. Such interactions include ionic-covalent σ-bonding, ΠΙ-bonding, electron correlation effects, all of which seem to play a role in determining class (a) and (b), or hard and soft character"

If it can be shown that solvation is the only reason why two distinct classes of acids (metal cations) exist, then HSAB is proved to be fundamentally flawed.

At the turn of the previous century, Abeg *et al*[17] was able to determine the overall formation constant for ML_n type complexes. However, Bjerrum *et al*[18] later showed that ML_n type complexes form in a sequence of stepwise ligand exchange reactions where several species can simultaneously exist at equilibrium, Diagram 1a.[2] To date a large number of investigations[6-12] have verified Bjerrum *et al's* findings that the amounts of species that form in a stepwise manner can be expressed in terms of a series of stability constants, K_n (n = 1 - 6) (Diagram 1a, equation 1).

$$K_n = \frac{[ML_n]}{[ML_{n-1}][L]} \qquad \ldots 1$$

However, the reaction scheme shown in Diagram 1a does not take stereoisomers into account, neglecting isomerization and 'cross' ligand substitution reactions, and is thus a simplification of the reaction scheme shown in Diagram 1b.

[2] In order to differentiate between the stability constants and thermodynamic parameters for diagram 1a and 1b, all diagram 1a parameters are denoted by a (*).

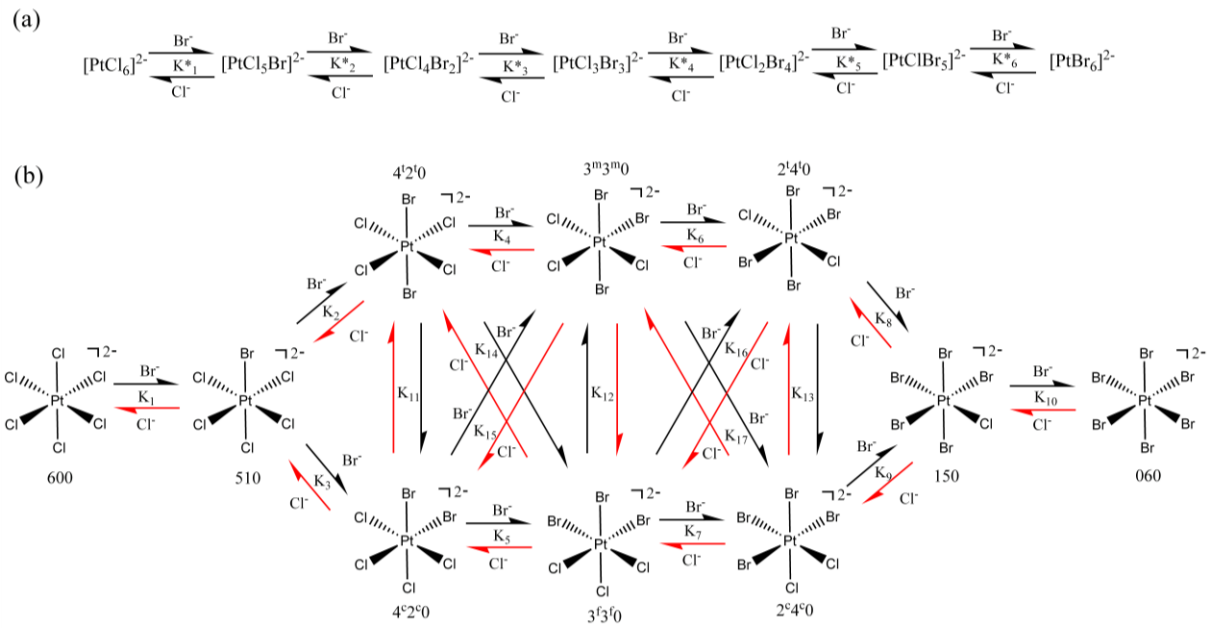

Diagram 1a and b. (a) Stability constants for the sequence of stepwise ligand exchange reactions of the $[PtCl_{6-n}Br_n]^{2-}$ (n = 0 - 6) species when the stereoisomers are not taken into account and (b) when the stereoisomers are taken into account. The red arrows in (b) indicate the direction of the spontaneous reaction. The notation used for the 10 species is an adaption of the nomenclature introduced by Drews and Preetz.[19] The first numeral represents the number of chlorides in the octahedral complex and the second the number of bromides. The configuration of the stereoisomers is given as a superscript; c for *cis*, t for *trans*, m for *meridional*, and f for *facial*.

This simplification not only results in the loss of thermodynamic information but also an internal self consistency check by which to quantitatively validate calculated ligand exchange stability constants. In addition, by neglecting stereoisomers a significant error is introduced when calculating certain standard reaction Gibbs free energies ($\Delta G^{o}_{rxn_T}$) using overall formation constants. To clarify this point, consider the multiple reaction paths by which $[PtCl_6]^{2-}$ can be transformed to $[PtBr_6]^{2-}$ as shown in Diagram 1b, reaction r1. Because $\Delta G^{o}_{rxn_T}$ is a state function, each individual reaction path must yield the same and correct $\Delta G^{o}_{rxn_T}$, e.g. $[PtCl_6]^{2-} \rightarrow [PtCl_5Br]^{2-}$ $\rightarrow$ *trans*-$[PtCl_4Br_2]^{2-}$ $\rightarrow$ *mer*-$[PtCl_3Br_3]^{2-}$ $\rightarrow$ *trans*-$[PtCl_2Br_4]^{2-}$ $\rightarrow$ $[PtClBr_5]^{2-}$ $\rightarrow$ $[PtBr_6]^{2-}$, equation 2. Whereas in Bjerrum's formulation the $\Delta G^{o*}_{rxn_T}$ for reaction r1 is the sum of two paths, i.e. $[PtCl_6]^{2-}$ $\rightarrow$ $[PtCl_5Br]^{2-}$ $\rightarrow$ *cis*-$[PtCl_4Br_2]^{2-}$ $\rightarrow$ *fac*-$[PtCl_3Br_3]^{2-}$ $\rightarrow$ *cis*-$[PtCl_2Br_4]^{2-}$ $\rightarrow$

$[PtClBr_5]^{2-} \rightarrow [PtBr_6]^{2-}$ and $[PtCl_6]^{2-} \rightarrow [PtCl_5Br]^{2-} \rightarrow$ *trans*-$[PtCl_4Br_2]^{2-} \rightarrow$ *mer*-$[PtCl_3Br_3]^{2-} \rightarrow$ *trans*-$[PtCl_2Br_4]^{2} \rightarrow [PtClBr_5]^{2-} \rightarrow [PtBr_6]^{2-}$, equation 3.[3]

$$[PtCl_6]^{2-} + 6Br^- \rightleftharpoons [PtBr_6]^{2-} + 6Cl^- \qquad ...r1$$

$$\Delta G^{o}_{rxnK_1} + \Delta G^{o}_{rxnK_2} + \Delta G^{o}_{rxnK_4} + \Delta G^{o}_{rxnK_6} + \Delta G^{o}_{rxnK_8} + \Delta G^{o}_{rxnK_{10}} = \Delta G^{o}_{rxn_T} \qquad ...2$$

$$\Delta G^{o*}_{rxnK^*_1} + (\Delta G^{o*}_{rxnK^*_2} + \Delta G^{o*}_{rxnK^*_3}) + (\Delta G^{o*}_{rxnK^*_4} + \Delta G^{o*}_{rxnK^*_5}) + (\Delta G^{o*}_{rxnK^*_6} + \Delta G^{o*}_{rxnK^*_7}) + (\Delta G^{o*}_{rxnK^*_8} + \Delta G^{o*}_{rxnK^*_9}) + \Delta G^{o*}_{rxnK^*_{10}} = \Delta G^{o*}_{rxn_T} \qquad ...3$$

This artificial inflation of $\Delta G^{o*}_{rxn_T}$ has several implications, including the evaluation of complex thermodynamic stability, determination of the thermodynamic driving force for these ligand exchange reactions, speciation calculations in a complex multi-component system and how thermodynamic data obtained with different experimental techniques can be compared if at all, e.g. standard reduction half cell potentials (E^o) vs. a direct spectrophotometric or calorimetric study. It should be noted that the main reason the reaction sequence (Diagram 1a) is still used arises from the inability of analytical methods, apart from NMR, to measure each species concentration 'directly'. Without this data a full speciation calculation incorporating all 10 species (Diagram 1b) is impossible (*vide infra*). However, several detailed investigations have been performed in which the stereo-specific substitutions of successive ligand exchange were successfully analyzed. In this manner portions of the reaction network similar to that shown in Diagram 1b could be elucidated.[20-26] To the best of our knowledge, the determination of all 17 stability constants has not been reported for an inorganic system.

In this manuscript we present a detailed equilibrium study of the Pt^{IV} chlorido-bromido halide exchange reaction network (HERN) shown in Diagram 1b and determine all 17 stability constants. Because the $\Delta G^{o}_{rxnK_n}$ (n = 1 - 17) could be determined for each ligand exchange reaction step shown in Diagram 1b, energy conservation relationships (ECRs) could be derived, e.g. equation 4, to test the accuracy and hence validate the calculated stability constants. Furthermore, using standard reaction half cell reduction potentials of $[PtCl_6]^{2-}$ and $[PtBr_6]^{2-}$ the overall formation constant or $\Delta G^{o}_{rxn_T}$ for reaction r1 can now also be validated.

[3] The mathematical details are given in the computational section.

$$\Delta G^0_{rxn\,3} + \Delta G^0_{rxn\,5} + \Delta G^0_{rxn\,7} + \Delta G^0_{rxn\,9} - (\Delta G^0_{rxn\,2} + \Delta G^0_{rxn\,4} + \Delta G^0_{rxn\,6} + \Delta G^0_{rxn\,8}) = 0 \quad \ldots 4$$

We then turn our focus to the determination of the thermodynamic driving force for the Pt^{IV} chlorido-bromido halide exchange reactions to ascertain why, or if, a second group of metal cations as defined by Ahrland exists and to test the validity of HSAB. Based on these findings new synthetic strategies are proposed for PGMs not possible in aqueous solutions. In addition, a generalised test could be devised to establish the bonding preferences of metal cations with halides.

Several investigations[27,28] show the spectacular success, or failure, of a particular density functional theory, DFT, functional(s) regarding the prediction of thermodynamic parameters for the same reaction or set of reactions. DFT is applied here to ascertain if it is possible to account for equilibrium geometry and the Gibbs free energy of the Pt^{IV} homoleptic and heteroleptic species using F^-, Cl^-, Br^- and I^- as ligands. In addition, several representative *p*- and *d*-block metal cations were chosen to compare their halido complexes' thermodynamic stability in the context of metal halide bonding preference.

Experimental

Reagents

HPLC grade acetonitrile was obtained from Merck (608-001-00- 3). All aqueous solutions were prepared using ultrapure Milli-Q water (>18 M). Analytical grade purity tetrabutyl-ammonium chloride (TBA^+Cl^-), sodium acetate and glacial acetic acid were obtained from Sigma–Aldrich. Mobile phases were prepared by the addition of acetonitrile to stock solutions of 0.05 M tetrabutyl-ammonium chloride and 0.1 M acetate buffer (pH = 4.6) to give 48% (v/v) CH_3CN:H_2O solutions. All mobile phases were filtered through 0.45 m HV filters (Mil-lipore Corporation, HVLP04700) under vacuum and degassed for 15 min in an ultrasonic bath before use. $Na_2PtCl_6{\cdot}2H_2O$ and H_2PtCl_6 (Johnson Matthey PLC, Precious Metals Division) was of analytical reagent grade quality and was dried in vacuo and stored in a desiccator prior to use.

High-performance liquid chromatography, with dual wavelength UV–Vis detection

Chromatographic separations were accomplished with a Varian Prostar liquid chromatograph equipped with a binary 210 solvent delivery module, a 410 auto-sampler with a 345 UV–Vis dual wave-length detector. The flow rate was set at 0.8 $mL.min^{-1}$ and the absorbance was measured at two fixed wavelengths, namely 262 and 315 nm. The column used throughout this study was a Microsorb C_{18}, 250 mm × 4.6 mm i.d., 5 μm particles. Column efficiency was tested by the injection of a solution comprising of acetophenone, phenol, aniline, caffeine, uracil, pyridine, benzene and 30% by volume acetonitrile. Column conditioning comprised of mobile phase passage through the column for 45 min prior to analysis.

ICP-OES

Determination of the samples' Pt, Cl^- and Br^- concentrations was accomplished with a SPECTRO *Arcos* ICP-OES spectrometer operating with a RF power set to 1400 W using a Burgener T2002 nebulizer and cyclonic spray chamber. The nebulizer flow rate was set at 0.8 $mL.min^{-1}$, auxiliary gas flow rate was set to 1 $L.min^{-1}$ and coolant flow rate to 13 $L.min^{-1}$. Pt standard solutions were prepared from a 1000 ppm ± 3 ppm stock solution in a 500 mL 10% HCl matrix obtained from De Bruyn Spectroscopy (Ultraspec). Cl^- and Br^- standard solutions were prepared from NaCl and NaBr (puriss; 99 %) obtained from Sigma-Aldrich, respectively. NaCl and NaBr was dried at 60ºC for 1 day and cooled in a vacuo desiccator prior to preparation of the relevant standard solutions. All standards and samples were matrix matched.

Sample preparation

Aqueous samples

21 samples were prepared in which the bromide mole fraction ($\alpha_{Br-} = \frac{n_{Br-}}{n_{Br-} + n_{Cl-}}$) was systematically varied. This stepwise incremental increase was 0.005 for the first 10 samples, and 0.5 for the remainder of the samples. All 21 samples were prepared such that the total $[Pt^{IV}]_T$ concentration of each was 10.0 mM. The ionic strength was kept constant for all samples by maintaining a total halide concentration such that $[Cl^-] + [Br^-] = 1.001$ M with $[H_3O^+]_T = 0.2$ M and $[Na^+]_T = 0.8$ M.

Organic sample

The mixed Pt^{IV} chlorido-bromido complex anions formed in an organic matrix was prepared by dissolving H_2PtCl_6 in chloroform containing equal portions of methyltrioctylammonium chloride and-bromide (Aliquat-336) such that the total halide concentration was 1.0 M, $[Pt]_T$ = 10 mM and the Cl^- to Br^- mole ratio equal to 1:1. The bromido form of Aliquat-336 was prepared by washing 20 % (v/v) Aliquat-336 in chloroform seven fold with 3.0 M HBr.

Computational Methods

Full and Partial Speciation Calculations of MX_AY_B systems applied to $[PtCl_{6-n}Br_n]^{2-}$ (n = 0 - 6)

To facilitate the discussion regarding the differences between speciation calculations utilizing the two reaction schemes shown in Diagram 1, consideration must be given to the formulation of the respective mass-balance equations and how this relates to the information that can be extracted from the data. For the 'conventional' case shown in Diagram 1a, the stepwise ligand exchange equilibria is expressed in terms of the overall formation constants, β_n^*, reaction r2 and equation 5.

$$[PtCl_6]^{2-} + nBr^- \rightleftharpoons [PtCl_{6-n}Br_n]^{2-} + nCl^- \quad (n = 1-6) \qquad \text{...r2}$$

$$\beta_n^* = \frac{([PtCl_{6-n}Br_n]^{2-})([Cl]^-)^n}{([PtCl_6]^{2-})([Br]^-)^n} \quad (n = 1-6) \qquad \text{...5}$$

Substitution of equation 5 into the mass-balance equations 6a-6c, yields a new set of mass balance equations 7a-7c with only three unknown variables (namely the $[PtCl_6]^{2-}$ and free unbound $[Cl^-]$, $[Br^-]$ concentrations).

$$[Pt]_T = \sum_{n=0}^{6} [PtCl_{6-n}Br_n]^{2-} \qquad \text{...6a}$$

$$[Cl]_T = \sum_{n=0}^{6} (6-n)[PtCl_{6-n}Br_n]^{2-} \qquad \text{...6b}$$

$$[\mathrm{Br}]_T = \sum_{n=0}^{6} n[\mathrm{PtCl}_{6-n}\mathrm{Br}_n]^{2-} \qquad \ldots 6c$$

$$[\mathrm{Pt}]_T = ([\mathrm{PtCl}_6]^{2-}) + \beta_1^*([\mathrm{PtCl}_6]^{2-})\frac{([\mathrm{Br}^-])}{([\mathrm{Cl}^-])} + \beta_2^*([\mathrm{PtCl}_6]^{2-})\frac{([\mathrm{Br}^-])^2}{([\mathrm{Cl}^-])^2} + \beta_3^*([\mathrm{PtCl}_6]^{2-})\frac{([\mathrm{Br}^-])^3}{([\mathrm{Cl}^-])^3} + \beta_4^*([\mathrm{PtCl}_6]^{2-})\frac{([\mathrm{Br}^-])^4}{([\mathrm{Cl}^-])^4} + \beta_5^*([\mathrm{PtCl}_6]^{2-})\frac{([\mathrm{Br}^-])^5}{([\mathrm{Cl}^-])^5} + \beta_6^*([\mathrm{PtCl}_6]^{2-})\frac{([\mathrm{Br}^-])^6}{([\mathrm{Cl}^-])^6} \qquad \ldots 7a$$

$$[\mathrm{Cl}]_T = ([\mathrm{Cl}]) + 6[\mathrm{PtCl}_6]^{2-} + 5\beta_1^*([\mathrm{PtCl}_6]^{2-})\frac{([\mathrm{Br}^-])}{([\mathrm{Cl}^-])} + 4\beta_2^*([\mathrm{PtCl}_6]^{2-})\frac{([\mathrm{Br}^-])^2}{([\mathrm{Cl}^-])^2} + 3\beta_3^*([\mathrm{PtCl}_6]^{2-})\frac{([\mathrm{Br}^-])^3}{([\mathrm{Cl}^-])^3} + 2\beta_4^*([\mathrm{PtCl}_6]^{2-})\frac{([\mathrm{Br}^-])^4}{([\mathrm{Cl}^-])^4} + \beta_5^*([\mathrm{PtCl}_6]^{2-})\frac{([\mathrm{Br}^-])^5}{([\mathrm{Cl}^-])^5} \qquad \ldots 7b$$

$$[\mathrm{Br}]_T = ([\mathrm{Br}]) + \beta_1^*([\mathrm{PtCl}_6]^{2-})\frac{([\mathrm{Br}^-])^2}{([\mathrm{Cl}^-])^2} + 2\beta_2^*([\mathrm{PtCl}_6]^{2-})\frac{([\mathrm{Br}^-])^3}{([\mathrm{Cl}^-])^3} + 3\beta_3^*([\mathrm{PtCl}_6]^{2-})\frac{([\mathrm{Br}^-])^4}{([\mathrm{Cl}^-])^4} + 4\beta_4^*([\mathrm{PtCl}_6]^{2-})\frac{([\mathrm{Br}^-])^5}{([\mathrm{Cl}^-])^5} + 5\beta_5^*([\mathrm{PtCl}_6]^{2-})\frac{([\mathrm{Br}^-])^6}{([\mathrm{Cl}^-])^6} + 6\beta_6^*([\mathrm{PtCl}_6]^{2-})\frac{([\mathrm{Br}^-])^6}{([\mathrm{Cl}^-])^6} \qquad \ldots 7c$$

In a similar manner as above, for the reactions shown in Diagram 1b and using reaction r3 and equation 8 the equivalent mass-balance equations 9a-9d are derived.

$$[\mathrm{PtCl}_6]^{2-} + m\mathrm{Br}^- \underset{}{\overset{\beta_n}{\rightleftharpoons}} [\mathrm{PtCl}_{6-m}\mathrm{Br}_m]^{2-} + m\mathrm{Cl}^- \quad (m = 1-6) \text{ and } (n = 1-10) \qquad \ldots r3$$

$$\beta_n = \frac{([\mathrm{PtCl}_{6-m}\mathrm{Br}_m]^{2-})([\mathrm{Cl}^-])^m}{([\mathrm{PtCl}_6]^{2-})([\mathrm{Br}^-])^m} \quad (m = 1-6) \text{ and } (n = 1-10) \qquad \ldots 8$$

$$[\mathrm{Pt}]_T = [\mathrm{PtCl}_6]^{2-} + [\mathrm{PtCl}_5\mathrm{Br}]^{2-} + [cis-\mathrm{PtCl}_4\mathrm{Br}_2]^{2-} + [trans-\mathrm{PtCl}_4\mathrm{Br}_2]^{2-} + [fac-\mathrm{PtCl}_3\mathrm{Br}_3]^{2-} + [mer-\mathrm{PtCl}_3\mathrm{Br}_3]^{2-} + [cis-\mathrm{PtCl}_2\mathrm{Br}_4]^{2-} + [trans\text{-}\mathrm{PtCl}_2\mathrm{Br}_4]^{2-} + [\mathrm{PtClBr}_5]^{2-} + [\mathrm{PtBr}_6]^{2-} \qquad \ldots 9a$$

$$[\mathrm{Pt}]_T = ([\mathrm{PtCl}_6]^{2-}) + \beta_1([\mathrm{PtCl}_6]^{2-})\frac{([\mathrm{Br}^-])}{([\mathrm{Cl}^-])} + (\beta_2 + \beta_3)([\mathrm{PtCl}_6]^{2-})\frac{([\mathrm{Br}^-])^2}{([\mathrm{Cl}^-])^2} + (\beta_4 + \beta_5)([\mathrm{PtCl}_6]^{2-})\frac{([\mathrm{Br}^-])^3}{([\mathrm{Cl}^-])^3} + (\beta_6 + \beta_7)([\mathrm{PtCl}_6]^{2-})\frac{([\mathrm{Br}^-])^4}{([\mathrm{Cl}^-])^4} + (\beta_8 \vee \beta_9)([\mathrm{PtCl}_6]^{2-})\frac{([Br]^-)^5}{([Cl]^-)^5} + \beta_{10}([\mathrm{PtCl}_6]^{2-})\frac{([\mathrm{Br}^-])^6}{([\mathrm{Cl}^-])^6} \qquad \ldots 9b$$

$$[Cl]_T = ([Cl])+6[PtCl_6]^{2-}+5\beta_1([PtCl_6]^{2-})\frac{([Br^-])}{([Cl^-])}+4(\beta_2+\beta_3)([PtCl_6]^{2-})\frac{([Br^-])^2}{([Cl^-])^2}+$$
$$3(\beta_4+\beta_5)([PtCl_6]^{2-})\frac{([Br^-])^3}{([Cl^-])^3}+2(\beta_6+\beta_7)([PtCl_6]^{2-})\frac{([Br^-])^4}{([Cl^-])^4}+ \quad ...9c$$
$$(\beta_8+\beta_9)([PtCl_6]^{2-})\frac{([Br^-])^5}{([Cl^-])^5}$$

$$[Br]_T = ([Br])+\beta_2^*([PtCl_6]^{2-})\frac{([Br^-])^2}{([Cl^-])^2}+2(\beta_2+\beta_3)([PtCl_6]^{2-})\frac{([Br^-])^3}{([Cl^-])^3}+$$
$$3(\beta_4+\beta_5)([PtCl_6]^{2-})\frac{([Br^-])^4}{([Cl^-])^4}+4(\beta_6+\beta_7)([PtCl_6]^{2-})\frac{([Br^-])^5}{([Cl^-])^5}+ \quad ...9d$$
$$5(\beta_8+\beta_9)([PtCl_6]^{2-})\frac{([Br^-])^6}{([Cl^-])^6}+6\beta_{10}^*([PtCl_6]^{2-})\frac{([Br^-])^6}{([Cl^-])^6}$$

On comparison of equations 7a and 9b two differences are noted: the terms that yield the concentration of stereoisomers show that the overall formation constant as defined in reaction r2 is actually the sum of two formation constants, e.g. $\beta_n^* = \beta_2+\beta_3$, and the term that yields the concentration of $[PtClBr_5]^{2-}$ contains either the formation constant β_8 or β_9. Moreover, since the change in Gibbs energy for the two reaction paths, *cis*-$[PtCl_4Br_2]^{2-}$ → *fac*-$[PtCl_3Br_3]^{2-}$ → *cis*-$[PtCl_2Br_4]^{2-}$ and *trans*-$[PtCl_4Br_2]^{2-}$ → *mer*-$[PtCl_3Br_3]^{2-}$ → *trans*-$[PtCl_2Br_4]^{2}$ are equal, it implies that $\beta_8 = \beta_9$ (equation 10) where $\beta_8 = K_1K_2K_4K_6K_8$ and $\beta_9 = K_1K_3K_5K_7K_9$.

$$e^{-\left(\frac{\Delta G^0_{rxn1}+\Delta G^0_{rxn3}+\Delta G^0_{rxn5}+\Delta G^0_{rxn7}+\Delta G^0_{rxn9}}{RT}\right)} = e^{-\left(\frac{\Delta G^0_{rxn1}+\Delta G^0_{rxn2}+\Delta G^0_{rxn4}+\Delta G^0_{rxn6}+\Delta G^0_{rxn8}}{RT}\right)} \Rightarrow \beta_8 = \beta_9 \quad ...10$$

To calculate the complex anion molar extinction coefficients, ε_i, and the 17 stability constants for the system shown in Diagram 1b it was necessary to develop a set of routines (called program EquiState.exe) in the Matlab 7.01 environment. The general workflow of program EquiState.exe is similar to that described by Meloun *et al*,[29] with some expected differences. The set of simultaneous non-linear mass balance equations, 9b-9d, derived from the model (Diagram 1b) were iteratively solved using the Levenberg-Marquardt algorithm[30] to obtain the $[PtCl_6]^{2-}$ and free unbound $[Cl^-]$ and $[Br^-]$ concentrations in exactly the same manner as for the reactions shown in Diagram 1a. Differentiating the non-linear least-squares objective function, equation 11, with respect to overall formation constants or molar extinction coefficients yields the n×n

Jacobian matrixes J(β) and J(ε), respectively. Because we obtain a response signal with no overlap for each of the 10 Pt^{IV} species, J(β) and J(ε) only have entries (partial derivates) along the diagonal. This is in contrast to the cases where a composite signal is obtained, e.g. spectral overlap in UV-Vis spectra when several species are present, and results in J(β) and J(ε) each having n×n entries. We therefore do not have to solve two sets of non-linear equations, as would be the case in Diagram 1a, but rather two sets of single variable equations, simplifying matters considerably. These equations are iteratively solved using the Newton-Raphson method.[31]

$$S = \sum_{i=1}^{j} (A_{\text{experimental}(j)} - A_{\text{theoretical}(j)})^2 \qquad \text{...11}$$

Utilizing the above procedure, the stability constants K_i (i = 1 - 10) as defined in Diagram 1b can be computed. The other 7 stability constants K_i (i = 11 - 17) pertaining to isomerisation and 'cross' ligand exchange are numerically 'fixed' since the Gibbs free energy is a state function. K_i (i = 11 - 17) are calculated as shown in the following two examples. Consider the stepwise ligand exchange reactions 2 and 3 shown in Diagram 1b. Dividing their stability constant expressions results in equation 12 and in effect accounts for the isomerization reaction between *cis*-$[PtCl_4Br_2]^{2-}$ and *trans*-$[PtCl_4Br_2]^{2-}$.

$$\frac{K_2}{K_3} = \frac{\dfrac{[cis\text{-}PtCl_4Br_2{}^{2-}][Cl^-]}{[PtCl_5Br^{2-}][Br^-]}}{\dfrac{[trans\text{-}PtCl_4Br_2{}^{2-}][Cl^-]}{[PtCl_5Br^{2-}][Br^-]}}$$

$$= \frac{[cis\text{-}PtCl_4Br_2{}^{2-}]}{[trans\text{-}PtCl_4Br_2{}^{2-}]} = K_{11} \qquad \text{...12}$$

The 'cross' ligand substitution reaction stability constants were calculated by making use of the two smaller reaction 'loops' that contain a 'cross' ligand exchange reaction, e.g. *fac*-$[PtCl_3Br_3]^{2-}$ to *trans*-$[PtCl_2Br_4]^{2-}$, and yields equation 14 or equivalently equation 15.

$$\Delta G^0_{rxn16} + \Delta G^0_{rxn13} - \Delta G^0_{rxn7} = 0 \qquad \text{...13}$$

$$K_7 \times K_{13} \times \frac{1}{K_{16}} = 1$$

$$= \frac{[cis\text{-}PtCl_2Br_4^{2-}][Cl^-]}{[fac\text{-}PtCl_3Br_3^{2-}][Br^-]} \times \frac{[trans\text{-}PtCl_2Br_4^{2-}]}{[cis\text{-}PtCl_2Br_4^{2-}]} \times \frac{[fac\text{-}PtCl_3Br_3^{2-}][Br^-]}{[trans\text{-}PtCl_2Br_4^{2-}][Cl^-]} \quad ...14$$

$$K_{16} = K_7 \times K_{13}$$

$$= \frac{[trans\text{-}PtCl_2Br_4^{2-}][Cl^-]}{[fac\text{-}PtCl_3Br_3^{2-}][Br^-]} \quad ...15$$

Results and Discussion

The 'semi-quantitative' experimental work of Schlesinger[32], led Ahrland[3-14] to conclude that Pt^{IV} unequivocally belongs to the second group of metal cations or class (b) in HSAB terminology. Here we extend the experimental work of Schlesinger[33] to a quantitative analysis of the Pt^{IV} halide exchange reaction network (HERN) shown in Diagram 1b.

In order to do so the difficulty associated with accurately measuring all ten $[PtCl_{6-n}Br_n]^{2-}$ (n = 0 - 6) complex anion concentrations in solution with 'direct' methods (Potentiometric,[6] Spectrophotometric[20-24] and Calorimetric[14]) must first be overcome for a full speciation calculation (*vide ante*). This analytical problem was recently solved with an ion-pair reversed phase chromatographic method capable of separating and quantifying all ten $[PtCl_{6-n}Br_n]^{2-}$ (n = 0 – 6) complex anions in well defined acidic chloride/bromide rich matrices.

To furnish the 10 Pt^{IV} complex anions in a 'stepwise' manner, the bromide mole fraction ($\alpha_{Br^-} = \frac{n_{Br^-}}{n_{Br^-} + n_{Cl^-}}$) was systematically varied in a series of samples whilst keeping the total $[Pt^{IV}]_T$ concentration (10.0 mM) constant. In light of our goal to also validate experimentally determined stepwise ligand exchange equilibrium constants using equation 4, it was imperative to keep the ionic strength the same for all samples (total halide concentration; $[Cl^-] + [Br^-]$ = 1.001 M, $[H_3O^+]_T$ = 0.2 M, $[Na^+]_T$ = 0.8 M), such that the activity coefficients of the complexes and halides do not vary significantly from one sample to another. Ultimately, the result obtained with equation 4 or similar energy conservation relationships (ECR) will settle concerns regarding the use of species concentration instead of activity when calculating $\Delta G^o_{rxn's}$. The Pt^{IV} samples were stored at 294.1 K for approximately 8 weeks and periodically irradiated with light to

accelerate ligand exchange.[33] Injection of a sample onto the reversed phase column was immediately done after sample dilution (15 times using an aqueous acetate solution – buffered at pH = 4.64), in order to ensure that no ligand exchange reactions take place for these relatively kinetically stable complex anions. The resulting UV-Vis chromatographic traces at 262 and 315 nm are shown in Figures 1a and b, together with the unambiguous assignment of the 10 Pt^{IV} complexes.[34] It is of interest to note that baseline separation for the $[PtCl_{6-n}Br_n]^{2-}$ (n = 0 - 6) complex anions is obtained and only a relatively small amount of peak overlap for the stereoisomers (n = 2, 3 and 4). Jeansonne *et al*[35] showed that peak deconvolution can be performed in these cases for accurate peak area determination using the exponentially modified Gaussian equation.[35]

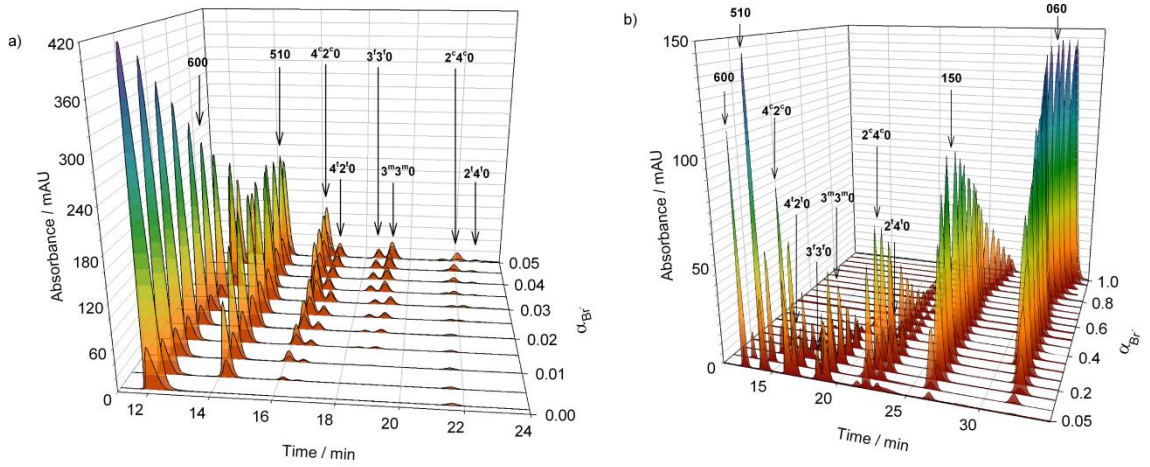

Figure 1. UV-Vis chromatographic traces depicting the stepwise manner in which $[PtCl_{6-n}Br_n]^{2-}$ (n = 0 – 6) complex anions increase and decrease as a function of Br^- mole fraction (a) Br^- mole fraction in the range of 0 to 0.05 and (b) Br^- mole fraction range of 0.05 to 1.0. Total $[Cl^-] + [Br^-]$ = 1.001 M.

In an acidic, ~1.0 M free chloride matrix, Pt^{IV} forms the $[PtCl_6]^{2-}$ complex anion in over 98% abundance, Figure 1a. As the α_{Br-} increase the heteroleptic $[PtCl_{6-n}Br_n]^{2-}$ (n = 1 – 6) complex anions amounts increase and decrease in a "stepwise" manner, best pictorially illustrated by the $[PtClBr_5]^{2-}$ species, Figure 1b. The peak associated with $[PtBr_6]^{2-}$ is already observed at a relatively low α_{Br-} and continues to increase in area until reaching a maximum when the α_{Br-}= 1 with no other Pt^{IV} species detected. Even though ligand exchange for these $[PtCl_{6-n}Br_n]^{2-}$ (n = 0 – 6) complex anions is relatively slow,[36] it was found that after 8 weeks and subsequent periodic injection of the samples for another 3 weeks, the Pt^{IV} complex anions' UV-Vis absorbance peak areas remain constant, giving an indication that equilibrium is attained. Moreover, the direct

determination of stereoisomer species concentrations allows for a straightforward test to confirm whether the Pt^0 chlorido bromido ligand exchange reactions are at equilibrium. From equation 16 it is clear that there is a linear relationship between the concentrations of species in stereoisomer pairs. To relate peak area (obtained in the UV-Vis chromatographic trace) and stereoisomer concentration (where j is a unique constant for each species, equation 16) equation 17 is derived. If all the samples are at equilibrium then a plot of stereoisomer pair peak areas (PA) must yield linear functions as shown in Figure 2. In total there are 14 stepwise ligand exchange and 3 isomerisation equilibria to consider for the HERN. As there are multiple paths by which one species can be converted into another, several ECR's can be derived for this system, Diagram 1b, of which equation 4 is one example. It should be made clear that whilst calculating the equilibrium constants, K_i (i = 1 – 10), no ECR's were used. ECR's only served to test the accuracy of calculated ΔG^o_{rxn}'s values. In addition, as discussed in the computational details section, it is only necessary to calculate the 10 stepwise ligand exchange equilibrium constants, K_i (i = 1 – 10), in order to 'fix' the numerical values of the remaining 7 equilibrium constants.

$$K_{17} = \frac{[trans - PtBr_4Cl_2^{2-}]}{[cis - PtBr_4Cl_2^{2-}]} = \frac{PA_{trans-[PtBr_4Cl_2]^{2-}} \bullet j_{trans-[PtBr_4Cl_2]^{2-}}}{PA_{cis-[PtBr_4Cl_2]^{2-}} \bullet j_{cis-[PtBr_4Cl_2]^{2-}}} \quad ...16$$

$$PA_{trans-[PtBr_4Cl_2]^{2-}} = K_{17} \frac{j_{cis-[PtBr_4Cl_2]^{2-}}}{j_{trans-[PtBr_4Cl_2]^{2-}}} PA_{cis-[PtBr_4Cl_2]^{2-}} \quad ...17$$

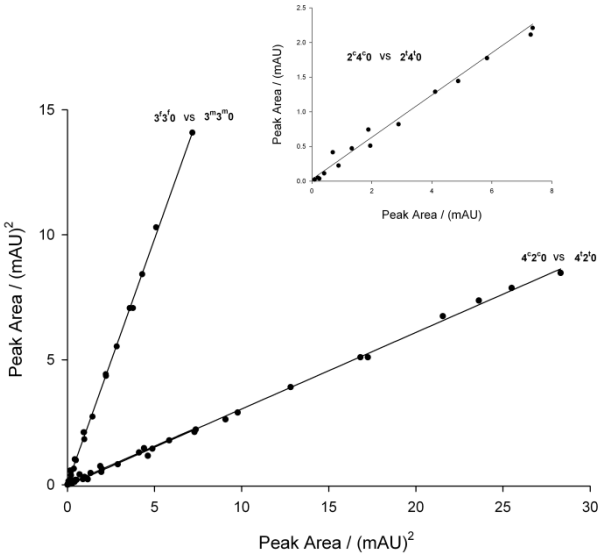

Figure 2. Linear relationships between peak areas observed at 262 nm for individual species in a stereoisomer pair illustrating that equilibrium has been attained. The 'larger' scatter of data observed in the insert figure is due to the signal-to-noise ratio being lower for the $2^{c}4^{c}0$ and $2^{t}4^{t}0$ stereoisomer pair.

Using the program EquiState the stepwise ligand exchange reaction model, Diagram 1b K_i (i = 1 – 10), was simulated and the non-linear least-squares fits obtained are shown in Figure 3.

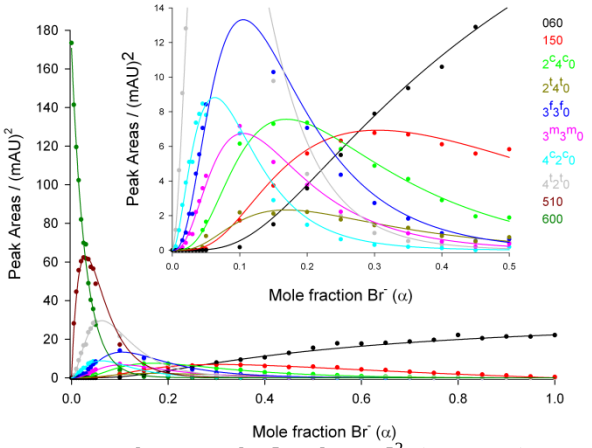

Figure 3. Fit between the $[PtCl_{6-n}Br_n]^{2-}$ (n = 0 – 6) species distribution calculated from peak areas obtained experimentally (·) and the simulated $[PtCl_{6-n}Br_n]^{2-}$ (n = 0 – 6) species distribution (-) detected at 262 nm.

Calculated ε_n's and K_i (i = 1 – 10) are listed in Tables 1 and 2 together with the 7 other numerically 'fixed' equilibrium constants. The excellent fits between the experimentally found Pt^{IV} species UV-Vis peak areas and those calculated, corroborate the model. Furthermore, it is

decidedly satisfying that the ECR (equation 4) yielded a value of 0.2 kJ.mol^{-1} which boasts well for the accuracy of the calculated K_i (i = 2 – 9) and unequivocally confirms for the first time the thermodynamic data for an 8 member inorganic reaction 'loop'. In addition, due to the fact that we do not simplify the HERN in Diagram 1b to 1a it is now possible to calculate the overall formation constant, β_{10}, using one reaction path, e.g. $\beta_{10} = K_1K_2K_4K_6K_8K_{10}$ = 472 239 and $\Delta G^o_{rxn(\beta 10)}$ = -31.94 kJ.mol^{-1}. When the HERN is simplified, as shown in Diagram 1a, the overall formation constant is incorrectly calculated as 'β_6*' = $K_1(K_2+K_3)(K_4+K_5)(K_6+K_7)(K_8+K_9)K_{10}$ = 17096544, introducing a significant error. Moreover, the ΔG^o_{rxn} for reaction r1 can also be verified with data obtained from standard half cell reduction potentials (E^0).[37] Combining the two half cell reactions r4 and r5 gives the overall reaction r1, from which equation 18 can be derived to calculate ΔG^o_{rxn}.

$$[PtCl_6]^{2-}_{(aq)} + 4e^- \rightleftharpoons Pt(s) + 6Cl^-_{(aq)} \qquad E^0_1 = 0.744 \text{ V} \qquad \text{...r4}$$

$$[PtBr_6]^{2-}_{(aq)} + 4e^- \rightleftharpoons Pt(s) + 6Br^-_{(aq)} \qquad E^0_2 = 0.657 \text{ V} \qquad \text{...5}$$

$$\Delta G^0_{rxn(B_{10})} = nFE^0_2 - nFE^0_1 = -33.6 \text{ kJ.mol}^{-1} \qquad \text{...18}$$

The exceptional agreement of the ΔG^o_{rxn}'s values (-31.94 and -33.6 kJ.mol^{-1}) obtained with two independent methods together with the result obtained with the ECR, equation 4, leaves little doubt regarding the accuracy of calculated thermodynamic parameters for this system. In light of the above results, the assumption concerning the use of species concentrations and not species activity for equilibrium constant calculations are well justified. A full species distribution diagram for the $[PtCl_{6-n}Br_n]^{2-}$ (n = 0 – 6) system is shown in Figure 4a, accompanied by an enlargement of the stereoisomer distributions, Figure 4b.

Table 1. Molar extinction coefficients, ε, for the $[PtCl_{6-n}Br_n]^{2-}$ (n = 0 - 6) complex anions at 262 nm.

Species	600	510	4^c2^c0	4^t2^t0	3^t3^t0	3^m30	2^c4^c0	2^t4^t0	150	060
ε /	24500 ±	23749 ±	19738 ±	15336 ±	9747 ±	10944 ±	5224 ±	4696 ±	2588 ±	3189 ±
L.mol^{-1}.cm^{-1}	351	285	592	460	292	328	156	140	77	95

Table 2. Stability constants K_i (i = 0 – 17) and Gibbs energy $\Delta G°_{rxn}$ (i = 0 – 17) for the $[PtCl_{6-n}Br_n]^{2-}$ (n = 0 – 6) complex anions at 294.1 K.

	i	K_i	$\Delta G°_{rxn}$ / kJ.mol^{-1}
Stepwise Ligand Substitution Reactions	1	36.34 ± 0.73	-8.79 ± 0.17
	2	12.46 ± 0.25	-6.17 ± 0.12
	3	4.78 ± 0.09	-3.83 ± 0.08
	4	5.30 ± 0.11	-4.08 ± 0.08
	5	24.30 ± 0.49	-7.80 ± 0.16
	6	13.93 ± 0.28	-6.44 ± 0.13
	7	2.71 ± 0.05	-2.44 ± 0.05
	8	6.54 ± 0.13	-4.59 ± 0.09
	9	19.11 ± 0.38	-7.21 ± 0.14
	10	2.16 ± 0.04	-1.88 ± 0.04
Isomerization Reactions	11	2.61 ± 0.05	-2.35 ± 0.05
	12	1.76 ± 0.03	-1.38 ± 0.03
	13	2.92 ± 0.06	-2.62 ± 0.05
'Cross' Ligand Substitution Reactions	14	13.48 ± 0.28	-1.74 ± 0.03
	15	9.34 ± 0.19	-2.71 ± 0.05
	16	4.77 ± 0.09	-3.82 ± 0.08
	17	7.92 ± 0.16	-4.99 ± 0.01

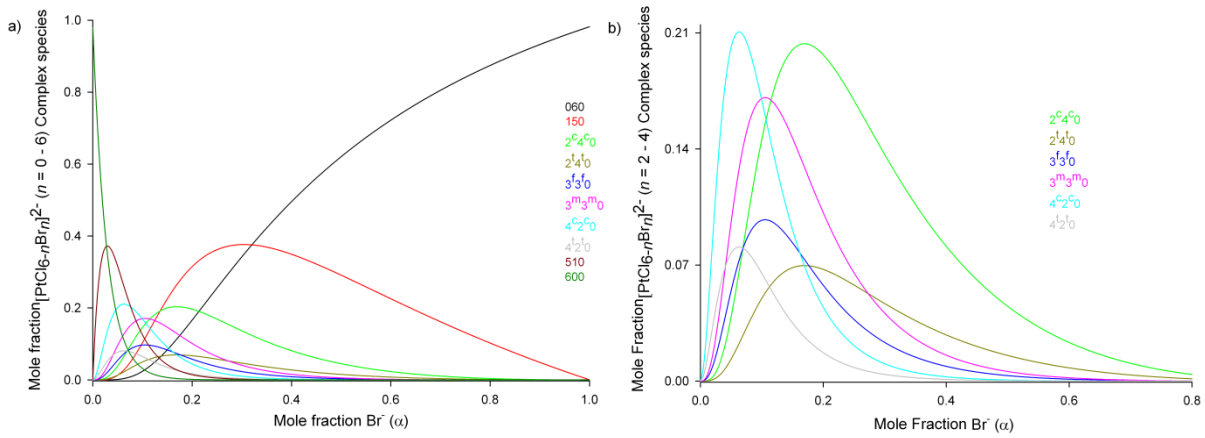

Figure 4. (a) The $[PtCl_{6-n}Br_n]^{2-}$ (n = 0 – 6) species distribution, (b) enlargement of the stereoisomers species distribution.

From the relatively large overall formation constant, β_{10} = 472 239, or from a visual inspection of the data in Figure 4a, it would seem justified to draw the same conclusion as done in many other related studies,[1] that the thermodynamic stability of the Pt^{IV} complexes containing bromido ligands is greater in comparison to their chlorido analogues. If the above statement regarding the thermodynamic stability of a complex was made when comparing for example stereoisomers, *cis*- and *trans*-$[PtCl_2Br_4]^{2-}$, it would be unambiguous, equation 19.

$$\Delta G^0_{rxn} = \Delta G^0_f(t\,rans - [PtCl_2Br_4]^{2-}) - \Delta G^0_f(cis - [PtCl_2Br_4]^{2-}) = -RT\ln(K_{17}) \quad ...19$$

However, for a ligand exchange reaction, e.g. the first exchange of a chloride by bromide for the $[PtCl_6]^{2-}$ complex, equation 21 and 22, it is clear that the contribution of the halides, $\Delta\Delta G^o_{f(halide)}$, to ΔG^o_{rxnK1} must also be taken into consideration before a conclusion can be made concerning the relative thermodynamic stability of these complexes.

$$\Delta G^0_{rxn} = \sum \Delta G^0_{f(products)} - \sum \Delta G^0_{f(reactants)} \quad ...20$$

$$\Delta G^0_{rxnK1} = \{\Delta G^0_f([PtCl_5Br]^{2-}) - \Delta G^0_f([PtCl_6]^{2-})\} + \{\Delta G^0_f([Cl]^-) - \Delta G^0_f([Br]^-)\} \quad ...21$$

$$\Delta G^0_{rxnK1} = \Delta\Delta G^0_{f(complex)} + \Delta\Delta G^0_{f(halide)} \quad ...22$$

From tabulated thermodynamic data[38] the $\Delta\Delta G_{f}^{o}{}_{(halide)}$ is equal to -27.2 kJ.mol^{-1} and $\Delta G^{o}{}_{rxnK1}$ determined experimentally is -8.7 kJ.mol^{-1}. Substituting these values into equation 22 yields a positive value for $\Delta\Delta G_{f}^{o}{}_{(complex)}$ of 18.9 kJ.mol^{-1}.For each subsequent stepwise ligand replacement reaction the $\Delta\Delta G_{f}^{o}{}_{(complex)}$ term becomes only slightly more positive (*vide infra*). Interestingly, the positive values for $\Delta\Delta G_{f}^{o}{}_{(complex)}$ clearly indicates that the chlorido complexes are energetically favoured above the corresponding bromido analogues. Moreover, the positive value for $\Delta\Delta G_{f}^{o}{}_{(complex)}$ and the overall negative value of $\Delta G^{o}{}_{rxnK1}$ implies that the replacement of chloride by bromide is thermodynamically driven by $\Delta\Delta G_{f}^{o}{}_{(halide)}$. In summary, the thermodynamic stability of Pt^{IV} complexes containing chlorido ligands are greater in comparison to their bromido analogues.

To generalize this result for all class (b) metal cations in order to determine whether the $\Delta\Delta G_{f}^{o}{}_{(complex)}$ term yields a positive or negative contribution to $\Delta G^{o}{}_{rxn}$, the above analysis was extended. To facilitate the discussion we use the convention that the lighter halide (X) is replaced by the heavier halide (Y) and note that the same conclusion(s) will be reached if this convention is reversed. Firstly, it is assumed that the $\Delta\Delta G_{f}^{o}{}_{(complex)}$ term is equal to zero, therefore $\Delta G^{o}{}_{rxn}$ is solely determined by the $\Delta\Delta G_{f}^{o}{}_{(halide)}$ contribution. The overall hypothetical formation constant, H_{10}, for replacing six X present in $[MX_6]^q$ (M is any metal cation, q is the charge) with six Y is then calculated using equation 23 which yield the H_{10} values shown in Table 3.

$$\Delta G^{0}_{rxn} = 6(\Delta\Delta G^{0}_{f\,(halide)}) = -RT\ln(H_{10}) \qquad \ldots 23$$

Table 3. Overall hypothetical formation constant, H_{10}, for replacing a lighter halide, X, by the heavier halide, Y.

X	F^-	Cl^-	Br^-	F^-
Y	Cl^-	Br^-	I^-	I^-
H_{10}	1.4×10^{155}	3.9×10^{28}	1.2×10^{55}	6.6×10^{238}

The experimentally determined β_{10} can now be compared to H_{10} to evaluate the $\Delta\Delta G_{f}^{o}{}_{(complex)}$ contribution to $\Delta G^{o}{}_{rxn}$. If $\beta_{10} < H_{10}$ then the $\Delta\Delta G_{f}^{o}{}_{(complex)}$ term is positive, implying that the lighter halide $[MX_6]^q$ complex is thermodynamically favoured relative to the heavier halide $[MY_6]^q$ analogue and vice versa. The listed H_{10}'s values in Table 3 are relatively large and we could not find one reported overall formation constant for any class (b) metal cation where $\beta_{10} > H_{10}$, even though many of the reported β_{10} (actually β_6*) values are artificially inflated as

discussed above. This striking experimental result indicates that the lighter metal halido complex is always thermodynamically favoured above the heavier metal halido analogue in solution. Stated differently, all class (b) metal cations prefer to bond with halides in the order $F^- > Cl^- > Br^- > I^-$, and thus is exactly the same for class (a) metal cations. Moreover, the numerical values of $\Delta\Delta G_f^o{}_{(complex)}$ and $\Delta\Delta G_f^o{}_{(halide)}$ are always opposite in sign. If this was not the case then the so-called class (b) metal cations would exhibit a $\beta_{10} > H_{10}$, increasing the thermodynamic stability of these metal halido complexes to such an extent that they would be unfavorable as synthetic starting materials in aqueous solution. It is apparent that HSAB classification of metal cations into two classes is erroneous and must be revised to include the $\Delta\Delta G_f^o{}_{(halide)}$ contribution to the $\Delta G^o{}_{rxn}$.

In the above context we propose that only one 'group' of metal cations exist, i.e. all homo- and heteroleptic metal halide complexes in solution *irrespective of the metal cation oxidation state* energetically favour to bond with halides in the order $F^- >> Cl^- > Br^- > I^-$. The '2^{nd} group' as defined by Ahrland only appears when the $\Delta\Delta G_f^o{}_{(halide)}$ contribution towards $\Delta G^o{}_{rxn}$ prevails, regardless of the metal cation preference to bond with the lighter halide.

$\Delta\Delta G_f^o{}_{(halide)}$ contribution to $\Delta G^o{}_{rxn}$ can be manipulated by performing these halide exchange reactions in chloroform. This was achieved by preparation of a Pt^{IV} sample such that the $[Pt]_T$ was 10 mM, 0.5 M methyltrioctylammonium chloride and 0.5 M methyltrioctylammonium bromide. The sample was left for 8 weeks to equilibrate at 298 K. The UV-Vis chromatographic trace obtained after the injection of 2 µl of this sample is shown in Figure 5. In contrast to the earlier observed species distribution obtained for this bromide mole fraction in water, (Figure 1b) where no $[PtCl_6]^{2-}$ species was present, there are now an abundant amount of $[PtCl_6]^{2-}$ species. This result unambiguously confirms the thermodynamically favoured stability of the chlorido complexes over that of the bromido species. It was noted by Preetz *et al*[1] that a 'class (b)' metal fluorido complexes are readily obtained in non-aqueous solutions by phase transfer of F^- by long-chain alkylammonium cations in solvents such as chloroform.[1]

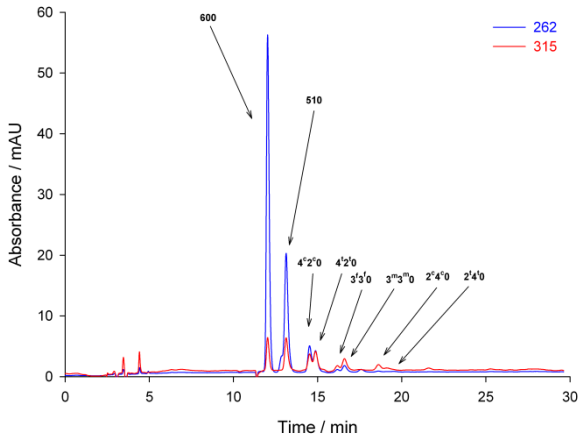

Figure 5. The $[PtCl_{6-n}Br_n]^{2-}$ (n = 0 – 6) species distribution in chloroform in the presence of 0.5 M Cl^- and 0.5 M Br^-.

Although the ΔG^o_{rxn} for some halide ligand exchange reactions are relatively small, Table 1, the opposing terms $\Delta\Delta G_f{}^o_{(complex)}$ and $\Delta\Delta G_f{}^o_{(halide)}$ are relatively large with respect to the chemical energetic accuracy that can be expected of modern DFT calculations for homo- and heteroleptic metal halido complexes.[27,28] In an attempt to gain better understanding of why all metal cations prefer to bond with halides in the order $F^- > Cl^- > Br^- > I^-$ we used several DFT functionals in both the gas phase and in the aqueous phase (conductor like screening model, COSMO) for the calculation of $\Delta\Delta G_f{}^o_{(complex)}$. Several representative *p*- and *d*-block metal cations were chosen that are known to form 4 – 6 coordinated halido complexes and in some cases the same metal cation in differing oxidation state and spin multiplicity were used. In addition, also establish at least qualitatively that the contributions of $\Delta\Delta G_f{}^o_{(complex)}$ and $\Delta\Delta G_f{}^o_{(halide)}$ towards ΔG^o_{rxn} are always opposite. The results for these calculations pertaining to Rh^{III}, Pt^{II} and Al^{III} are listed in Table 4 and the data for the other 5 metal cations tested are listed in Table S1.

Table 4. $\Delta\Delta G_{f\,(complex)}^{o}$ for the stepwise halide substitution reactions for Rh^{III}, Pt^{II} and Al^{III} complexes in $kJ.mol^{-1}$.

i	$[RhF_{6-n}Cl_n]^{3-}$ (n = 0 – 6)[a]		$[RhCl_{6-n}Br_n]^{3-}$ (n = 0 – 6)[a]		$[PtF_{4-n}Cl_n]^{2-}$ (n = 0 – 4)[b]		$[PtCl_{4-n}Br_n]^{2-}$ (n = 0 – 4)[b]		$[AlF_{4-n}Cl_n]^{-}$ (n = 0 – 4)[c]		$[AlCl_{4-n}Br_n]^{-}$ (n = 0 – 4)[c]	
	Gas phase	COSMO	Gas phase	COSMO	Gas phase	COSMO	Gas phase	COSMO	Gas phase	COSMO	Gas phase	COSMO
1	24.49	136.64	14.31	34.56	64.38	114.70	30.41	36.65	185.90	209.84	57.73	60.36
2	69.20	145.38	19.74	40.52	71.56	120.02	35.71	41.30	191.81	212.03	60.13	63.34
3	61.76	136.17	17.97	36.87	70.86	115.29	34.96	40.46	197.71	214.69	62.17	64.34
4	63.16	132.00	16.68	35.64	74.50	114.19	33.73	38.16	202.47	218.43	64.32	66.67
5	68.91	138.07	21.32	40.95	75.21	118.91	34.51	39.01				
6	78.27	141.86	22.55	41.01	84.35	123.78	38.82	42.18				
7	75.01	137.39	17.99	37.75								
8	76.97	130.71	20.00	38.63								
9	81.92	138.32	21.70	40.24								
10	89.97	143.80	24.65	41.96								

[a]Refer to Scheme S1 for *i* values (octahedral)
[b]Refer to Scheme S2 for *i* values (square planar)
[c]Refer to Scheme S3 for *i* values (tetrahedral)

From the $\Delta\Delta G_{f\,(complex)}^{o}$ data shown in Tables 4 and S1 one distinctive trend stands out, all $\Delta\Delta G_{f\,(complex)}^{o}$ values are positive. Thus confirms that metal cations prefer to bond with halides in the order $F^- > Cl^- > Br^- > I^-$, the same trend as found experimentally. This result remains the same irrespective of the metal cation oxidation state, level of DFT functional used, basis set size, the spin-multiplicity of a complex, omission or inclusion of relativistic effects and for both gas and liquid phases. Moreover, the trends regarding the magnitude of $\Delta\Delta G_{f\,(complex)}^{o}$ corresponds with the expected ligand field stabilization energy (LFSE) with respect to metal cation oxidation state and position of halide ligand in the spectrochemical series as encapsulated in ligand field theory (LFT). A detailed DFT investigation for quantitative comparison with experimentally obtained stability constants for all the metal cations listed in Tables 4 and S1 is beyond the ambit of this investigation and is currently being pursued. Here we first focus on whether it is possible to obtain quantitative agreement between experiment and theory (DFT) concerning Pt^{IV} chlorido bromido complexes with respect to the thermodynamic parameters such as the $\Delta\Delta G_{f\,(complex)}^{o}$ term. Especially encouraging is the chemically energetic accuracy, < 20 $kJ.mol^{-1}$, obtained for the $\Delta\Delta G_{f\,(complex)}^{o}$ terms for chlorido-bromido halide exchange for Pt^{IV}, Figure 6. It is also noted that the $\Delta\Delta G_{f\,(complex)}^{o}$ energy difference only slightly increases for each successive ligand exchange reaction, similarly to that found experimentally. Moreover, the gas phase energies are in better agreement with experimental values compared to the COSMO model calculations. Calculated stereoisomer ΔG_{rxn}^{o} values for the Pt^{IV} chlorido bromido system, Table 4, using DFT agree quantitatively with the experimentally obtained values. This relatively high accuracy may be due to some fortuitous error cancellation.[28] However, accurate stereoisomer stability constants can be expected for metal cation halide complexes using the computational methodology as outlined here. Furthermore, the $\Delta\Delta G_{f\,(complex)}^{o}$ calculated for the $[PtF_{6-n}Br_n]^{2-}$, $[PtF_{6-n}Br_n]^{2-}$ and $[PtCl_{6-n}I_n]^{2-}$ (n = 0 – 6) systems decreases in the order $F^- > Cl^- > Br^- > I^-$ in the gas and liquid (COSMO) phases indicating clearly the bonding preference of Pt^{IV} to halides, Table S2.

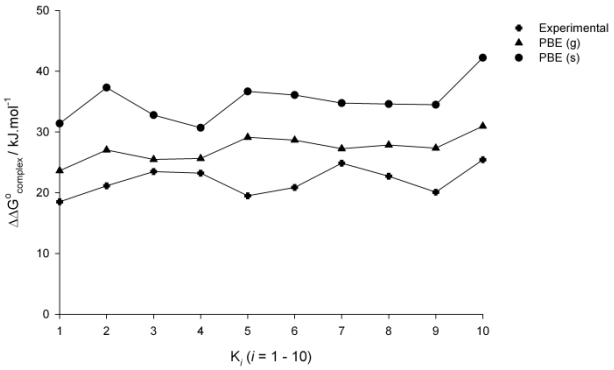

Figure 6. Comparison between the $\Delta\Delta G_f^{o}{}_{(complex)}$ values for the $[PtCl_{6-n}Br_n]^{2-}$ (n = 0 – 6) species (kJ.mol-1) obtained experimentally and those calculated by DFT in the gas phase and aqueous solvent.

Table 4. DFT calculated and experimentally determined ΔG_{rxn}^{o} values (kJ.mol^{-}1) for the isomerization reactions of $PtCl_{6-n}Br_n]^{2-}$ (n = 0 – 6).

i	PBE		LDA		PW91		MO6L		
	Gas phase	COSMO	Gas phase	COSMO	Gas phase	COSMO	Gas phase	COSMO	Experimental
11	-1.56	-4.54	-1.75	-2.82	-1.66	-2.47	-1.18	-3.56	-2.35± 0.05
12	-1.93	-1.44	-2.97	-2.13	-3.08	-2.04	-2.68	1.68	-1.38± 0.03
13	0.51	0.12	-1.72	-2.82	-1.55	-2.02	-4.76	-9.38	-2.62± 0.05

Conclusions

The ability to quantify each individual $[PtCl_{6-n}Br_n]^{2-}$ (n = 0 – 6) species by means of ion-paring HPLC-UV-Vis allowed for the determination of all 17 stability constants for the Pt^{IV} chlorido-bromido halide exchange reaction network. The associated Gibbs free energies were determined for each ligand exchange reaction step, $\Delta G_{rxnK_n}^{o}$ (n = 1 - 17), and together with energy conservation relationships served to validate the accuracy of the experimentally calculated stability constants. The good agreement between the experimentally determined overall formation constant or ΔG_{rxn}^{o} and those calculated using the standard reaction half cell reduction potentials of $[PtCl_6]^{2-}$ and $[PtBr_6]^{2-}$ is further confirmation of these experimentally obtained thermodynamic parameters. The hydration energy differences between halide ligands contribution to $\Delta G_{rxnK_n}^{o}$ (n = 1 - 17), $\Delta\Delta G_f^{o}{}_{(halide)}$ = -27.2 kJ.mol^{-1}, drives the reaction towards the

bromido Pt^{IV} species in aqueous solutions, even though the chlorido Pt^{IV} complexes were determined to be energetically favoured in this reaction network. This result was generalized for other metal cation halido exchange reactions and showed that all metal halido complexes exhibit the $F^- >> Cl^- > Br^- > I^-$ order of thermodynamic stability and that inversion of this order was only due to the solvation of the relevant halide ligands. This result exposed the fundamentally flawed nature of HSAB in predicting metal cation halido thermodynamic stabilities. Moreover, density functional theory (DFT) was used to confirm the thermodynamic stabilities with respect to the isodesmic reactions involving chlorido-bromido Pt^{IV} stereoisomer pairs and chlorido-bromido Pt^{IV} ligand exchange reactions of the $[PtCl_{6-n}Br_n]^{2-}$ (n = 0 – 6) species and confirmed the $F^- >> Cl^- > Br^- > I^-$ order of thermodynamic stability as well as determining the $\Delta\Delta G^o_{rxn}$ within the range of 8 - 20 $kJ.mol^{-1}$ to the experimentally determined $\Delta\Delta G^o_{rxn}$.

COMPUTATIONAL DETAILS

Geometries were fully optimised at the relativistic spin-orbit ZORA level, using the LDA,[39] GGA's PBE[40] and PW91,[41] and the M06L[42] functionals, together with an all-electron quadruple-ζ plus polarisation function (QZ4P) basis set on the Pt and I and even-tempered pVQZ basis set on the F, Cl and Br. Optimization in the gas phase as well as for those using the conductor-like screening model (COSMO),[43] with the parameters of water, were done with the abovementioned combinations of functionals and basis sets. The obtained structures were characterized as minima by analyzing the Hessian matrix. These calculations employed the ADF2010.02 program.[44]

References

1. G. Peters, W. Preetz, D. Bublitz, *Chemical Reviews*, **1996**, *96*, 977.
2. R. A. Grant, F. L. Bernardis, D. C. Sherrington, *Reactive & Functional Polymers*, **2005**, *65*, 205.
3. S. Ahraland, *Acta Chemica Scandinavica*, **1956**, *10*, 723.
4. S. Ahraland, I. Grenthe, *Acta Chemica Scandinavica*, **1957**, *11*, 1111.
5. S. Ahraland, I. Grenthe, L. Johansson, B. Norén, *Acta Chemica Scandinavica*, **1963**, *17*, 1567.
6. S. Ahraland, J. Rawsthorne, *Acta Chemica Scandinavica*, **1970**, *24*, 157.
7. S. Ahraland, N-O, Björk, *Acta Chemica Scandinavica*, **1976**, *30*, 249.

8. S. Ahraland, B. Tagesson, *Acta Chemica Scandinavica*, **1977**, *31*, 615.

9. S. Ahraland, B. Tagesson, D. Tuhtar, *Acta Chemica Scandinavica*, **1977**, *31*, 625.

10. S. Ahraland, L. Kullberg, R. Portanova, *Acta Chemica Scandinavica*, **1978**, *32*, 251.

11. S. Ahraland, N-O, Björk, I. Persson, *Acta Chemica Scandinavica*, **1981**, *35*, 67.

12. S. Ahraland, K. Nilsson, B. Tagesson, *Acta Chemica Scandinavica*, **1983**, *37*, 193.

13. S. Ahraland, S, Ishiguro, I. Persson, *Acta Chemica Scandinavica*, **1986**, *40*, 418.

14. S. Ahraland, G. Hefter, B. Norén, *Acta Chemica Scandinavica*, **1990**, *44*, 1.

15. R. G. Pearson, *Journal of the American Chemical society*, **1963**, *22*, 3533.

16. H, Mayr, M. Breugst, A, R, Ofial, *Angewandte Chemie, International Edition*, **2011**, *50*, 6470.

17. R. Abegg, G. Bodländer, *Zeitschift für Anorganiche und Allgemeine Chemie*, **1899**, 20, 453.

18. J. Bjerrum, *Chemical Reviews*, **1950**, *46*, 381.

19. H. H. Drews, W. Z. Preetz, *Naturrforsch. B*, **1996**, *51*, 1563.

20. L. I. Elding, L. Gustafson, *Inorganica Chimica Acta*, **1976**, *19*, 31.

21. L. I. Elding, L. Gustafson, *Inorganica Chimica Acta*, **1977**, *22*, 201.

22. L. I. Elding, L. Gustafson, *Inorganica Chimica Acta*, **1977**, *24*, 239.

23. L. I. Elding, A. Groning, *Chemica Scripta*, **1977**, *11*, 8.

24. L. I. Elding, *Inorganica Chimica Acta*, **1978**, *28*, 255.

25. L. I. Elding, L. Drougge, *Inorganica Chimica Acta*, **1986**, *121*, 175.

26. W. Robb, G. M. Harris, *Journal of the American Chemical Society*, **1965**, *87*, 4472.

27. P. E. M. Siegbahn, *Theoretica Chimica Acta*, **1993**, *86*, 219.

28. P. R. Varadwaj, I. Cukrowski, C. B. Perry, H. M. Marques, *Journal of Physical Chemistry A*, **2011**, *115*, 6629.

29. M. Meloun, J. Havel, E. Högfeldt, *Computation of Solution Equilibria- A Guide to Methods in Potentiometry, Extraction, and Spectrophotometry*, Ellis Horwood, Chichester, **1987**.

30. K. Levenberg, *Quarterly of Applied Mathermatics*, **1944**, *2*, 164.

31. R. L. Burden, J. D Faires, Numerical Analysis, 6th ed., Brooks/Cole Publishing Company, **1997**.

32. H. I. Schlesinger, M. W. Tapley, Journal of the American Chemical Society, **1924**, *46*, 276.

33. I. V. Khmelinski, V. P. Grivin, V. F. Plyusnin, *Journal of Photochemistry and Photobiology, A: Chemistry*, **1990**, *51*, 379.

34. P-H. Van Wyk, W. J Gerber, K. R. Koch, *Analytica Chimica Acta*, **2011**, *704*, 154.

35. J. P. Foley, M. S. Jeansonne, *Journal of Chromatography*, **1992**, *1*, 594.

36. A. Wilkinson, G. Cotton, Advanced Inorganic Chemistry, John Wiley & Sons: New York, **1988**.

37. G. Inzelt, *Standard Potentials*, *Encyclopedia of Electrochemistry*, 2007, John Wiley & Sons, Ltd.

38. T. Engel, P. Reid, *Thermodynamics, Statistical Thermodynamics and Kinetics*, Prentice Hall, Inc. 2006.

39. S. H. Vosko, L. Wilk, M. Nusair, *Canadian Journal of Physics*, **1980**, *58*, 1200.

40. J. P. Perdew, K. Burke, M. Ernzerhof, *Physical Review Letters*, **1996**, *77*, 3865.

41. J. P. Perdew, J. A. Chevary, S. H. Vosko, K. A. Jackson, M. R. Pederson, D. J. Sing, C. Fiolhais, *Physical Review B*, **1992**, *46*, 6671.

42. (a) Y. Zhao, D. G. Truhlar, *Journal of Chemical Physics*, **2006**, *125*, 194101. (b) Y. Zhao, D. G. Truhlar, *Theoretical Chemistry Accounts*, **2008**, *120*, 215.

43. (a) A. Klamt, G. Schüürmann, *Journal of the Chemical Society, Perkin Transactions*, **1993**, *2*, 799. (b) A. Klamt, *Journal of Physical Chemistry*, **1995**, *99*, 2224. (c) A. Klamt, V. Jonas, *Journal of Chemical Physics*, **1996**, *105*, 9972.

44. E. J. Baerends, T. Ziegler, J. Autschbach, D. Bashford, A. Bérces, F.M. Bickelhaupt, C. Bo, P. M. Boerrigter, L. Cavallo, D. P. Chong, L. Deng, R. M. Dickson, D. E. Ellis, M. van Faassen, L. Fan, T. H. Fischer, C. Fonseca Guerra, A. Ghysels, A. Giammona, S. J. A. van Gisbergen, A. W. Götz, J. A. Groeneveld, O. V. Gritsenko, M. Grüning, S. Gusarov, F. E. Harris, P. van den Hoek, C. R. Jacob, H. Jacobsen, L. Jensen, J. W. Kaminski, G. van Kessel, F. Kootstra, A. Kovalenko, M. V. Krykunov, E. van Lenthe, D. A. McCormack, A. Michalak, M. Mitoraj, J. Neugebauer, V. P. Nicu, L. Noodleman, V. P. Osinga, S. Patchkovskii, P. H. T. Philipsen, D. Post, C. C. Pye, W. Ravenek, J. I. Rodríguez, P. Ros, P. R. T. Schipper, G. Schreckenbach, J. S. Seldenthuis, M. Seth, J. G. Snijders, M. Solà, M. Swart, D. Swerhone, G. te Velde, P. Vernooijs, L. Versluis, L. Visscher, O. Visser, F. Wang, T. A. Wesolowski, E. M. van Wezenbeek, G. Wiesenekker, S. K. Wolff, T. K. Woo, A. L. Yakovlev, *ADF2010*; SCM, Theoretical Chemistry, Vrije Universiteit: Amsterdam, The Netherlands; see http://www.scm.com.

Supporting Information

Table S1. DFT calculated $\Delta\Delta G_f^{o}{}_{(complex)}$ for the stepwise halide substitution reactions for MXY type Au^{III}, Cd^{II} and Fe^{III} complexes in $kJ.mol^{-1}$.

i	$[AuF_{6-n}Cl_n]^-$ (n = 0 – 4)[b]		$[AuCl_{6-n}Br_n]^-$ (n = 0 – 4)[b]		$[CdF_{4-n}Cl_n]^{2-}$ (n = 0 – 4)[c]		$[CdCl_{4-n}Br_n]^{2-}$ (n = 0 – 4)[c]		$[FeF_{4-n}Cl_n]^-$ (n = 0 – 4)[c]		$[FeCl_{4-n}Br_n]^-$ (n = 0 – 4)[c]	
	Gas phase	COSMO	Gas phase	COSMO	Gas phase	COSMO	Gas phase	COSMO	Gas phase	COSMO	Gas phase	COSMO
1	96.24	111.40	34.03	36.02	67.65	126.97	31.49	43.83	136.98	158.02	39.21	42.30
2	102.46	121.98	38.95	41.95	76.51	129.73	34.39	46.17	141.59	159.87	39.70	42.97
3	99.95	113.43	37.87	40.15	84.04	134.67	36.66	47.75	145.21	162.16	41.89	44.65
4	98.59	110.89	36.15	38.41	91.25	136.78	39.33	50.43	149.76	165.11	44.05	46.35
5	101.10	119.45	37.24	40.22								
6	105.57	123.20	41.36	43.69								

[a]Refer to Scheme S1 for *i* values (octahedral)
[b]Refer to Scheme S2 for *i* values (square planar)
[c]Refer to Scheme S3 for *i* values (tetrahedral)

Table S1 *cont*. DFT calculated $\Delta\Delta G_{f\,(complex)}^{o}$ for the stepwise halide substitution reactions for MXY type Sn^{II} and Zn^{II} complexes in kJ.mol^{-1}.

i	$[SnF_{6-n}Cl_n]$ (n = 0 – 4)[c]		$[SnCl_{6-n}Br_n]$ (n = 0 – 4)[c]		$[ZnF_{4-n}Cl_n]^{2-}$ (n = 0 – 4)[c]		$[ZnCl_{4-n}Br_n]^{2-}$ (n = 0 – 4)[c]	
	Gas phase	COSMO	Gas phase	COSMO	Gas phase	COSMO	Gas phase	COSMO
1	136.90	140.07	35.45	36.03	73.42	135.29	26.11	41.46
2	141.11	148.25	37.52	37.99	85.76	139.43	29.14	44.14
3	146.49	154.96	38.72	41.48	95.59	144.03	31.36	45.49
4	150.90	160.22	41.57	43.65	104.66	148.63	34.05	47.40

[a]Refer to Scheme S1 for *i* values (octahedral)
[b]Refer to Scheme S2 for *i* values (square planar)
[c]Refer to Scheme S3 for *i* values (tetrahedral)

Table S2. DFT calculated $\Delta\Delta G_{f\,(complex)}^{o}$ for the stepwise halide substitution reactions of $[PtX_{6-n}Y_n]^{2-}$ (n = 0 – 6)[a] complexes in kJ.mol^{-1}.

i	$[PtF_{6-n}Cl_n]^{2-}$ (n = 0 – 6)		$[PtF_{6-n}Br_n]^{2-}$ (n = 0 – 6)		$[PtCl_{6-n}I_n]^{2-}$ (n = 0 – 6)	
	Gas phase	COSMO	Gas phase	COSMO	Gas phase	COSMO
1	89.77	124.93	118.64	164.28	62.65	82.31
2	100.62	135.48	126.37	172.69	67.27	92.21
3	95.75	126.35	125.67	163.55	65.38	84.34
4	96.20	124.501	127.06	158.63	66.64	84.92
5	101.22	129.69	132.01	165.16	73.17	91.23
6	105.70	136.06	133.68	174.16	71.97	95.22
7	101.81	130.81	127.78	163.45	67.20	90.52
8	102.02	124.49	131.12	156.13	71.55	88.40
9	105.76	133.68	132.77	169.45	71.69	94.67
10	110.18	135.93	136.02	168.59	76.47	96.56

[a]Refer to Scheme S1 for *i* values (octahedral)
[b]Refer to Scheme S2 for *i* values (square planar)
[c]Refer to Scheme S3 for *i* values (tetrahedral)

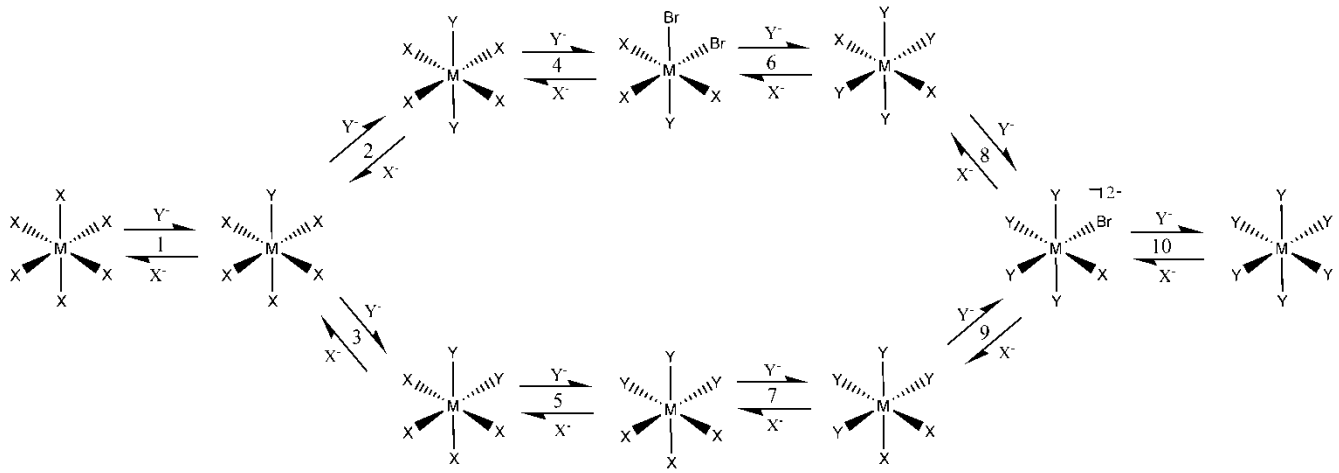

Scheme S1. The stepwise halide substitution reactions, *i* = 1 - 10, for an octahedral system.

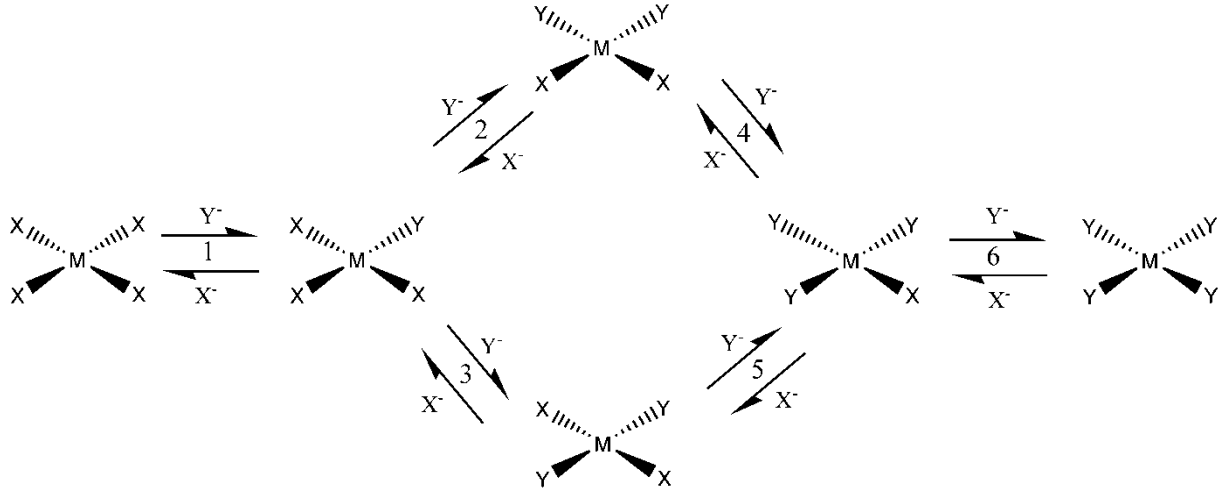

Scheme S2. The stepwise halide substitution reactions, *i* = 1 - 6, for a square planar system.

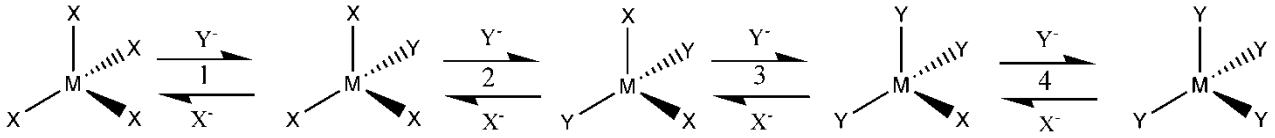

Scheme S3. The stepwise halide substitution reactions, *i* = 1 - 4, for a tetrahedral system.

Concluding Remarks

In this thesis, the development of an ion-paring reversed phase liquid chromatographic method for the analysis of platinum complex anions present in acidic, halide rich (Cl^- and Br^-) solutions of interest to the PGMs recovery industry was presented. This study commenced with the development of the ion-pairing RP-HPLC method and its successful application to the separation, characterization and quantification of all possible $[PtCl_{6-n}Br_n]^{2-}$ (n = 0 – 6) and $[PtCl_{4-n}Br_n]^{2-}$ (n = 0 – 4) complex anions using UV-Vis detection. High resolution ^{195}Pt NMR of more concentrated $Pt^{II/IV}$ solutions served to validate the relevant species assignments, particularly those of the stereoisomer species. The relevant $Pt^{II/IV}$ species were quantified by means of IP-RP-HPLC coupled to ICP-MS or ICP-OES, and together with the UV-Vis absorption spectra obtained by photodiode array (PDA) recording of all eluted species, the photometric characteristics (λ_{max} and ε) of all the $Pt^{II/IV}$ species was determined. Characterization of Pt species observed chromatographically was still, however, to an extent dependent on ^{195}Pt NMR validation. The determination of the Pt to halide mole ratio of individually separated species enabled the characterization of Pt species without the need for ^{195}Pt NMR validation using concentrated samples. The Pt to chloride and/or Pt to bromide mole ratio of the $[PtCl_4]^{2-}$ and the series of $[PtCl_{6-n}Br_n]^{2-}$ (n = 0 – 6) complexes were determined using HPLC-ICP-OES based on the 177.708 nm Pt, 134.724 nm Cl and 148.845 nm Br emission lines. The limits of quantification (LOQs) for the HPLC-ICP-OES method of 2.97×10^{-3}, 0.67 and 0.29 $mmol.L^{-1}$, respectively, indicate the lower limit of concentration at which a particular separated species can be unambiguously characterized. Nevertheless, species present in low abundance could still not be characterized based on their Pt to halide mole ratio. In order to obtain structural information of the $[PtCl_{5-n}Br_n(H_2O)]^-$ (n = 0 – 5) complex anions present in low concentrations, ESI-Q-TOF-MS was used. Additionally, using reversed phase ion-pairing UHPLC, based on tributylamine,

allowed for shorter analysis times, thus further improving sensitivity. The developed UHPLC-ESI-Q-TOF-MS method was capable of separating and characterizing all the homoleptic and heteroleptic $[PtCl_{6-n}Br_n]^{2-}$ (n = 0 – 6) complexes as a proof-of-concept study, whereupon separation and characterization of the mono-aquated $[PtCl_{5-n}Br_n(H_2O)]^-$ (n = 0 – 5) complex anions was achieved. The estimated LOQ of 0.1 $mg.L^{-1}$ represents a significant improvement in the level of concentration at which these Pt^{IV} species can be characterized. Quantification of the $[PtCl_{5-n}Br_n(H_2O)]^-$ (n = 0 – 5) complex anions by means of IP-HPLC-ICP-OES using the 214.423 nm Pt emission line forms part of future work concerning this study. The ability to quantify each of the $[PtCl_{6-n}Br_n]^{2-}$ (n = 0 – 6) species by means of ion-paring HPLC-UV-Vis allowed for the determination of all 17 stability constants for the Pt^{IV} chlorido-bromido halide exchange reaction network. The associated Gibbs free energies were determined for each ligand exchange reaction step, $\Delta G^{o}_{rxnK_n}$ (n = 1 - 17), and together with energy conservation relationships served to validate the accuracy of the experimentally calculated stability constants. The good agreement between the experimentally determined overall formation constant or ΔG^{o}_{rxn} and those calculated using the standard reaction half cell reduction potentials of $[PtCl_6]^{2-}$ and $[PtBr_6]^{2-}$ is further confirmation of these experimentally obtained thermodynamic parameters. The thermodynamic driving force in aqueous solutions was determined to be the hydration of the halide ligands, contributing $\Delta\Delta G_f{}^{o}_{(halide)}$ = -27.4 $kJ.mol^{-1}$ to $\Delta G^{o}_{rxnK_n}$ (n = 1 - 17). This results in the formation of the bromido Pt^{IV} complexes, even though the chlorido Pt^{IV} complexes were determined to be energetically favoured in this reaction network. This result was generalized for other metal cation halido exchange reactions and showed that all metal halido complexes exhibit the $F^- >> Cl^- > Br^- > I^-$ order of thermodynamic stability and that inversion of this order was only due to the solvation of the relevant halide ligands, a result that exposes the fundamentally flawed nature of HSAB in predicting metal cation halido thermodynamic stabilities. Moreover, density functional theory (DFT) was used to predict the thermodynamic stabilities with respect to the isodesmic reactions involving chlorido-bromido Pt^{IV} stereoisomer pairs and chlorido-bromido Pt^{IV} ligand exchange reactions of the $[PtCl_{6-n}Br_n]^{2-}$ (n = 0 – 6) species and used to confirm the $F^- >> Cl^- > Br^- > I^-$ order of thermodynamic stability for these Pt^{IV} species.

This work represents a significant advancement in the ability to analyse mixed chlorido-bromido $Pt^{II/IV}$ complex anions present at low concentration in acidic, halide rich or halide deficient solutions.